Aus dem Institut für Zahnärztliche Prothetik, Alterszahnmedizin und Funktionslehre Bereich zahnärztliche Werkstoffkunde und Biomaterialforschung der Medizinischen Fakultät Charité – Universitätsmedizin Berlin

DISSERTATION

The submicron dimensional behavior of post-cure dental composites: an Electronic Speckle Pattern-correlation Interferometry study

zur Erlangung des akademischen Grades

Doctor medicinae dentariae (Dr. med. dent.)

vorgelegt der Medizinischen Fakultät

Charité – Universitätsmedizin Berlin

von

Nikolaos Kachrimanis

Aus Agrinio

25. Oktober 2013

Acknowledgements:

To Prof. Dr. Wolf-Dieter Müller for supervising this Thesis and for supporting me throughout these years.

To Dr. Paul Zaslansky for his valuable advices and teaching.

To Dr. Uwe Blunck for his unconventional support and guidance since my very first day in Germany. To Dr. Carolina Mochales Palau for her priceless professional and personal assistance. To Clemens Randow for sharing his knowledge with me. And last but not least, to my family and my partner for the effort to always sustain the good feeling no matter the circumstances.

Contents

1. Introduction

Intraoral cavity preparation and immediate restoration is one of the basic treatments performed by almost every general dental practitioner. For direct filling restorations, three materials are nowadays available: glassionomer cements, amalgam and dental composite resins. The choice between these is governed by the advantages and disadvantages exhibited by each material and the restorative needs.

Glassionomer cements are generally recommended as temporary filling materials due to their inadequate mechanical properties and the swelling they exhibit. Their use is thus indicated only under particular circumstances [1, 2].

Amalgam has been used for a much longer period of time than the relatively new composites [1]. Although it doesn't comply with the aesthetic requirements, it has served well into restoring the teeth's function following decay. Amalgam is robust, and its application is a less sensitive procedure. It performs well in the humid environment of the oral cavity, a fact that may be the reason for the lower failure rate it exhibits when compared to composite fillings. Moreover, when carefully placed, the absence of initial shrinkage results in good marginal adaptation [3]. Nevertheless, amalgam fillings swell over time [4]. The lack of adhesion between this material and the tooth substances results in larger cavities, with particular retention configurations [4]. The filling and the tooth do not function as one entity, a situation posing danger to the tooth integrity [1].

These problems of amalgam were circumvented by the use of composite resins. Apart from their improved aesthetic quality, their application requires adhesion to the hard dental tissues, such that the material and the tooth operate as one system. Due to these major advantages, composites often substitute amalgam in clinical practice, attracting more attention leading to further developments and improvements.

Adhesion of composite materials to the tooth substances makes it necessary to form an interface following a sensitive and demanding procedure. This interface is subjected to various challenges during the life time of the filling and is susceptible to degradation. Indeed, the main disadvantage of composites is related to failure of the adhesive layer, usually expressed as a failure in their marginal adaptation [1, 5]. It is generally proposed that a large part of the challenges this interface has to withstand is related to the

dimensional behavior of the composite material, since any dimensional changes lead to the formation of stresses at the interface.

After the composite is placed and polymerized in the cavity, it appears that three phenomena start occurring simultaneously intraorally: post-polymerization reactions, water absorption connected with the elution of species from the material and changes in the temperature the filling is constantly exposed to, starting with the rise in temperature from room temperature to mouth temperature. Although each of these individual phenomena have been extensively investigated, the relationship between them is not clear. This relationship is important due to the fact that they exert their influence over the material in the same time span.

The complicated dimensional behavior of composites is connected with their chemical composition and constitutes a large field of scientific interest since it has not been fully investigated yet. However, answering the questions connected with this behavior is significant regarding the improvement of the material, so that it will better serve the clinical purposes for which it is used.

2. State of the art

2.1. Chemical composition of dental composite resins

Regardless of their type, all composite resins share the same basic chemical structure: an organic matrix and an inorganic phase, bound together by a coupling agent [6, 7].

2.1.1. Organic matrix

The organic matrix mainly consists of mono-, di- and tri-functional monomers [8]. The monomers that are used are principally BisGMA solved by TEGDMA, BISDMA, EGDMA, and UDMA [5]. BisGMA are the basic monomers used [Fig. 1]. Their high viscosity renders their use problematic, requiring their combination in particular percentages with one or more of other monomers with a lower molecular weight, for example TEGDMA , shown in Fig. 2 [6, 9, 10].

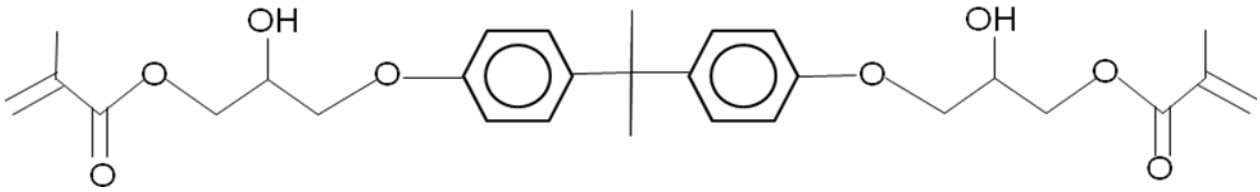

Fig. 1: BisGMA monomer chemical formula.

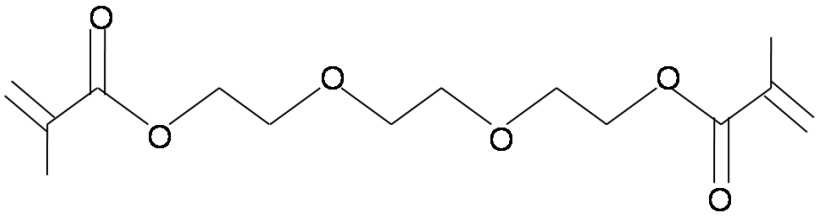

Fig. 2: TEGDMA monomer chemical formula.

The following substances are added to the organic phase of composites:

- A free radical polymerization initiation system, which in the case of photopolymerized composites, is an alpha diketone (e.g. camphoroquinone) [6, 11, 12]. For chemical polymerization a benzoyl peroxide initiator is required together with an amine activator (dihydroxyethyl-p-toluidine or N, N-dimethyl-*p*-toluidine) [5, 11, 12].
- An acceleration system for the initiator, for the light- cured materials (dimethylaminoethyl methacrylate DMAEM, or ethyl-4-dimethylaminobenzoate EDMAB, or n,n-cyanoethyl-methylaniline CEMA) [11, 12].
- An inhibitor system that prevents polymerization to ensure the material's shelf life and its stability after use (such as hydroquinone monomethyl ether) [12].
- UV absorbers (2-hydroxy-4-methoxybenzophenone) for eliminating the effects of UV light on the amine groups of the initiator, which are responsible for color instability of the material [13].
- Color pigments such as metal oxide particles, in order to achieve aesthetic similarities with the tooth substances [5, 13].

2.1.2. Inorganic phase

Concerning the inorganic phase of the composites, the basic filler that is used is silicon dioxide. Boron silicates, lithium aluminium silicates and barium fillers are also used [1, 6, 14].

Due to the soft nature of the matrix, the total filler content, the type, size and morphology of the fillers are mainly responsible for the mechanical properties of the material [11, 15-17]. A proportional correlation was found to exist between hardness and the filler load of the composite [1, 18, 19]. The maximal filler load that can be achieved is determined by the size of the filler particles, which in turn is connected with the distance between them in the mass of the material [16, 17]. Due to this fact, the size of the filler particles is of great importance. Nanotechnology made possible the use of

particles of a size of up to 25nm, making it possible to reach a filler load of up to 79.5 w/w % for some composites. The small size of these fillers is responsible for better aesthetics, lower degradation and lower polymerization shrinkage [1, 17, 18, 20].

2.1.3. Coupling agent

The coupling agent, a silane, that is used to connect the two phases of the composite resins is a molecule with silane groups at one end, able to form ion bonds to SiO_2 of the fillers and methacrylate groups at the other that form covalent bonds with the resin matrix [1, 5, 6]. These bonds distribute the stresses applied on the material between the stronger fillers, through the weaker matrix, thus raising the strength of the composite [13, 19].

Silane coupling protects the fillers from hydrolytic degradation, either due to its hydrophobic nature or by generating compressive stress between the matrix and the filler, not allowing the movement of water molecules through that space [21, 22]. However this bond exhibits a low hydrolytic stability [22-24].

2.2. Polymerization of dental composite resins

The first phenomenon affecting the dimensions of the composites- thus posing a challenge to the interface of the restoration- is their polymerization.

The polymerization of dental composites used as direct filling materials is mostly light-initiated and starts with the activation of camphoroquinone. The free radicals activate the monomer molecules by opening their methacrylate bonds. These in turn react with further monomers of the material leading to the creation of chains, extending and polymerizing until no more reactions can take place [12, 25].

The chains form covalent bonds with each other resulting in the formation of a cross-linked polymer structure connected to the fillers by the silane coupling agent [Fig. 3, 4]. This structure of the composite resins is rigid, exhibits a high molecular weight and increased strength [12, 25].

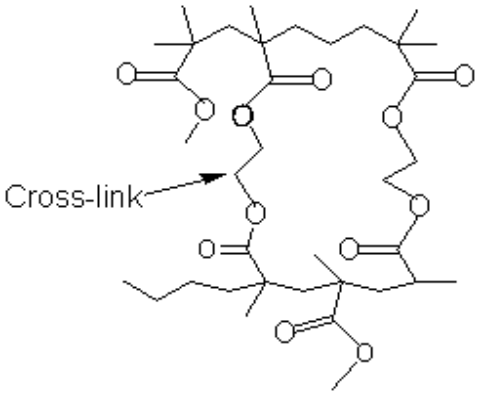

Fig. 3: Cross- linking of direct dental composites, following Anusavice [5].

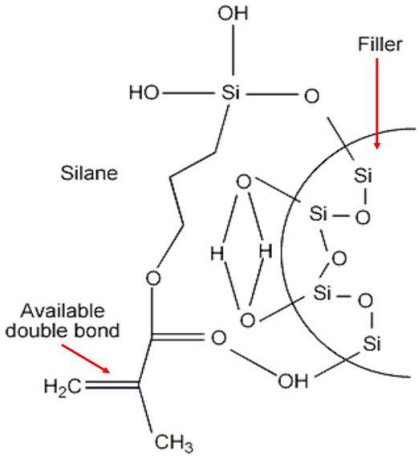

Fig. 4: Silane attached to filler particle following Anusavice [5].

Since the distances between the monomers reduce as the polymerization reactions take place, all composite resins exhibit shrinkage during their polymerization, for which the organic matrix is mainly responsible [5, 10]. Table 1 lists typical shrinkage values.

Material	Polymerization shrinkage
Photo-cured composite resins	1.5-3vol%
Flow composites	5vol%
BisGMA	5.2vol%
TEGDMA	12.5vol%

Table 1: Polymerization shrinkage of various materials [1, 26-28]. The values depend on the degree of polymerization but are not significantly influenced by the curing time [29].

In order to eliminate polymerization shrinkage effects and ensure at the same time acceptable mechanical properties, many monomer combinations are proposed, for example BisGMA with TEGDMA [9]. A negative correlation was demonstrated between the filler load and polymerization shrinkage [29, 30].

It has been demonstrated that shrinkage is linked to the development of internal stresses of the material [31-33]. Such stresses are either original contraction stresses in the material, or shear stresses parallel to the adhesive interface; neither, however, is uniform throughout the restoration [34].

The polymerization of the composites is never complete after light cure. Polymerization reactions take place at a high speed so the order of the structure formed is never homogeneous. Significant amounts of monomer react only at one end or not at all [Fig. 5].

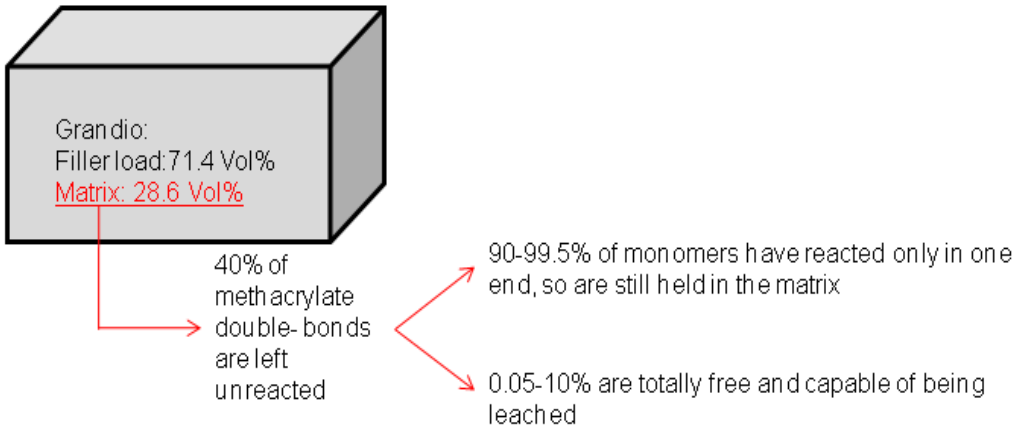

Fig. 5: Chemical state of the monomers of the matrix after polymerization [1, 5, 14, 35, 36].

The unreacted monomers can react with other molecules or can be leached. An important observation concerning polymerization is the fact that it does not reach its end following light cure, but constantly increases for at least 7 days [37].

The number of the C=C bonds that have reacted at the end of polymerization is described as the degree of polymerization of the material [5]. This is influenced by the type of the monomers used and by the initiation of polymerization, i.e. whether it is light-heating- or chemically induced. For the light-cured composites, influential factors include the type of the illumination lamp used, the quality of the light and the duration of the light curing [38-40].

The degree of polymerization is linked to the mechanical properties of the material [18]. It has been demonstrated that the higher the degree of polymerization, the harder is the material [1, 19, 41, 42].

2.3. Composites and water

The dimensional instability of composites does not only include the initial polymerization shrinkage, but is also induced after light-curing by many factors constantly encountered by the material after its application. This instability is also mediated by the wet environment of the mouth.

Observed phenomena include dissolution,[43, 44] hydrolysis,[21, 45] expansion, [9, 46-48] plasticization, [49-51] microcrack formation[21, 51] and fatigue[44, 52] and are attributed to the presence of water inside the material.

Two processes take place when a composite is put in a wet environment: water absorption followed by swelling and water solubility. These two phenomena (water absorption and solubility) interact with each other and therefore must be taken into account simultaneously.

2.3.1. Water absorption

The absorption of water inside composite resins is a diffusion process through porosities and intermolecular spaces of the resin matrix [8, 24, 53, 54], controlled by the laws of diffusion- a fact demonstrated by the Fickian character of the phenomenon [9, 49, 55-59].

Similar to other diffusion processes, water sorption is controlled by the diffusion coefficient of the material under examination.

The following factors modify the diffusion coefficient of dental composites:

- The monomers of the matrix, since sorption is mainly observed through it [45, 60-66]
- The chemical structure and functional groups of the molecules involved, due to the bipolar character of the H_2O molecules.

- The degree of polymerization [8]. It is generally accepted that the higher the quality of the polymerization, the lower the diffusion coefficient of the material [38].

- The concentration of water on the environment around the diffusion “front” [67].During sorption (when the concentration of the water is lower since it exists only in the surrounding environment) a higher diffusion coefficient is found than during desorption (when water is simultaneously inside the material and in the space surrounding it) [24, 59, 68].

- The thickness of the specimens tested. The thicker the specimens, the higher the sorption and desorption coefficients [48, 69].

- The temperature- since it is demonstrated that water uptake increases as the temperature increases [9].

Conflicting information exists in the literature concerning the time span in which the sorption takes place [Table 2].

	Time span in which water absorption takes place
Musanje et al. 2001 [70], Lagouvardos et al. 2003 [71]	3 days
Ferracane et al. 1990 [60], Ortengren et al. 2001 [62], Asaoka et al. 2003 [69]	7 days
Indrani et al. 1995 [72]	13 days
Fan et al. 1985 [73], Ortengren et al. 2001 [61]	60 days

Table 2: Time needed for the water absorption to take place, according to different authors.

The fillers by themselves appear to have no impact on the actual process of water sorption [50, 60]. The only connection mentioned between the filler load and the water sorption is a negative correlation, since the higher filler load reduces the proportion of the polymer matrix [43].

The silane bond between the matrix and the filler protects the latter from hydrolysis and degradation [22]. Moreover, the hydrophobic nature of this bond causes stress on the

matrix- filler interface, preventing water molecules from entering that space [22, 24, 56, 68].

It has been proved however, that the chemistry of the solvent into which the material is placed plays an important role concerning the magnitude of the sorption. Higher diffusion coefficients were found when ethanol/ water solvent was used in comparison to pure water [66, 74]. Other solutions have also been used, such as artificial saliva however it was demonstrated that no significant differences in sorption were found in comparison to pure water [75, 76].

Two distinct phases of water are found inside polymers, after the sorption had taken place [67]. The first phase involves water molecules normally dissolved inside the polymer matrix [64]. The second phase involves water molecules trapped inside pre-existing polymer microvoids [43]. These molecules are hydrogen-bonded and form clusters [48, 77]. However, it is suggested that the later phase is not to be found inside composite resins [24, 71].

Water sorption also influences the weight of the material, provoking an increase of up to 1% within 30 days [78]. Moreover, water also has an impact on the hardness of the material- dry-stored specimens demonstrate higher hardness values in comparison to wet-stored ones made of the same material [79]. The plasticizing effect and the hydrolysis the water imposes on the composites are proposed as responsible for this phenomenon [79].

2.3.2. Water solubility and elution

The presence of water inside the material following absorption leads to the elution of particular chemical substances from the composite [60]. The species, capable of being eluted in a wet environment, include monomers and oligomers from the matrix, [60, 61, 80, 81] polymerization promoters [81, 82] and ions from filler particles [21, 22, 43]. The solubility of the components of composite resins and the subsequent elution of substances are connected with the fact that polymerization is never complete right after curing [1, 35]. Furthermore, solubility affects, among other characteristics, the material's

weight over time [16, 43, 50, 83], leading to a loss of approximately 2%w/w of the material [1, 14, 60].

Elution was shown to take place in a short time after water immersion, as shown in Fig. 6. However, there is also evidence in the literature that it requires from 1 up to 7 days of water immersion [61, 62].

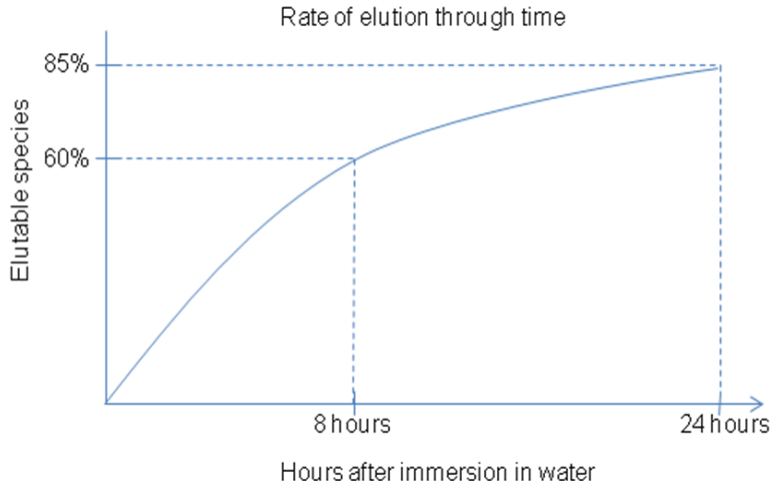

Fig. 6: Rate of elution. 60% of the free monomers are leached within the first 8h of water immersion [84]. 85%-100% of the elution is completed within the first 24h [1, 14, 60].

Various factors affect the rate of elution; factors that are connected, in particular, with the nature of the leachable species and with the solvent in which the elution takes place [85].

Concerning the leachable species, the size and the chemical composition of the elutable species plays an important role [60]. Smaller or more hydrophilic molecules demonstrate a larger capability of elution [61]. A great influence on the elution is also attributed to the degree of polymerization of the composite, since inadequate polymerization means more unreacted monomers [38, 64].

Regarding the factors related to the nature of the solvent, it is shown that the rate of elution varies proportionally to the pH of the solution in which the material is immersed [62]. Experiments have also shown that elution is more pronounced when the composite is kept in an organic solvent, as for example in ethanol[60, 66], than in distilled water or artificial saliva [85].

This connection between the solvent and the solubility is expressed by the solubility parameter (δ), which represents the potential of the polymer network for hydrogen bonding and polar interactions [8]. The extent of solvent uptake by a polymer is a function of the differences between the solubility parameter of the polymer and that of the solvent, being greater when this difference is small. This parameter in composites is typically measured by the swelling of the material, since it is caused by the water that is dissolved in it [8].

The solubility of fillers generally depends on the type of the glass used. Pure silica and quartz fillers do not react with water, while zinc, barium and strontium glasses show the highest total ion leaching [43]. Silicon ions, boron, barium, sodium, lithium and strontium are detected in the solutions used in elution tests [1, 21, 22, 43]. However, their origin is obscure; no degradation of the fillers inside the mass of the material was found [19, 49] since they are protected by the silane coupling [22]. In addition, no correlation was found between the filler load and solubility [19, 54]. The unprotected fillers however that exist on the polished surface of the composite are leached rapidly after immersion and may therefore be responsible for the detection of the ions mentioned above [86].

2.4. Dimensional changes of composites due to water absorption

One of the main results of water sorption is the swelling of the material over time [1, 9, 29, 44, 46-48, 77, 87]. Whether a composite will swell because of water uptake, depends on the mechanism of absorption and the chemical composition of the material [9].

Expansion is also influenced by solubility, suggesting that water molecules inside the material are replacing dissolved species [29]. This is indicated by the fact that a positive correlation was demonstrated between water sorption and hygroscopic expansion, while a negative correlation was shown between solubility and hygroscopic expansion [29, 87, 88].

Regarding the swelling mechanism, the cause for expansion depends on which of the two phases of the water molecules described above predominate in the material. Expansion is caused by the water molecules that are dissolved in the polymer network, since they are the ones that act as a plasticizer and separate the polymer chains [29, 64]. The second phase of water molecules formulate clusters, act rather like filler particles and do not exhibit any effect on the dimensions of the material [48].

Consequently, materials with rigid structures, where the fluid is in porosities and not between the polymer chains, exhibit no dimensional change when absorbing or desorbing fluids [64, 77].

It is demonstrated that 63% of the expansion due to water sorption occurs in the first 10 days of water immersion [89]. This swelling phenomenon is responsible for the relaxation of the stresses caused by polymerization [51]. In addition, the expansion compensates, to some extent, for the shrinkage observed during the polymerization, however it can never bring the material to its original dimensions as they were before the polymerization took place [1, 29, 89]. A point of interest however, is that this dimensional change was found to generate radial pressure inside the material [67].

An osmotic effect is described in order to explain the swelling of some composites during water absorption [90]. This effect is caused by the presence of zones inside the material structure, in which water may be concentrated with residual components of the

polymerization [77]. This concentration results in continued absorption. The osmotic pressure generated may be great enough to overcome the restraining effects of the cavity in which the material is placed, or to cause internal tearing of its polymer chains [91].

A second theory proposed for the sorption process is connected with the free volume of the material, i.e. the space in the material available for chemical interactions to take place. According to this theory, the molecules that enter the material induce a softening of the polymer structure creating extra free volume, thus inducing expansion [92].

The forces that are expected to counterbalance this expansion originate from the walls of the cavity the material is placed in and the luting agents that are used [77]. It is possible that the pressure inside the material, generated by the water uptake, equals the restraining pressure imposed by the cavity walls and the pressure generated by the elastic response of the material. It is therefore suspected, that the value of the stress caused by the hygroscopic expansion of the composite resins is related to the cavity configuration and the size of the surfaces of the material that are exposed to fluids [77, 93].

If the pressure generated by sorption is larger than the existing restraining forces, the tooth integrity may be in danger [94]. This possibility of a tooth fracture is, as inducted, related to the tensile bond strength between the material and enamel or dentin, to the cavity dimensions and to the residual tooth structure thickness [94].

2.5. Composites and thermal fluctuations

The third phenomenon responsible for the dimensional changes a composite filling undergoes, in addition to polymerization shrinkage and swelling due to water absorption, is connected to the thermal changes occurring constantly in the mouth environment.

The complicated thermal behavior of wet composite resins is of great clinical interest, since the temperatures that develop *in vivo* in the mouth cover a large range between 5°C and 55°C [95] and are constantly changing during the lifetime of the filling.

2.5.1. Dimensional changes due to thermal fluctuations

It should be stated that generally, dry composite resins exhibit a non-linear expansion when heated [96].

The coefficient of thermal expansion (CTE) is used to describe the dimensional change a material shows when it is heated. The difference of the CTE between composite resins and dental hard tissues is responsible for the generation of stresses at the interface between them, as shown in Fig. 7, which can result in microleakage at the interface [97].

The CTE generally decreases as the filler load of the composites increases [98-100]. Furthermore, for the CTE of any given composite is not fixed, exhibiting a decrease as the thickness of the material increases [96]. Also for heated specimens, the dimensional change at higher temperatures is greater than at lower ones [99].

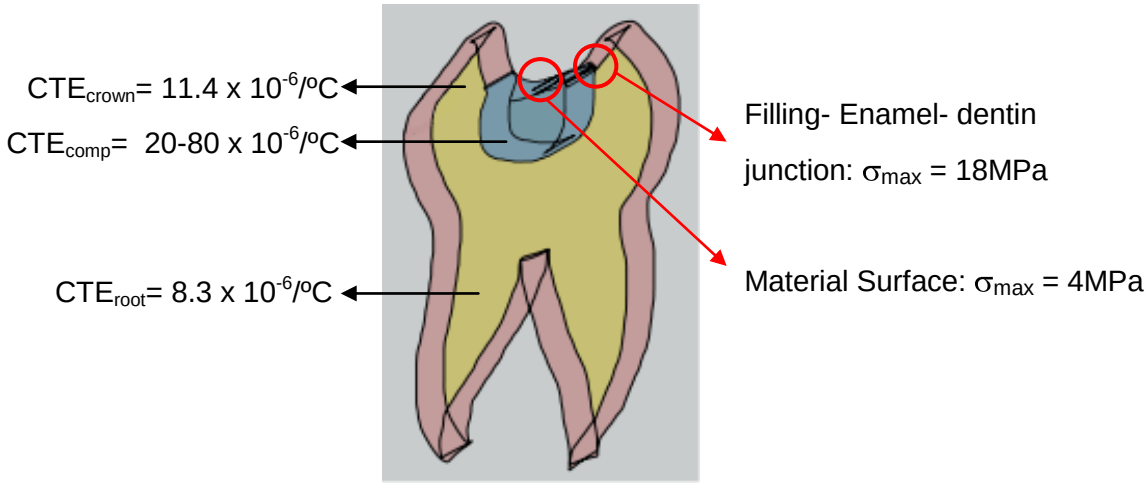

Fig. 7: CTE values and stresses generated when the tooth- filling complex is heated (for composites measured in a range of 26°C<T<120°C, for hard tissues measured in a range of 20°C<T<50°C) [101, 102]. During heating, the greatest stress is found to be generated between the composite and enamel. The maximum tensile stress, 4MPa, is exhibited at the surface of the material and the maximum compressive stress, 18MPa, at the interface of the material with the enamel-dentin junction [103].

This dimensional response of composites towards thermal fluctuations is also influenced by the presence of water. Wet composites show higher CTEs than dry ones [96].

The final dimensional change expected when a wet material is being heated depends on which of the two phases of the water (the dissolved phase or the water molecules forming clusters, as mentioned) predominates [96]. Sidhu et al. suggested the following equation as a means for extracting useful information [104]:

$$CDC = CTE + CDCf \qquad \text{[Eq. 1]}$$

where:

CDC= coefficient of dimensional change

CTE= coefficient of thermal expansion

CDCf= coefficient of dimensional change due to fluid movement

CDCf represents the shrinkage a material undergoes, as the absorbed water inside it starts evaporating due to rise of the temperature.

Depending on the material, either the CTE or the CDCf predominates; consequently, a material either contracts or expands due to heating, depending of the amount of the absorbed water inside it.

Another important value connected with the dimensional change is the glass transition temperature (T_g) of the material. It is demonstrated that this temperature is the threshold above which the evaporation of the absorbed water takes place in a dry environment [105]. This evaporation, as will be seen, is a critical point concerning this study. T_g – similarly to CTE- is not affected by the presence of water clusters in the composite, but rather by the diffused water [96]. Its value appears to be lower in the case of wet specimens [96]. For most of the composite resins its value ranges between 40 and 45 °C [96].

2.6. Methods applied for measuring deformations

Until now, various methods have been applied for the purpose of measuring dimensional changes, as described in Table 3. Each of these methods possesses particular advantages and disadvantages.

Methods other than profilometry, optical scanning systems and finite element models are not suitable for small scale three- dimensional measurements. This is either because of the nature of the setup (electronic micrometer, custom automatic laser radial micrometer), or because with some methods the deformation measurements are indirect (Archimedes' principle), based on the measurement of stress generated (stress-strain analyzer, universal testing machine, strain gauges, glass strips), or because the specimens are confined within moulds that don't allow free deformations in all directions (bonded disk method).

Profilomentry and finite element models give results regarding dimensional changes occurring over time in all three directions, as described in Table 3. However, the finite element models are based on simulations and not real measurements.

	Methods applied for measuring strain	Actual results acquired
Chutinan et al. 2003 [106], Sideridou et al. 2008 [88]	Archimedes' principle of buoyancy	The density of the specimen defined from the mass upthrust after placement in an immersion liquid
Hirasawa et al. 1983 [87]	Electronic micrometer	The dimensional changes regarding the length of the specimen.
Martin et al. 2003 [89]	Custom automatic laser radial micrometer	The diameter of the specimen during a stepwise rotation.
Marchesi et al. 2010 [107]	Stress- strain analyzer	The contraction force generated during deformations.
Marchesi et al. 2010 [107]	Universal testing machine	The force required in order to keep the specimen's height stable.
Versluis et al. 2003 [32], Takahashi et al. 2010 [31]	Strain gauges	The shrinkage of a composite specimen placed over a strain gauge as change in resistance.
Feilzer et al. 1990 [93]	Glass strips	The curvatures of glass strips, on which the specimen was adhered.
Min et al. 2010 [108], Takahashi et al. 2010 [31]	Bonded disk method	The axial shrinkage strain of a composite placed between one slide glass and one flexible cover glass.
McCabe et al. 2003 [77]	Profilometry	The swelling of the material, by comparing the profile of the mould - specimen surface before and after wet storage.
Versluis et al. 2010 [94]	Optical scanning systems	The lingual and buccal tooth surface flexure, after comparing digitized tooth images before and after storage.
Barink et al. 2003 [34], Versluis et al. 2003 [32]	Finite element models	The simulation of residual shrinkage stress by software, after specifying known parameters such as light intensity, elastic modulus, creep and shrinkage.

Table 3: Methods applied for measuring deformations of composites.

3. Statement of the problem

There is a need for investigating the relationship between the three phenomena taking place after the composite filling is placed, namely post-polymerization, water uptake and thermal fluctuations. To investigate this relationship, it is important to be able to record the deformations as expressions of these phenomena at the same time as they are taking place in all three dimensions.

The null hypothesis of this study was that the post-cure dimensional behavior of the composite when heated up to mouth temperature is influenced by post-polymerization and water absorption phenomena that take place after curing.

The second hypothesis of this study was that it is possible to measure the minute deformations of the composite when exposed to mouth temperature, as they occur after polymerization in different storage conditions, in a high precision in all three directions with electronic speckle pattern interferometry (ESPI).

4. Aim

The basic aim of this study was to investigate the dimensional behavior of a standard composite in response to particular phenomena taking place after polymerization. Through deformation measurements, the interaction of post-cure phenomena will be explored in order to acquire information concerning the magnitude of their influences.

Within the scope of investigating the dimensional behavior of the material after its polymerization, the capacity of ESPI as a measurement technique was investigated.

The unique advantage of ESPI is that it performs non-destructive measurements of the deformations as they occur over time in the nm scale, simultaneously in three dimensions.

This combination of features renders ESPI a promising technique for conducting a wide range of measurements. Therefore, the second aim of this study was to establish the reliability of ESPI as a measurement technique and develop a measurement protocol which could be thereafter applied for performing diverse investigations.

5. Materials and Methods

5.1. Materials and specimens' preparation

For the purposes of this study, the following two light-curing direct restorative materials were selected [Tables 4, 5].

	Company	Classification	Matrix	Filler load
ADIMRA	VOCO, Cuxhaven	Ormocer®	Bis-GMA, UDMA, TEGDMA	56 Vol. %
GRANDIO	VOCO, Cuxhaven	Nanohybrid	Bis-GMA, TEGDMA	71. 4 Vol. %

Table 4: Materials used for the measurements.

Measurements	ESPI evaluation and protocol definition	Impact of water and air storage/ Specimens' control/ Water inside dry- stored specimens/ Procedure of water absorption	Impact of post-polymerization/ Relationship between the 3 phenomena
Material	Admira	Grandio	Grandio
Batch Nr.	0816094	0917243	1047455
Reference	02423E1	1800	1812

Table 5: Batch numbers and references of the materials tested in the equivalent measurements.

Both materials are used in combination with an adhesive, according to the principles of the layering technique, for direct restorations in the clinical practice [13].

All specimens used in this study had a diameter of ~ 15mm and a thickness of 1mm, and were produced with a standardized method [Fig. 8, 9]. A mass of the material was shaped and thinned between two glass plates, pressed until the distance between the glass plates reached 1mm, then polymerized from both sides for a total time of 80 sec, 40 sec from each side.

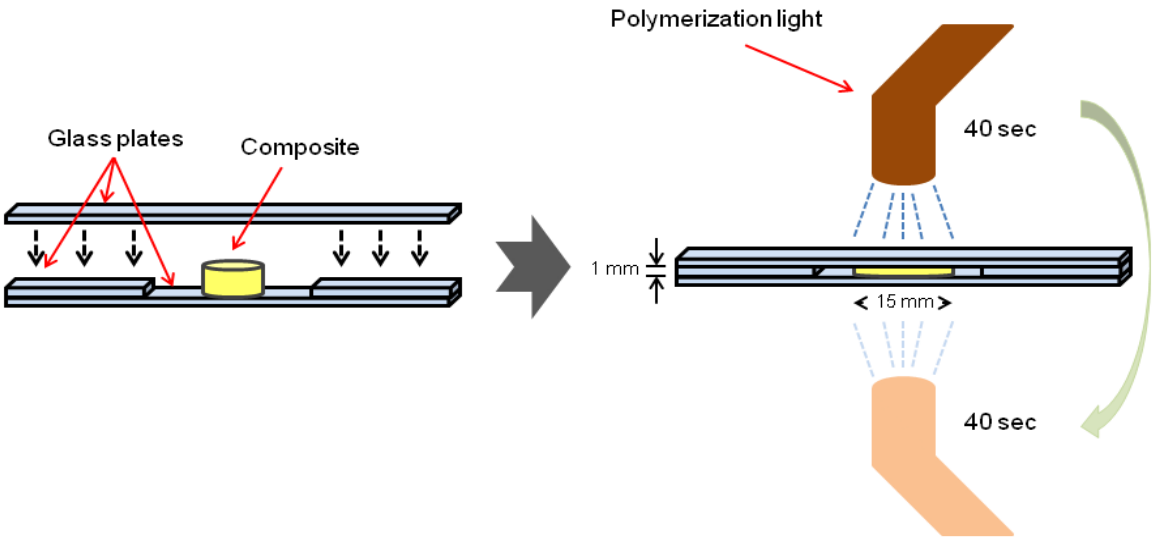

Fig. 8: Standardized method followed for the production of the specimens.

The duration of polymerization is strongly positively correlated with the degree of conversion [19, 109]. This long duration of polymerization ensured the achievement of the highest degree of conversion, so that no possibility of inadequate polymerization would exist. The polymerization was accomplished by using a LED curing light, CELALUX 2 (VOCO, Cuxhaven), with a wavelength of 420- 480 nm and intensity 900-2000 mW/cm^2 in the normal light-curing mode [Fig. 10].

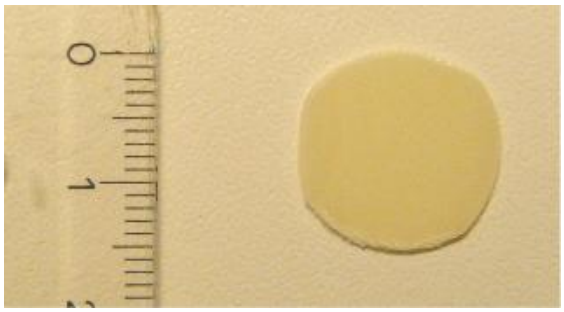

Fig. 9: Specimen with dimensions.

Fig. 10: Polymerization light.

5.2. Methods

In order to measure the deformations of the material, an ESPI (Dantec Dymanics) method was used.

5.2.1. Electronic speckle pattern interferometry for measurements of deformations

Electronic speckle pattern interferometry (ESPI), shown in Fig. 11 and 12, is a non-contact, non-destructive laser imaging method for measuring small deformations and minute strains of surfaces [110].

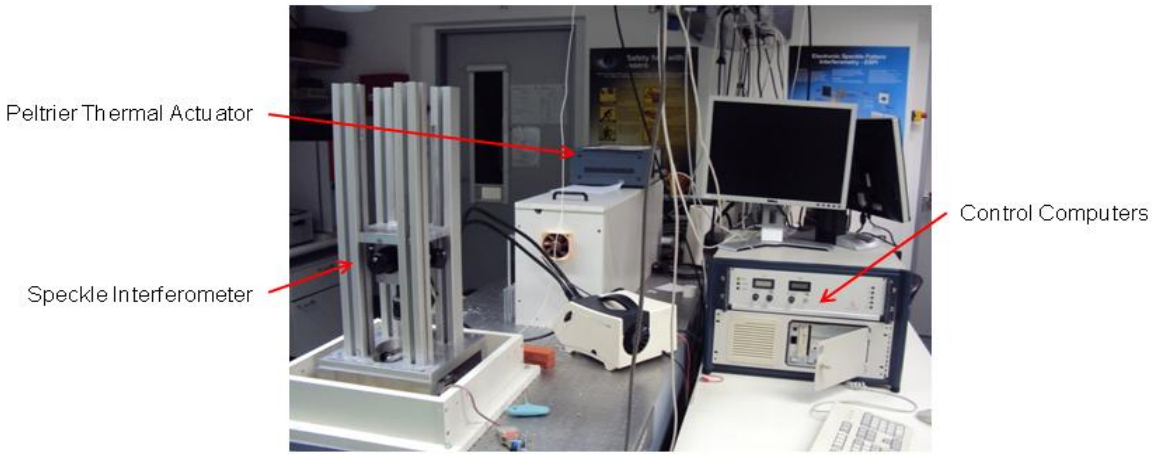

Fig. 11: ESPI.

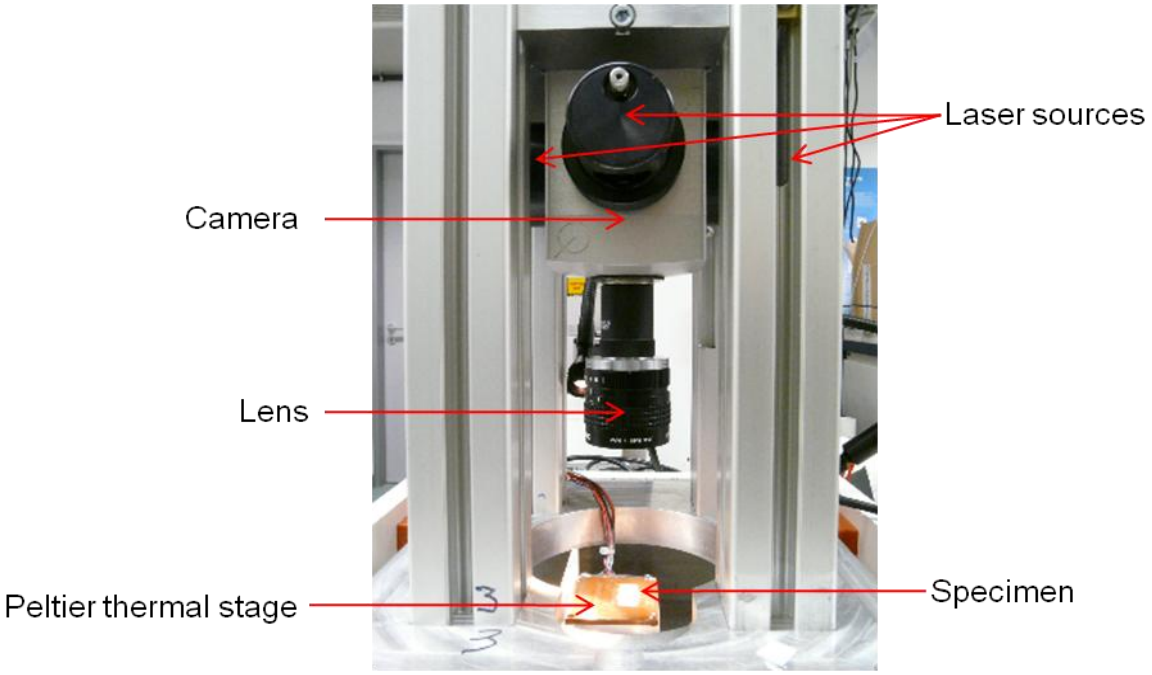

Fig. 12: Detailed view of ESPI with specimen.

The non-contact and non-destructive character of the measurement procedure enables the recording of deformations occurring in the material over time as a response to thermal fluctuations or mechanical strain.

5.2.1.1. Principles

In this section, a brief description of the ESPI principles is given according to the technical information from Dantec Dymanics and their description from Zaslansky et al. [111-113]. The basic principle of the ESPI measurement involves the illumination of the surface of the specimen by a coherent laser beam split in two, the first creating statistical random interference patterns, intrinsic to the surface, called speckles and the second serving as a reference beam. The light-field is recorded by a CCD camera, through a lens [Fig. 13].

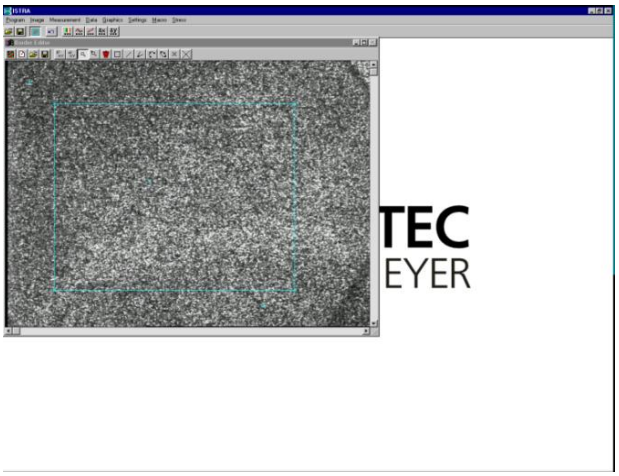

Fig.13: Typical speckle image

The superimposition of the two beams creates an interferogram, which is the basis of measuring the deformations. As displacement takes place on the surface, each image created by the laser beam changes; as a result, the interferogram changes [Fig. 14].

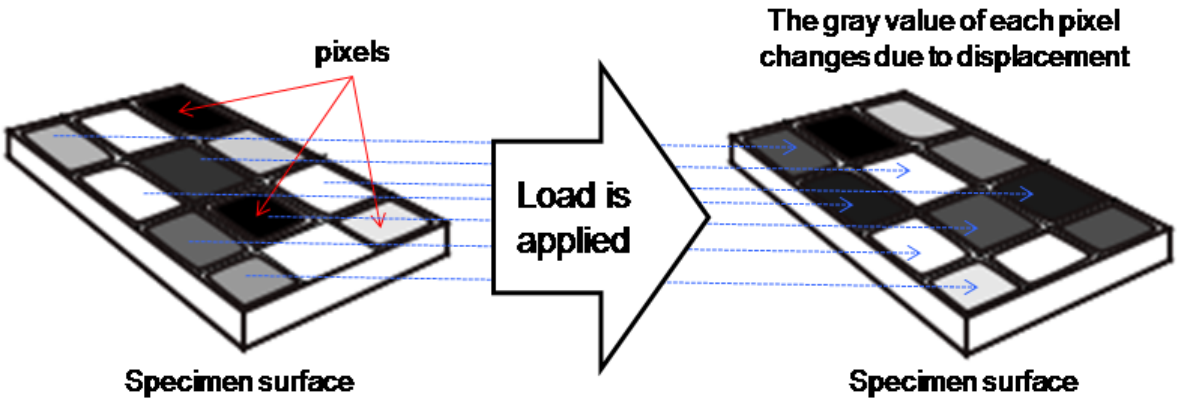

Fig. 14: Each time a load is applied on the specimen, the displacement occurring is expressed as a change on the gray value of each pixel on the image of its surface.

These changes of the interferogram are recorded and the quantitative estimates of surface deformations are acquired.

The ESPI measurement is full-field, which means that it images the whole specimen simultaneously. Measurements are conducted along the x axis, then also along the y axis and z axis in the same image to provide the opportunity of calculating the three dimensional distribution of displacement and strain. The x and y directions are measured by an in-plane arrangement and the z direction by an out-of-plane arrangement, all quasi simultaneously [Fig. 15].

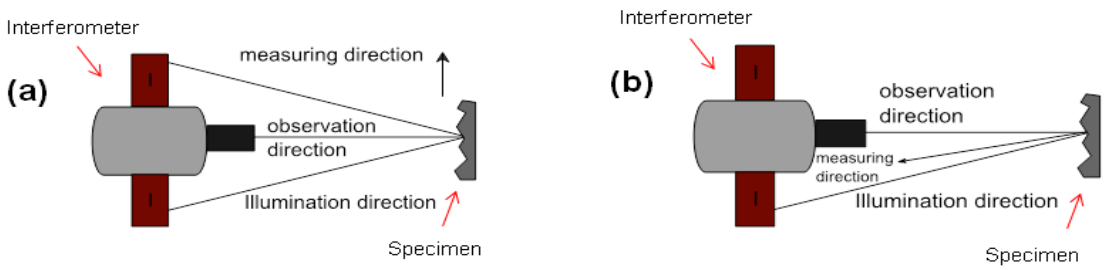

Fig. 15: Illumination and measuring directions of ESPI according to Zaslansky et al. [113]. (a) shows the in-plane arrangement for the calculation of strain in the x and y directions. (b) shows the out-of-plane arrangement for the calculation of strain in the z direction.

At the in-plane arrangement, the laser beam is split in two beams, each illuminating the surface from two opposite angles [Fig. 15(a)]. The phase of only one of the two beams changes, the other serving as a reference. Interference occurs between the two speckle images acquired. At the out-of-plane arrangement, although the laser beam is also split in two only one beam illuminates the surface, which is also the one that changes phase, while the other one serving as a reference is directed towards the camera [Fig. 15(b)]. The change in the phase of the beams takes place by the use of a mirror mounted on the interferometers.

5.2.1.2. Acquirement of the data:

The total duration of the measurement is determined by the user, in terms of number of measurement steps, with each step requiring 4 sec. A detailed description of this process is given in Appendix A.

For the duration of the measurement step, comparing the two interferograms leads to the creation of a fringe pattern related to the specimen surface. This imaging of the surface consists of consecutive black, gray and white patterns representing the displacement of the specimen surface regions [Fig. 16].

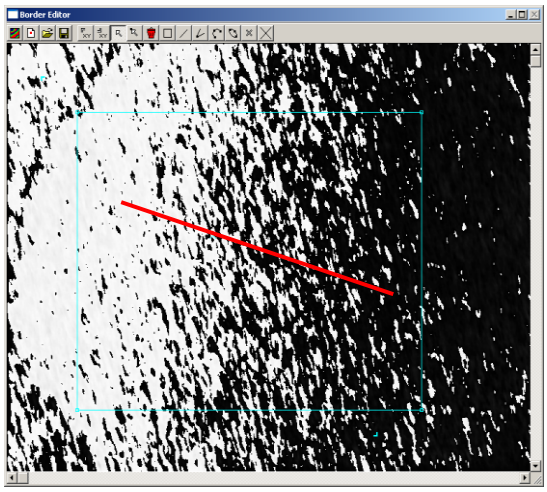

Fig. 16: Fringe patterns on the surface of the specimen. The red line depicts a slope in the data (from white to black) corresponding to a gradient of displacements which indicates that the specimen experiences strain.

With a reference point set, the image acquired from each step shows whether the surface of the material expanded or contracted during this step.

The fringe patterns provide quantitative information after phase unwrapping is applied. The result is a submicron displacement map. For every point of the surface, three displacement values are acquired per step. As a simple approximation, these values are the variables that represent a plane. Thus these points satisfy the equation a+b*x+c*y=z, and consequently a plane regression can take place to estimate the slope and strain. The b and c variables stand for the slope of the plane in the x and y directions (μm/ μm). Smoothing can also be performed [Fig. 17, 18].

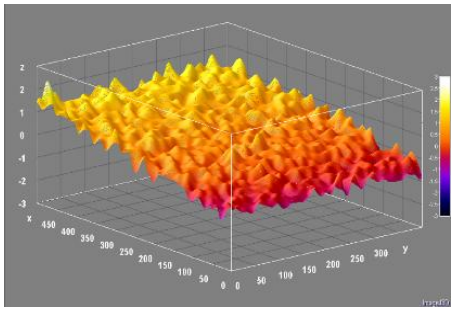

Fig. 17: Plane regression after phase shifting.

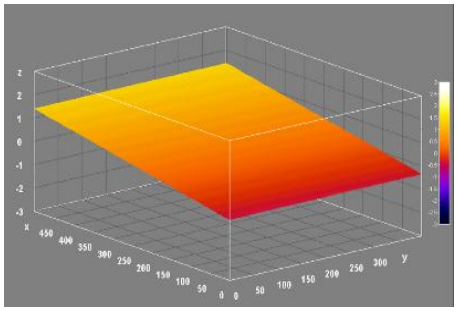

Fig. 18: Smoothed plane.

5.2.1.3. Evaluation of the data

The data, after unwrapping and smoothing, are transferred to ImageJ, a free image processing program [114].

The slope per step represents the strain accumulated in each particular step for the equivalent direction on the surface of the specimen: the larger the slope, the greater the strain.

From these strain values, the strain percentage values are easily calculated by multiplying by 100.

The strain equation [Eq. 2] according to Craig [115] shows that if the strain is known and the initial length equals 100 (as is the case when the calculations are done in percentages), the deformation percentage (ΔL) equals to the strain percentage:

$$\varepsilon = \frac{\Delta L}{L_0} \qquad \text{[Eq. 2]}$$

where ε= strain

$\Delta L / L_0$ = the change in length per unit original length

In this way, the deformation percentage that took place during each step can be calculated as the actual strain percentage recorded by the ESPI during that step.

Summing up all the slope values until the last measurement step provides the value of the total strain developed over the duration of the measurement. The total deformation percentage value that took place up until each step therefore equals to the sum of the strain percentage value in this step with all the strain percentage values exhibited in the previous steps. In this manner it is possible to follow the deformations taking place throughout the duration of the experiments.

The positive deformation values acquired represent expansion, while the negative ones shrinkage.

5.2.1.4. Purposes of application of the ESPI

It is demonstrated that the measurements conducted with ESPI provide reliable results, with the unique advantage of the non- destructive character of the method [116]. Generally, ESPI has been successfully used for mechanical tests of bones, [117, 118] for recording thermally induced deformations in dentin [119], for the development of cuspal strain [120], for measuring the strain and Young's modulus of dentin [113] or the strain at the dentin- enamel junction[112].

5.2.1.5. ESPI requirements

The illuminated surface under examination must be optically rough which means that transparent materials or finely polished surfaces must be coated in order to be measured. This way, reflections recorded are from the laser beams, as they hit the surface of the specimen. Reflections coming from the bulk of the material or from the surrounding environment distort the recording and provide inaccurate results. The materials proposed for coating are either talcum powder, white industrial crack-visualization spray (Diffu-Therm, Helmut Klumpf Technische Chemie AG) or Tipp-Ex (Tipp-Ex GmbH & Co. KG).

The precision of the ESPI measurements on such a small scale has the drawback of a great sensitivity during the measurements. External vibrations or uncontrolled temperature of the surrounding space can distort the measurement. It is therefore important that the ESPI is mounted on a vibration isolation platform in a carefully controlled environment.

5.2.2. Specimen storage

The specimens prepared to be measured were stored either in ambient conditions at room temperature or in water at room temperature. The water used for this purpose was regular tap water. The reason why water was used was that no different impact on water sorption characteristics was observed between water and artificial saliva as a storage medium [75, 76]. Tap water was preferred instead of distilled water, as the former exhibits a larger contact angle than the latter thus achieving a better wettability [121].

The storage durations chosen for each measurement were defined by the facts already demonstrated in the literature concerning water sorption, solubility and post-polymerization of dental composite resins.

The temperature of interest in these measurements was the mouth temperature, 37°C, relevant to the clinical conditions where these materials are used. In addition, at 37°C the absorbed water would not evaporate from the material: it is much lower than the T_g of composites which is, as explained in Chapter 2.5.1, the temperature above which this evaporation takes place.

5.2.3. Experimental prerequisites for specimen mounting and thermal measurement

Prior to each measurement, the specimen was mounted on a custom- made Peltier Thermal stage which was used to regulate the temperature [Fig. 19, Appendix B1]. The surface of the specimen in contact with the Peltier copper plate was coated with AMASAN (Armack Löttechnik), a thermal coupling paste, in order to optimize the thermal contact and ensure an even transition of the temperature over the entire surface of the specimen. The visible surface of the partially transparent specimen was coated with Diffu-Therm, a white industrial crack visualization spray, or with Tipp-Ex, in order to make the measurement with the Electronic Speckle Pattern Interferometer possible.

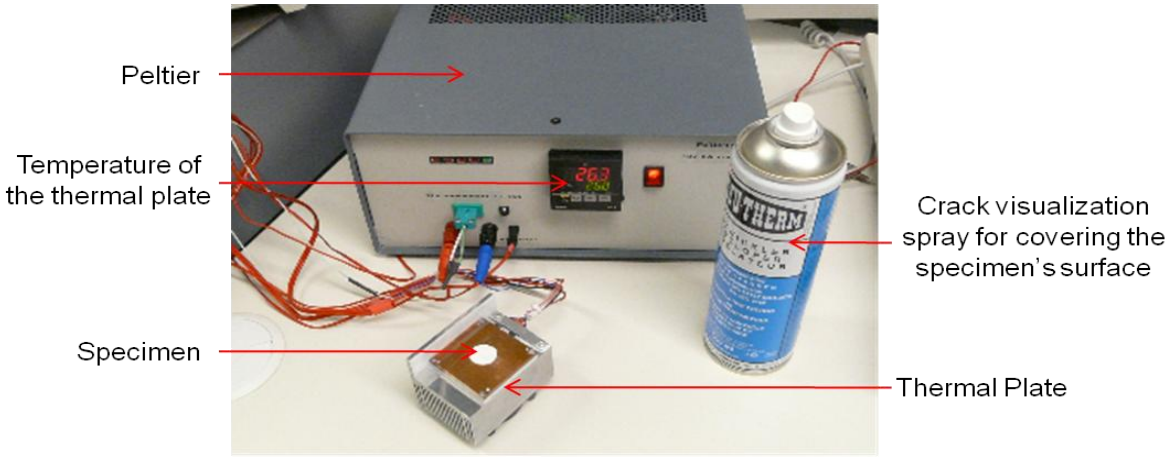

Fig. 19: Peltier Thermal stage with specimen mounted on it.

5.2.4. Evaluation of the ESPI and protocol definition

5.2.4.1. Evaluation of the ESPI technique

In order to investigate the potential of applying ESPI to measure the differences in the dimensional behavior of the material, when stored for different lengths of time, two specimens of ADMIRA were produced and immersed in water for two different lengths of time, at room temperature [Fig. 20]. The specimens were coated with talcum powder and then mounted on the Peltier thermal stage. The ESPI parameters for this measurement are described in Table 6.

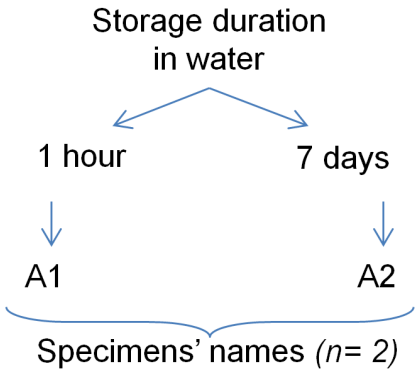

Fig. 20: Specimens and water storage durations.

Aperture	7.5
Focus	1.3
Laser Intensity	50 mA
Lens- Specimen Distance	250mm
Temperature	From 26°C to 44°C and held until the end. 44°C reached at step No 30
Number of steps	300, equivalent to 20min

Table 6: ESPI configuration.

5.2.4.2. Establishment of an ESPI measurement protocol

A second, more controlled series of measurements was performed in order to acquire better knowledge concerning the best combinations of laser intensity, aperture, focus and position of the ESPI lens.

The impact of the storage medium in this measurement was also taken into account. The storage durations for this set of measurements were chosen in such a way as to be able to additionally acquire an indication of the general behavior of the material and the potential influence of the storage conditions (storage medium and duration).

6 ADMIRA specimens were produced and stored for different lengths of time in different mediums, at room temperature, as seen in Fig. 21.

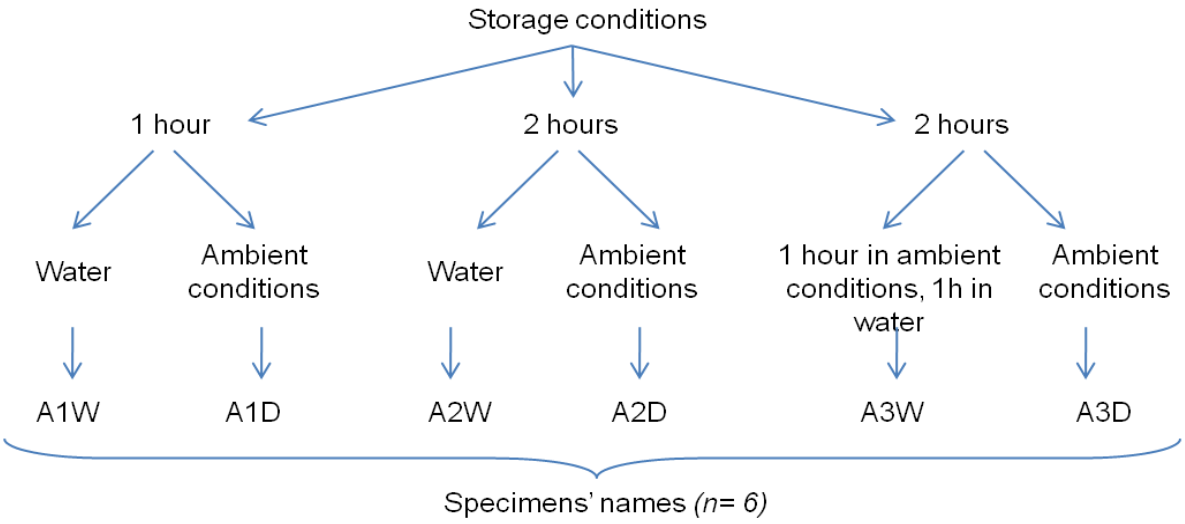

Fig. 21: Specimens' names and storage conditions.

All specimens were talcum coated and then mounted on the Peltier thermal stage. The ESPI measurement configuration for this measurement is shown in Table 7.

Aperture	11
Focus	8
Laser Intensity	60 mA
Lens- Specimen Distance	266mm
Temperature	From 26°C to 44°C and held until the end. 44°C reached at step No 55
Number of steps	400, equivalent to app. 27 min

Table 7: ESPI configuration.

5.2.5. Investigation of the dimensional behavior by using the ESPI

Having established the ESPI measurement protocol, the investigations of the dimensional behavior of the material could take place.

The target temperature of interest was set to be at body temperature, 37°C, relevant to the clinical conditions where these materials are used. All measurements start at room temperature, include an initial heating period and a holding period at 37°C.

Upon reaching the designated storage duration, each specimen was mounted on the Peltier precision heating stage with thermal coupling paste (Amasan), coated with white industrial crack-visualization spray (Diffu-Therm) before heating and kept at 37˚C [Fig. 22].

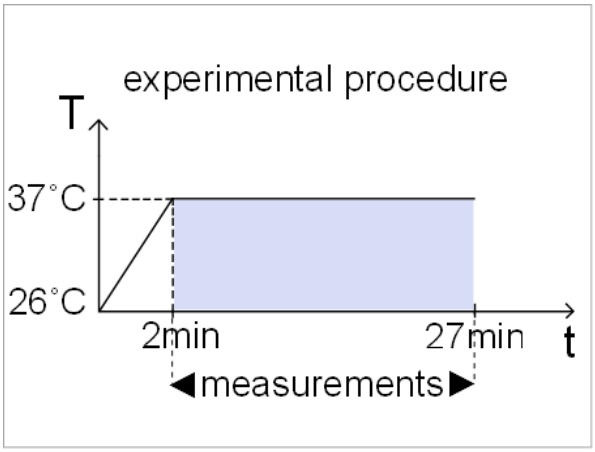

Fig. 22: Experimental timeline: the specimen reached 37°C on the 2nd minute and kept at this temperature until the end of the measurement.

5.2.5.1. Investigation of the different impact of water and air storage on the post-cure dimensional behavior of the composite

The different influence of water and air storage on the dimensional response of the material to heating was first investigated.

Two groups of GRANDIO specimens (n= 6, each) were produced and stored according to Fig. 23. The ESPI configuration is shown in Table 8.

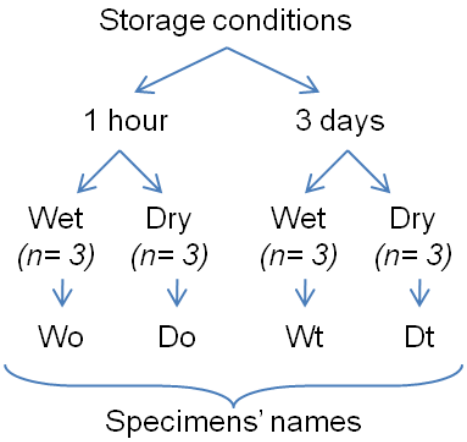

Fig. 23: Specimens' names and storage conditions.

Aperture	11
Focus	1.3
Laser Intensity	55 mA
Lens- Specimen Distance	257mm
Temperature	From 26°C to 37°C and held until the end. 37°C reached at step No 30
Number of steps	400, equivalent to app. 27 min

Table 8: ESPI configuration.

The 400 steps acquired for each specimen were divided in groups of 10 and for each group of 10 the mean slope value was calculated. When a slope value was found to be defective, it was replaced by the average of the three values before and three after it, as explained in Chapter 7.1.

The statistical significance of the results was tested by 2-way ANOVA followed by a Tukey test, since there are two observations (wet and dry specimens) for every storage duration.

5.2.5.2. Investigation of the presence of water inside dry- stored specimens

Since a large part of these investigations involve water absorption it would prove useful to examine the possibility of water being present inside the material even before it is polymerized. For this purpose, two more Grandio specimens were produced, stored in vacuum, measured with ESPI and the results compared with 2 dry- stored specimens from the previous measurement [Fig. 24, Table 9].

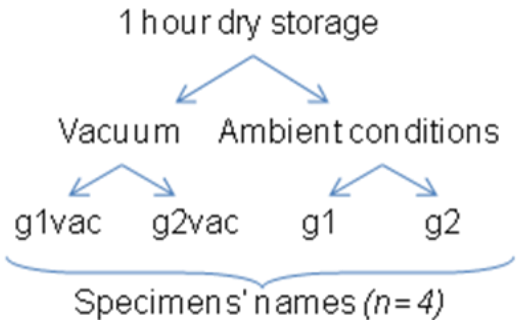

Fig. 24: Specimens names and storage conditions.

Aperture	11
Focus	1.3
Laser Intensity	55 mA
Lens- Specimen Distance	257mm
Temperature	From 26°C to 37°C and held until the end. 37°C reached at step No 55
Number of steps	400, equivalent to app. 27 min

Table 9: ESPI configuration.

The statistical significance of the results was evaluated by a Student's t-test.

5.2.5.3. Investigation of the impact of post-polymerization on the dimensional behavior of the composite

The final investigation concerning the dimensional behavior of the composite had to do with the way the post-polymerization determines different responses of the material to heating.

42 Grandio specimens were produced. For these measurements, all specimens were stored wet before being measured for different time periods [Fig. 25]. At the end of the storage period, each specimen was mounted on the Peltier heating stage with coupling paste and Tipp-Ex applied on the surface being measured.

The ESPI configuration is shown in Table 10.

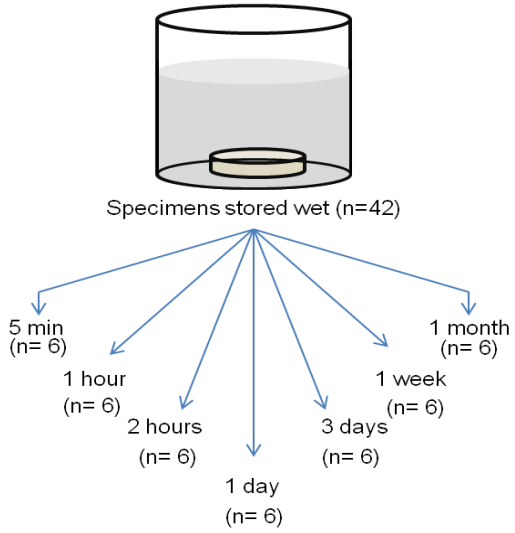

Fig. 25: Groups of specimens.

Aperture	8
Focus	2
Laser Intensity	60 mA
Lens- Specimen Distance	484mm
Temperature	From 26°C to 37°C and held until the end. 37°C reached at step No 30
Number of steps	400, equivalent to app. 27 min

Table 10: ESPI configuration.

The statistical significance of the results was tested by one way ANOVA followed by Tukey test.

5.2.6. Control of the specimens' production reliability

In order to control the reliability of the production of the specimens, measuring the values of their Vickers microhardness (HV) is a useful tool. Differences in the HV values between the specimens reveal potential inhomogeneities and problems in the production of the specimens [122].

For this purpose, a Microindenter (MHT-10, Anton Paar) [Fig. 26] was used. The diamond pyramid shaped tip indents an impression on the surface of the material. The force of the tip and the duration of its application are predetermined.

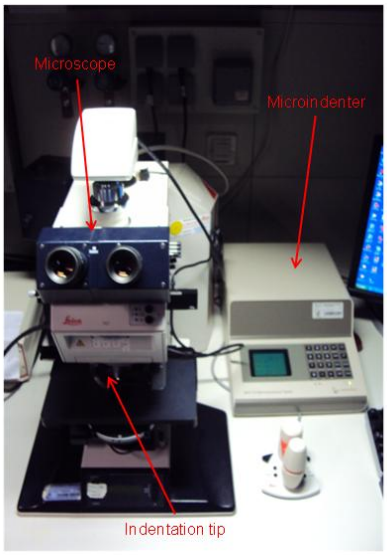

Fig. 26: Microindenter.

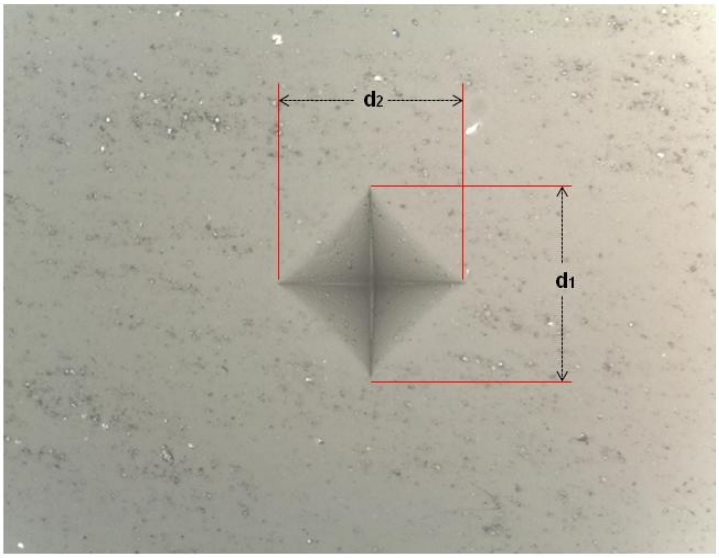

Fig. 27: An indentation on the surface of a composite specimen: d_1 is the length of the vertical line and d_2 of the horizontal line.

Each indentation is visualized by a microscope lens. In the acquired picture, two lines are depicted, one vertical and one horizontal, which correspond to the pyramid tip. The lengths of these lines, determined as d_1 and d_2 respectively, are indicative of the depth of the indentation achieved, making it possible to determine the HV of the material [Fig. 27]. The storage conditions the specimens were subjected to and the measurement setup are given in Figure 28 and Table 11.

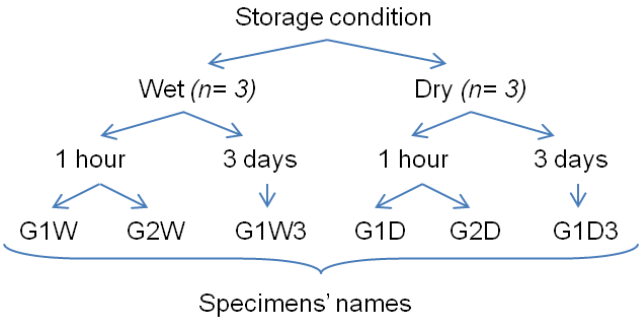

Fig. 28: Specimens' names and storage.

Force	4 N
Duration of application	5 sec
Slope	0.9
Number of indentations/ specimen	12
Lens magnification	20*

Table 11: Measurement configuration.

In order to calculate the HV, Equation 3 was used [123]:

$$HV = \frac{0.01891 \cdot F}{d^2} \qquad \text{[Eq. 3]}$$

where F= Force (N)

d= (d_1+d_2)/2 (mm)

A total of 6 Grandio specimens were produced in the same way as the specimens used for the ESPI measurements [Fig. 28, Table 11].

The HV for each specimen was calculated as the mean value of the HV acquired from 12 indentations.

Statistical significance was tested by a 2-Way ANOVA.

5.2.7. Investigation of the magnitude and influence of water absorption

Water absorption increases the weight of the specimens. Consequently, measuring the weight of the specimens following particular immersion times would provide useful information about the extent of water uptake.

For this purpose two sets of weighing measurements were conducted for a series of specimens by using a high-precision weigh machine in a range of 0.1E^{-04} g [Fig. 29].

Fig. 29: Weigh precision stage.

5.2.7.1. Investigation of the water absorption procedure of composites over time

The investigation of water absorption involved the measurement of the weight of 10 Grandio specimens (marked G1 to G10) subjected to various conditions – stored dry or wet or heated to 37°C- throughout a time span of 2 months [Fig. 30].

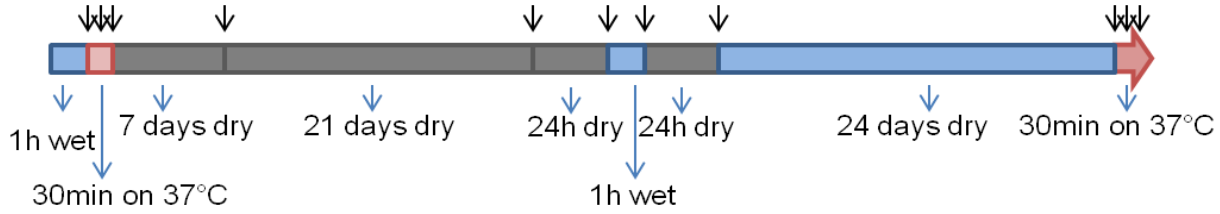

Fig. 30: Storage conditions of the specimens. The black arrows represent the measurements of weight for each specimen.

The actual weight of each specimen after each storage condition was subtracted from its original weight right after polymerization, which served as the control weight. The percentage differences of the weigh between the two conditions were calculated. These percentage differences signified whether the material had gained or lost weight, making comparisons possible.

5.2.7.2. Investigation of the relationship between water absorption, post-polymerization and heating

Differences in the weight may be used to reveal information concerning the relationship between water absorption and post-polymerization.

For this purpose, 24 Grandio specimens were divided into 4 groups (n=6 each). Each group was subjected to a different set of storage conditions, the specimens being weighed at particular times [Fig. 31].

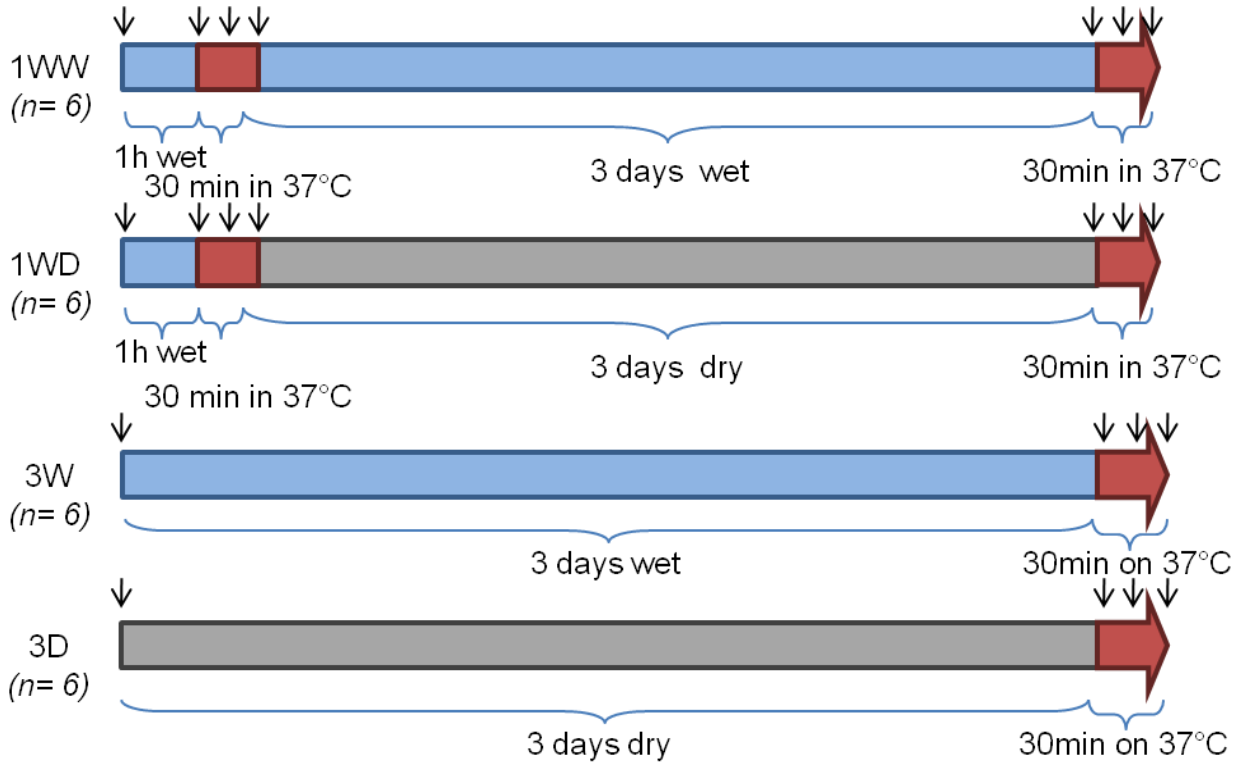

Fig. 31: Specimen groups and storage conditions. The black arrows represent time points of the weigh measurements.

Comparisons were made between the weight averages of each group.

6. Results

The investigation concerning the application of the ESPI technique is presented, followed by a description of the results of the measurements for assessing the dimensional behavior of the composite.

6.1. Evaluation of the ESPI and protocol definition

The ability to detect dimensional changes of the composite resulting from heat transfer was first investigated in the range of the ESPI resolution. The efficiency of the proposed setup for this type of measurements was examined using this procedure

6.1.1. Evaluation of the ESPI technique

The strain values acquired for the two Admira specimens are shown in Fig. 32. For this particular measurement, and unlike the rest of the measurements, no summing of the values was performed. Each value shown is the actual strain value in percentage recorded at each measurement step and not the shrinkage that took place up until that step.

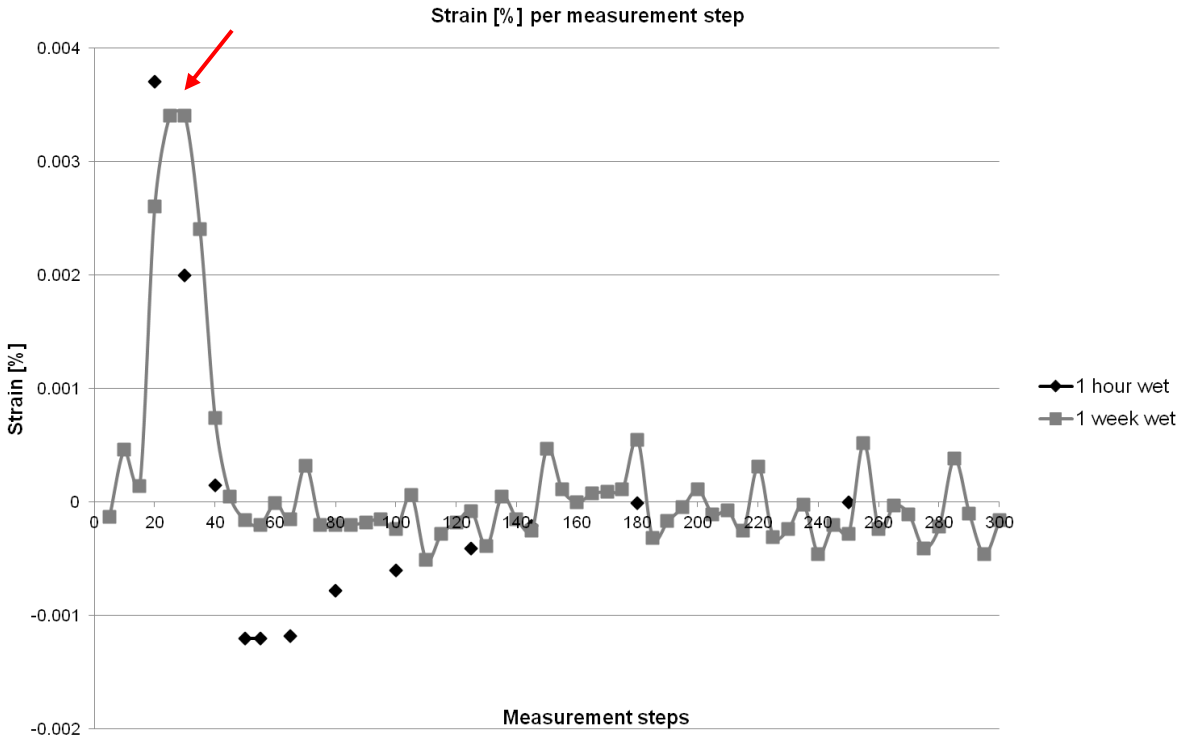

Fig. 32: Strain values in percentage acquired at each measurement step. The red arrow shows the highest strain value acquired, which corresponds to the step when the temperature reached 44°C.

As demonstrated, both specimens exhibited positive strain values, increasing during the first 30 steps of the measurement. The peak on the graph (red arrow in Fig. 32)) coincides with step No. 30 for both specimens. This marks the end of the time period when the specimens were heated from 26°C to 44°C, during which the material expanded.

Following initial heating and after the temperature was stabilized at 44°C, the strain values decreased rapidly. After step No. 40 negative strain values are mainly seen showing that shrinkage takes place. For the one week wet specimen (marked gray in Fig. 32), after step No.160 both positive and negative strains are acquired, which means that overall, the material is reaching a relatively stable dimensional state. A smoother transition to a stable state is observed for the 1 h wet specimen (marked black in Fig. 32).

The smallest strain value percentage acquired was $-9E^{-05}$%, corresponding to step No. 14 for the specimen stored wet for 7 days. Since the specimen diameter was 15 mm,

Equation 2 can be used to demonstrate that during that step, the specimen shrank by 13. 5nm.

The 1 hour wet stored specimen exhibited a more dramatic behavior in comparison to the 1 week wet stored specimen during this heating procedure. Not only did it expand more, but it also shrank more and continued shrinking at a higher rate than the 1 week stored specimen. In addition, it reached a stable state in less time.

6.1.2. Establishment of the ESPI measurement protocol

In order to quantify the deformation of the material over time, it is essential to have stable, controlled temperatures. Consequently a rapid, initial warming of the specimens was introduced (reaching 37°C in 2 min). These first 2 min of recording correspond to an initial expansion phase, as seen from the positive strain values in Fig. 32. This expansion phase is outside the scope of this study and will therefore be omitted as explained in Appendix B2.

The evaluation procedure described in Chapter 5.2.1.3 was followed, summing up the strain values in percentages in order to investigate the progress of the deformation over time.

These total deformation values in percentages acquired within the framework of establishing the measurement protocol are shown in Fig. 33.

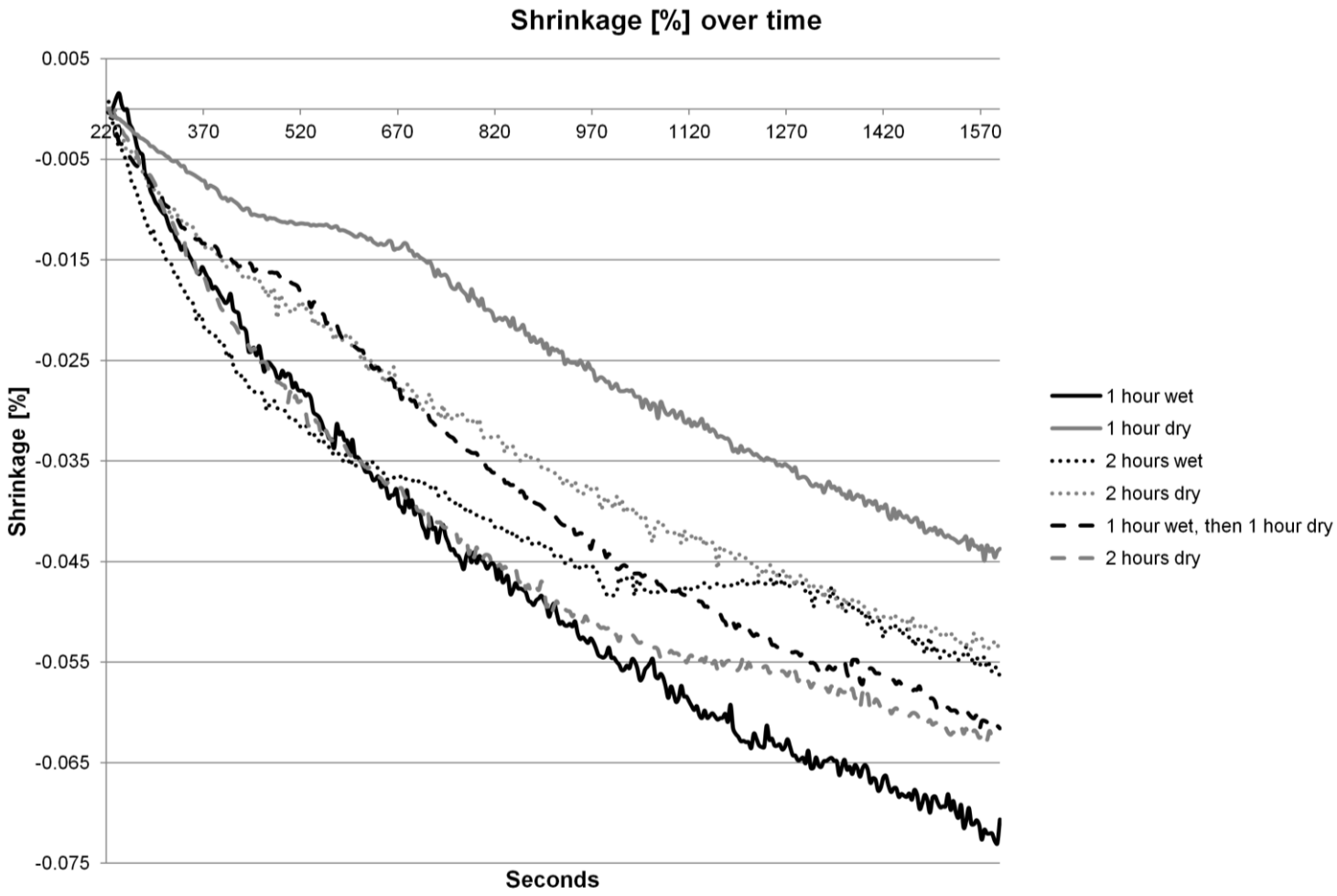

Fig. 33: Shrinkage [%] values per measurement step. Gray color stands for dry storage and black for wet. Specimens belonging to the same group are shown with the same line style.

The slopes on this particular measurement start from 220 sec after the start of the experiment, which corresponds to the time when the temperature was stabilized. The duration of this measurement was 1380 sec.

The total deformation exhibited for the duration of the measurement is given in Table 9.

	A1W	A1D	A2W	A2D	A3W	A3D
Total deformation [%]	-0.07%	-0.04%	-0.06%	-0.05%	-0.06%	-0.06%

Table 9: Total deformation [%] values for each specimen for the duration of the measurement (1380 sec).

The negative deformation values found in all the steps demonstrate that given the conditions of measurement, all specimens were gradually shrinking.

None of the specimens reached a stable state up to a time of 1380 sec at 37°C. The greatest shrinkage, 0.07%, was exhibited by the specimen stored wet for 1 hour. Inside each group of specimens, the wet specimen always shrank more than the dry one.

Nevertheless, no remarkable differences were found in the shrinkage between the three groups, implying that the different storage durations of each group didn’t play an important role, at least within the 2 hours of the total experimental storage duration.

6.2. Investigation of the dimensional behavior by using the ESPI

In this chapter, the results of the impact of the storage medium and of the storage duration on the dimensional behavior of the material will be presented.

6.2.1. Investigation of the impact of water and air storage on the dimensional behavior of the composite

The cumulative shrinkage values of each specimen, after following the evaluation procedure described in Chapter 5.2.1.3, are given in Fig. 34. The values presented are in shrinkage percentages.

The specimens were grouped according to the storage conditions in 1 hour wet specimens, 1 hour dry specimens, 72 hours wet specimens and 72 hours dry specimens. The acquired mean total shrinkage percentage values for each group with their standard deviations are given in Table 11.

	1 hour wet	1 hour dry	72 hours wet	72 hours dry
Mean deformation [%]	-0.042%	-0.031%	-0.021%	-0.014%
Standard deviation	0.010	0.008	0.020	0.004

Table 11: Mean total shrinkage percentage values per group, with standard deviations.

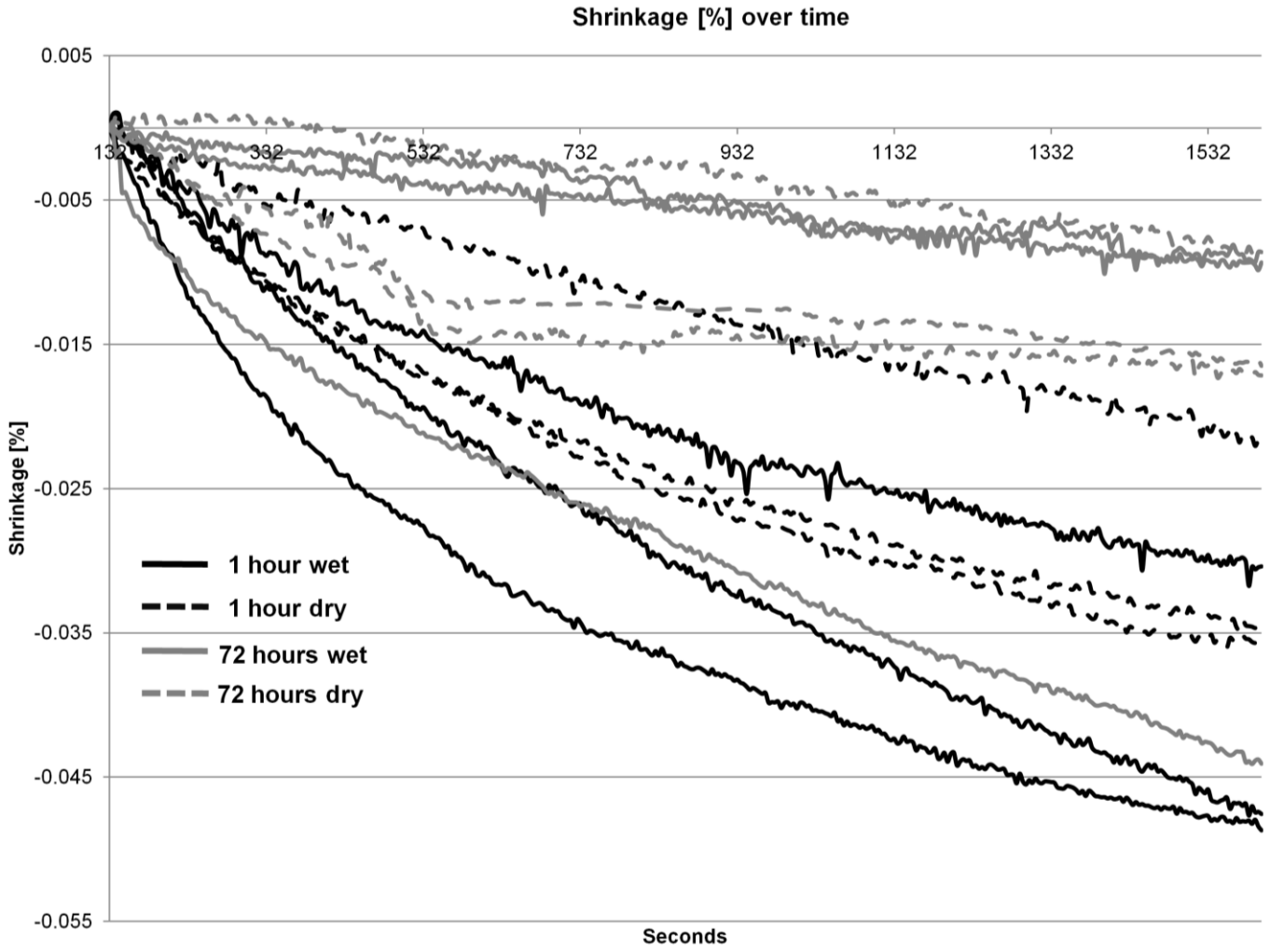

Fig. 34: Shrinkage percentage per measurement step for wet and dry specimens. Black color indicates specimens stored for 1 hour, gray for the specimens stored for 72 hours. Constant lines stand for the wet specimens, dotted lines for the dry.

All specimens shrank during the measurement. These shrinkage percentage values of each group are shown in Fig. 35.

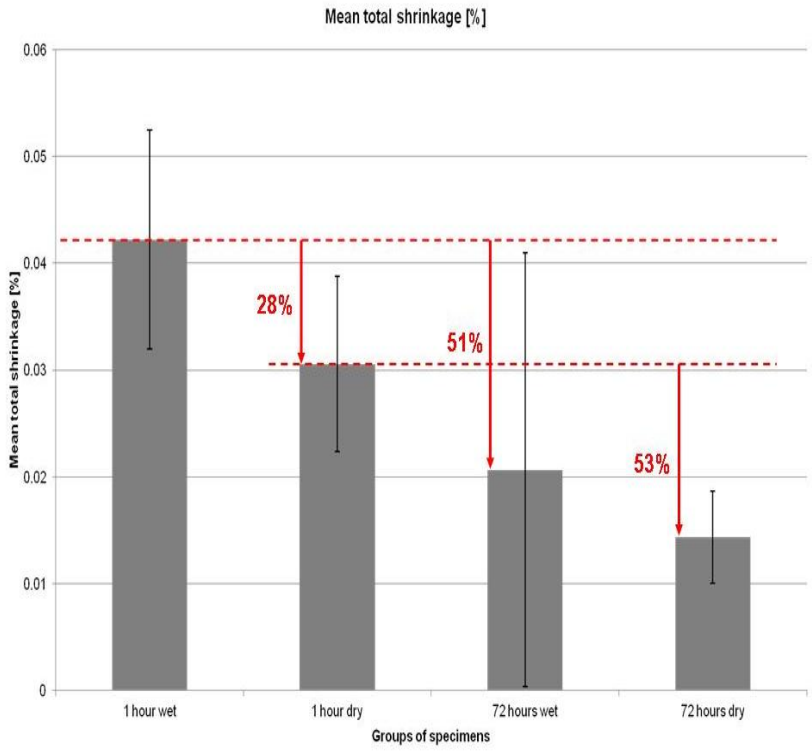

Fig. 35: Absolute mean shrinkage percentage values per group of specimens.

The 1 hour wet-stored specimens shrank the most, followed by the 1 hour dry-stored specimens. The 72 hours wet stored specimens shrank slightly more than the 72 hours dry stored ones

In particular, the 1 hour wet specimens exhibited 28% larger shrinkage than the 1 hour dry specimens. The 72 hours dry specimens shrank 53% less than the 1 hour dry specimens and the 72 hours wet specimens 51% less than the 1 hour wet specimens.

To better understand the dynamics of shrinkage, the deformation was divided into three distinct time frames, of 8min each [Fig. 36].

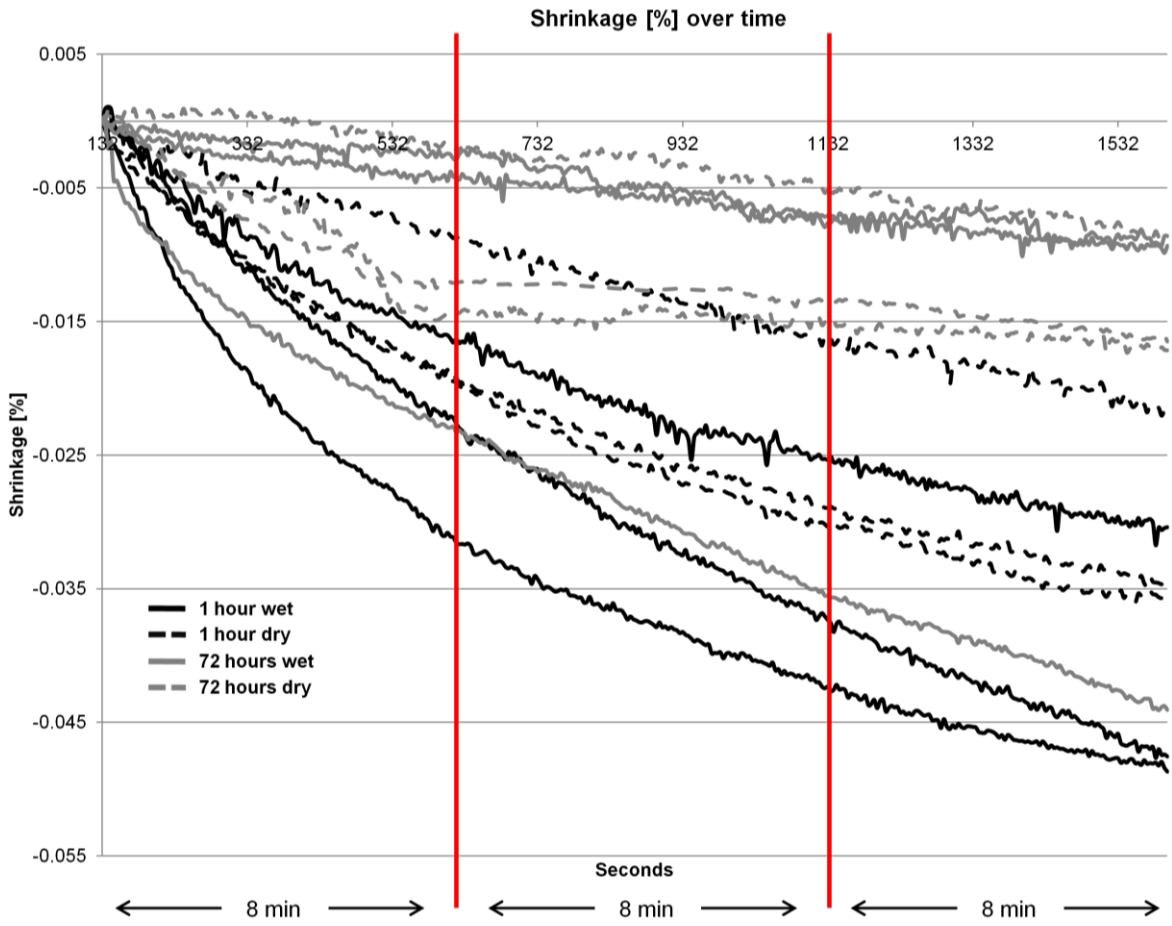

Fig. 36: Division of the measurements duration into 8 min intervals. Black color corresponds to 1 hour storage, gray to 72 hours storage. Constant lines correspond to wet storage and broken lines to dry storage.

In the first time frame, the slopes of the specimens are greater and most of the shrinkage takes place rapidly. During the two following phases the procedure is gradually slowed down.

The visualization of shrinkage occurring during each particular time frame is given in Fig. 37.

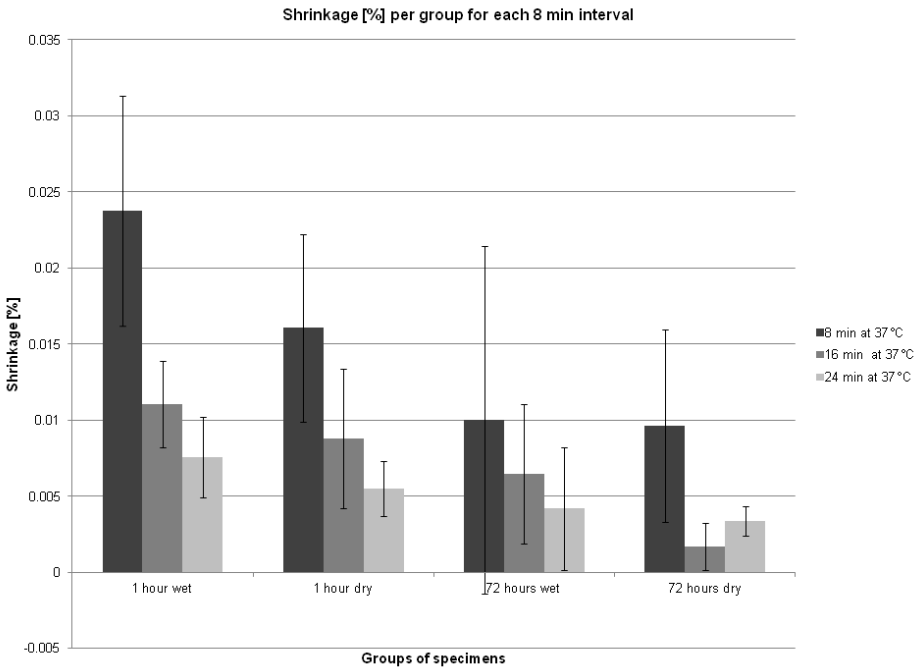

Fig. 37: Shrinkage percentage values of each group of specimens during each 8min interval of the measurement.

The highest rate in shrinkage percentage was exhibited by all specimens during the first 8 min at 37°C, gradually slowing down.

Examining the values in 8 min intervals, the 1 hour wet specimens shrank 23% more that the 1 hour dry specimens, in the first 8 min of measurement, whereas the 72 hours wet specimens only shrank 4% more than the 72 hours dry specimens in the same time period. The smallest differences in the shrinkage percentage values between the intervals were shown by the 72 hours wet specimens. The smallest shrinkage percentage was found after the 16 min interval for the 72 hours dry specimens.

In this measurement, two conditions were potentially influencing the deformation of the material at 37°C: the storage medium and the storage time. In order to investigate the impact of each of these two conditions, the specimens were grouped according to Table 12 and the total shrinkage value in percentage for each group was calculated [Fig. 38].

Wet	**Dry**	**1 hour**	**72 hours**
wet 1 h+ wet 72 h	dry 1 h+ dry 72 h	wet 1 h+ dry 1 h	wet 72 h+ dry 72 h

Table 12: Groups of specimens according to storage conditions.

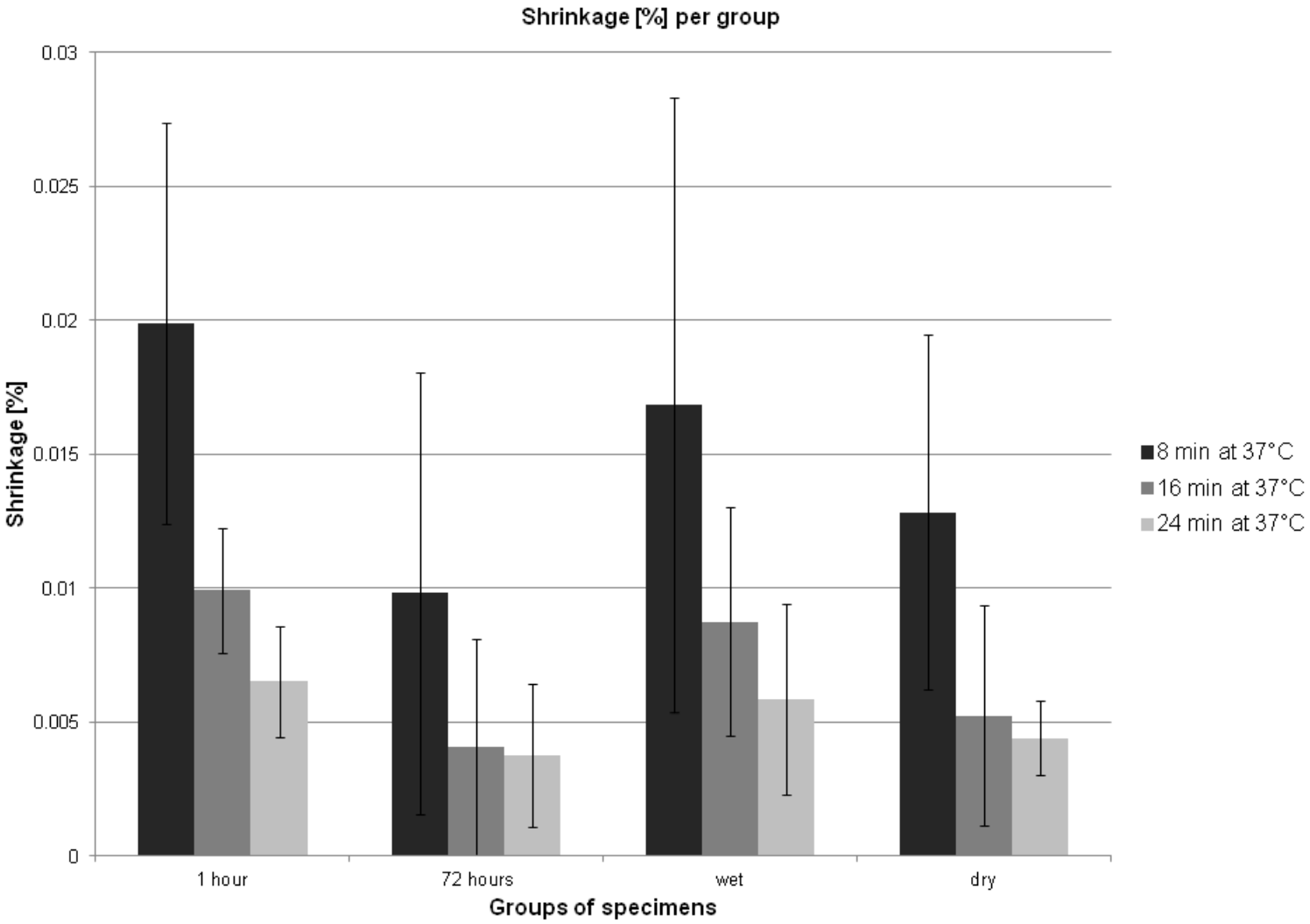

Graph 38: Shrinkage percentage per group of specimens during each 8min interval.

No difference can be seen for any time interval between the grouped wet versus the grouped dry specimens. The grouped 1 hour specimens shrank remarkably more in comparison with the grouped 72 hours specimens.

Indeed, the statistical analysis (2-way ANOVA) demonstrated that the grouped 1 hour stored specimens shrank more in a statistically significant way than the grouped 72 hours stored specimens, regardless of the storage medium, for the duration of the measurement ($p < 0.05$).

No statistically significant difference in shrinkage percentage was found when comparing the grouped wet versus the grouped dry specimens for the duration of the measurement ($p > 0.05$).

6.2.2. Investigation of the existence of water inside dry- stored specimens

The total percentages of shrinkage acquired from these measurements for each group of specimens are given in Fig. 39. The slopes start from the 208th sec of measurement, when the temperature reached the designated 37°C.

The mean total shrinkage percentage values of the specimens stored in ambient conditions or in vacuum are given in Table 13.

	1h stored in vacuum	1h stored in ambient conditions
Mean total shrinkage [%]	0.04	0.03
Standard deviation	0.0004	0.0005

Table 13: Mean total shrinkages in percentage of specimens grouped according to the storage conditions, with standard deviations.

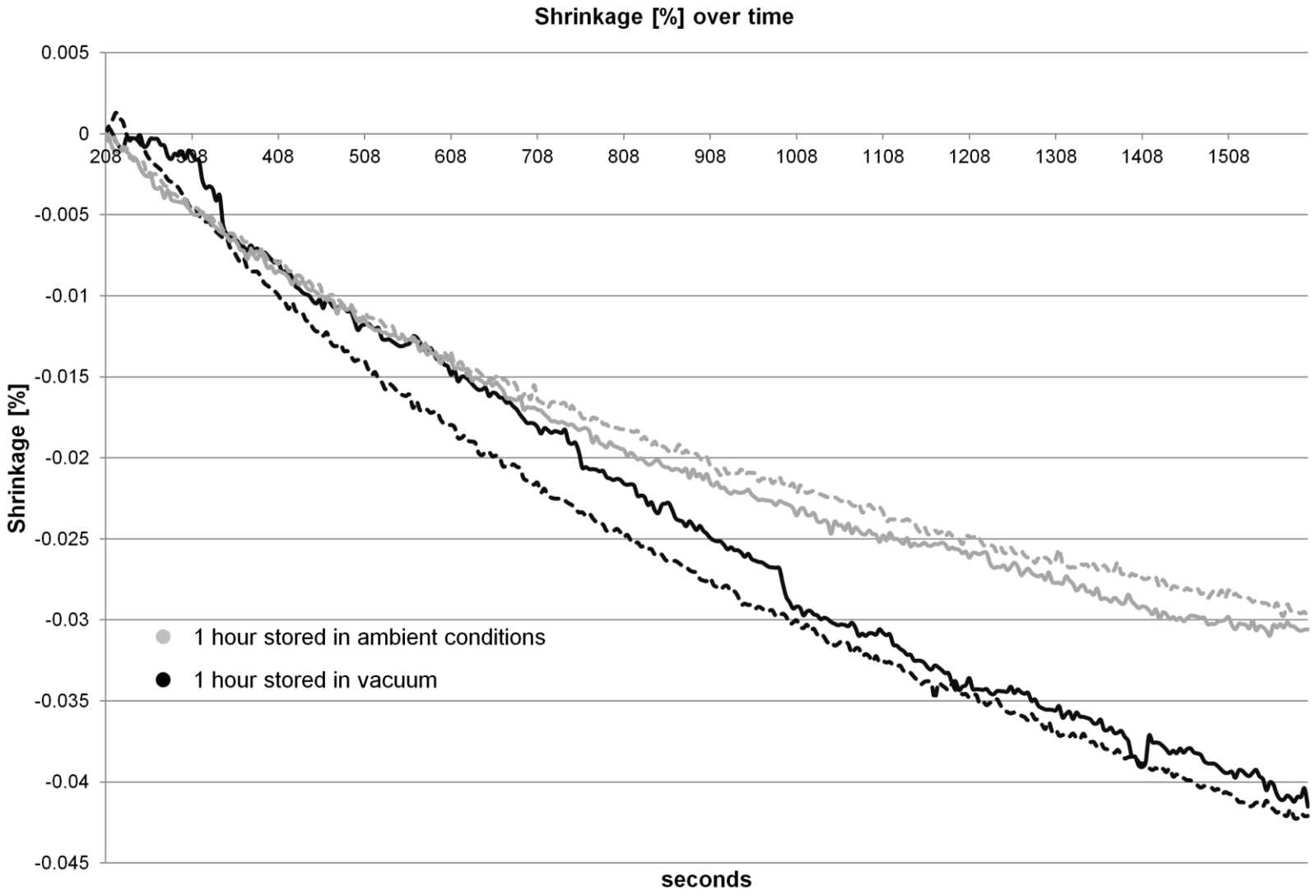

Fig. 39: Shrinkage percentage values of the two specimens stored dry for 1 hour in vacuum (black slopes) versus the values of the specimens stored dry for 1 hour in ambient conditions (gray slopes).

The specimens stored in vacuum shrank 28% more than the specimens stored in ambient conditions, for the duration of the measurement.

The statistical analysis (Student's t-test) showed that the shrinkage of the specimens stored in vacuum was different from the shrinkage of the specimens stored in ambient conditions, in a statistically significant way ($p \sim 0.01$).

6.2.3. Investigation of the impact of post-polymerization on the dimensional behavior of the composite

Having examined the influence of the storage medium and duration, the influence of the post-polymerization was investigated. The point of interest was set on the storage duration and not the storage medium, so only wet specimens stored for different storage durations were measured.

The cumulative shrinkage values in percentage for every specimen are shown in Appendix C. Due to the large amount of information presented, it is difficult to evaluate the behavior of the different groups of specimens in this Figure. Thus, the mean value of shrinkage exhibited in each step from all specimens inside each group was calculated, concentrating the different slopes of the specimens into one slope per group [Fig. 40].

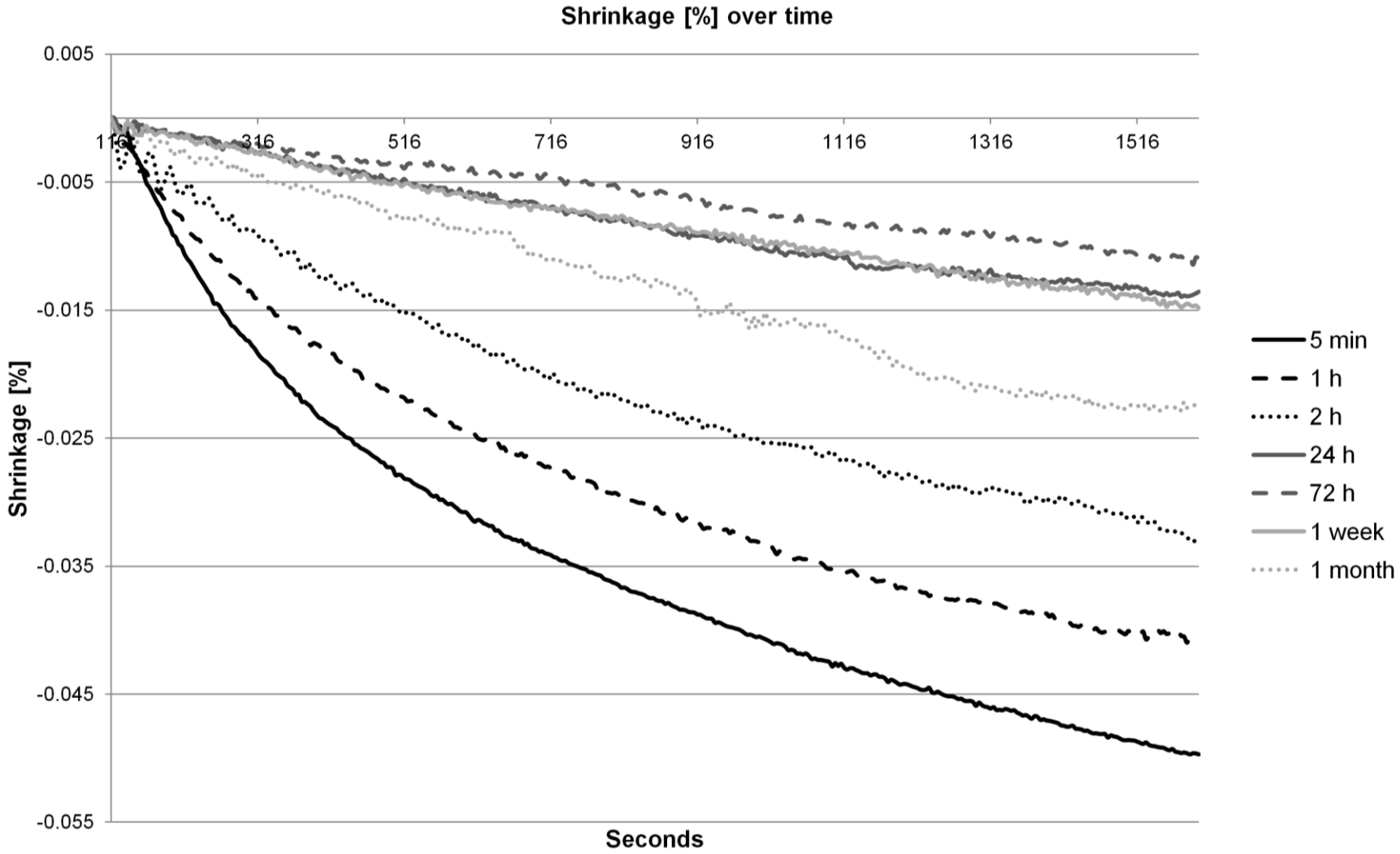

Fig. 40: Shrinkage percentage values through time for each group of specimens, after calculating the mean shrinkage values of the specimens of every group during every measurement step.

As demonstrated in Fig. 40, all groups of specimens shrank during the measurement.

The group with the largest mean shrinkage percentage, 0.0497%, was the 5 min stored specimens. Moreover, they were the ones that appeared to be shrinking most dramatically, as the slopes recorded from them were the steepest.

The second-highest shrinkage percentage was found for the 1 hour stored specimens, followed by the 2 hours stored specimens; with equal slope value reductions.

From the 24 hours stored specimens onwards, the shrinkage values acquired were lower in comparison to the previous specimens. In particular, the smallest shrinkage value, which was 0.011%, was recorded from the specimens stored 72 hours. These specimens also exhibited the smallest slopes. The slope values for the specimens stored between 24 hours and 72 hours were also found to be comparable to each other.

The specimens stored wet for 1 week shrank more than the specimens stored 72 hours, whereas the specimens stored for 1 month shrank remarkably more than all the long-stored specimens, with shrinkage values comparable to the ones of the specimens stored for up to 24 hours.

Although the shrinkage decreases gradually until 72 hours of storage, no group reached a stable state in the course of the measurement but continued shrinking until the end of it.

The mean total shrinkage values in percentage exhibited from each group during this measurement are presented with their standard deviations in Table 14 and Fig. 41.

A more detailed depiction of Fig. 41 is Fig. 42, where the build-up of shrinkage every 5 min of measurement can be seen for each storage duration.

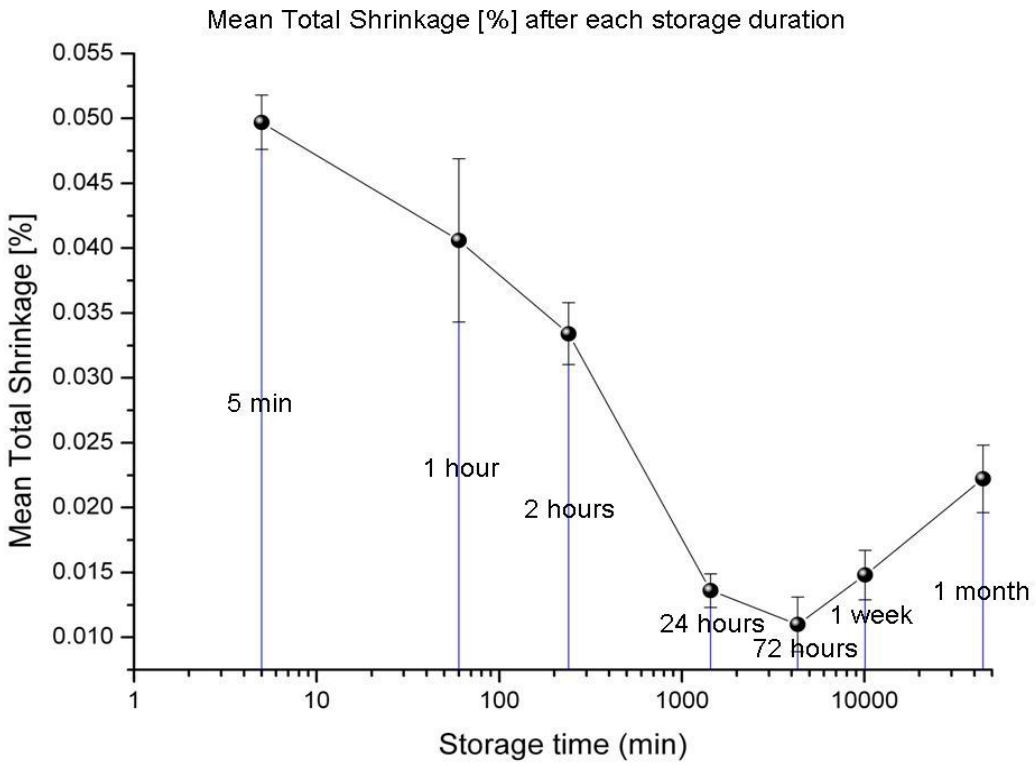

Fig. 41: Mean total shrinkage percentage after each wet storage period.

	5 min	1 hour	2 hours	24 hours	72 hours	1 week	1 month
Mean total shrinkage [%]	0.0497	0.0406	0.0334	0.0136	0.011	0.0148	0.0222
Standard deviation	0.0021	0.0063	0.0024	0.0013	0.0021	0.0019	0.0026

Table 14: Mean total shrinkage percentage values of all groups of specimens with standard deviations.

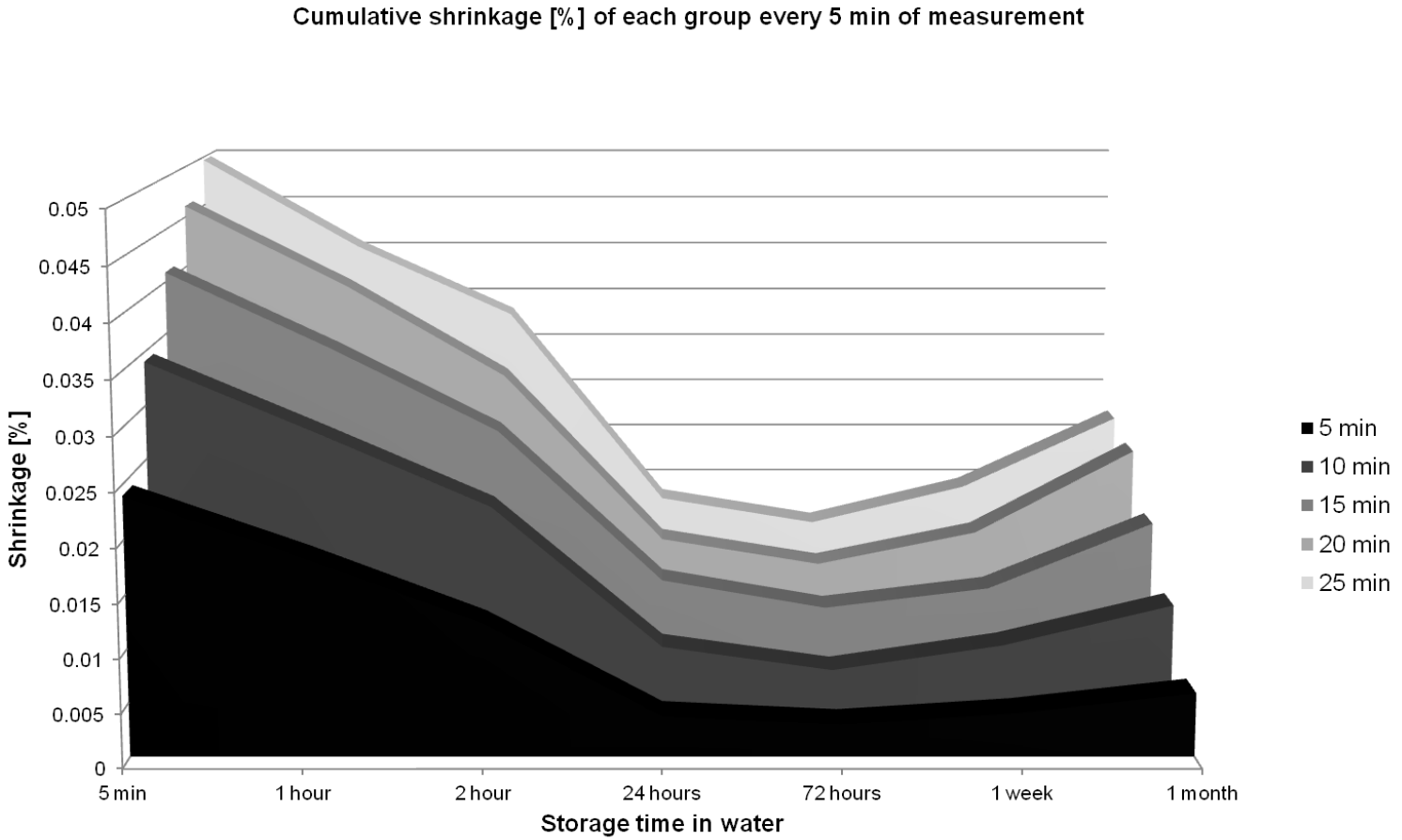

Fig. 42: Cumulative shrinkage trend for each storage period as it evolved during every 5 min of measurement.

In Fig. 41 the great variation of the shrinkage between the groups is pronounced. The shrinkage values decline for storage durations up until 72 hours. For storages longer than 72 hours, the shrinkage values start increasing again. The largest shrinkage takes place in the first 10 min of measurement, gradually declining until the end.

Statistical analysis (One Way ANOVA) between the shrinkage percentage values of the groups demonstrated the following significant differences ($p \leq 0.05$):

- The 5min group was different in a significant way to all the rest of the groups, except the 1 hour group.
- The 1 hour group was different to all the rest of the groups, except the 5min and the 2 hours group, where no difference was found.
- The 2 hours group was different to all the rest of the groups, except the 1 hour group.
- No difference was found between the 24 hours group, the 72 hours group and the 1 week group.
- The 72 hours group was different to the 1 month group.
- The 1 month group was different to the 5 min group, the 1 hour group, the 2 hours group and the 72 hours group. No difference was found between the 1 month group and the 24 hours group and 1 week group.

A better visualization of the development of shrinkage during the measurements was achieved after grouping the measurement into 8 min intervals and calculating the shrinkage percentage that took place during each interval, as described above. The total shrinkage percentage measured at the end of each interval for each group is given in Fig. 43.

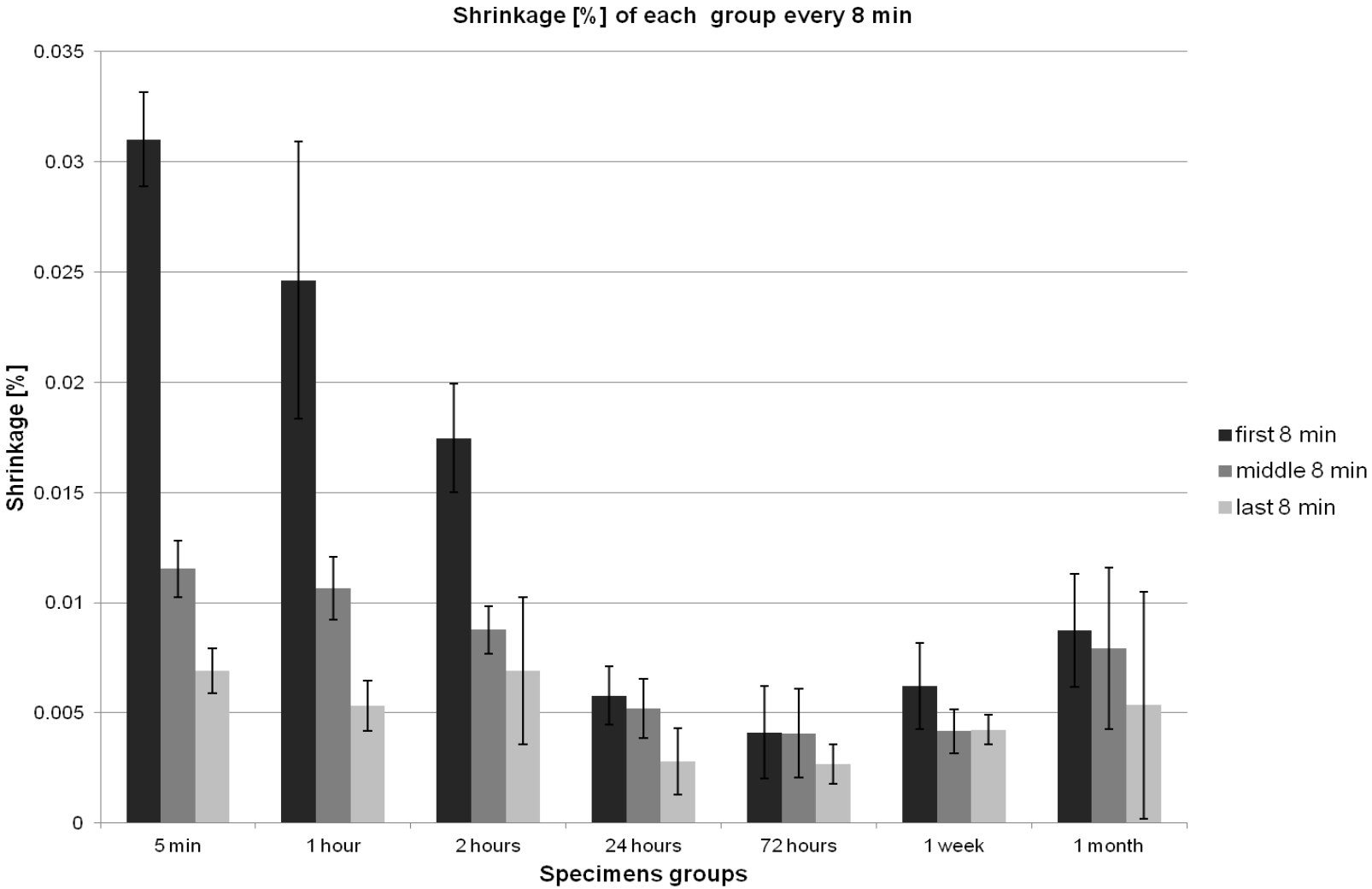

Fig. 43: Shrinkage percentage for each group at 8 min intervals.

The greatest shrinkage was exhibited in the first 8 min of heating in all groups and especially for the short-period storages of up to 2 hours. These first 8 min of measurement is the time when the greatest slope values are seen, demonstrating that it is then that the greatest changes take place, regardless of the storage duration.

In the second interval, the shrinkage gradually slows down as is also the case for the later periods, when the specimens seem to be reaching a relatively more stable state.

For the long-period storages, the differences in the shrinkage values between the intervals were smaller. Nevertheless, no group reached a stable state over the duration of the measurement.

6.3. Control of the specimens' production reliability

The HV values acquired for each specimen are given in Table 15 and Fig. 44.

	G1W	G2W	G1W3	G1D	G2D	G1D3
HV	107.3	113.3	105.9	106.7	106.2	107.2
Standard Deviation	2.105	3.287	3.318	5.433	2.130	3.319

Table 15: HV values of each specimen tested.

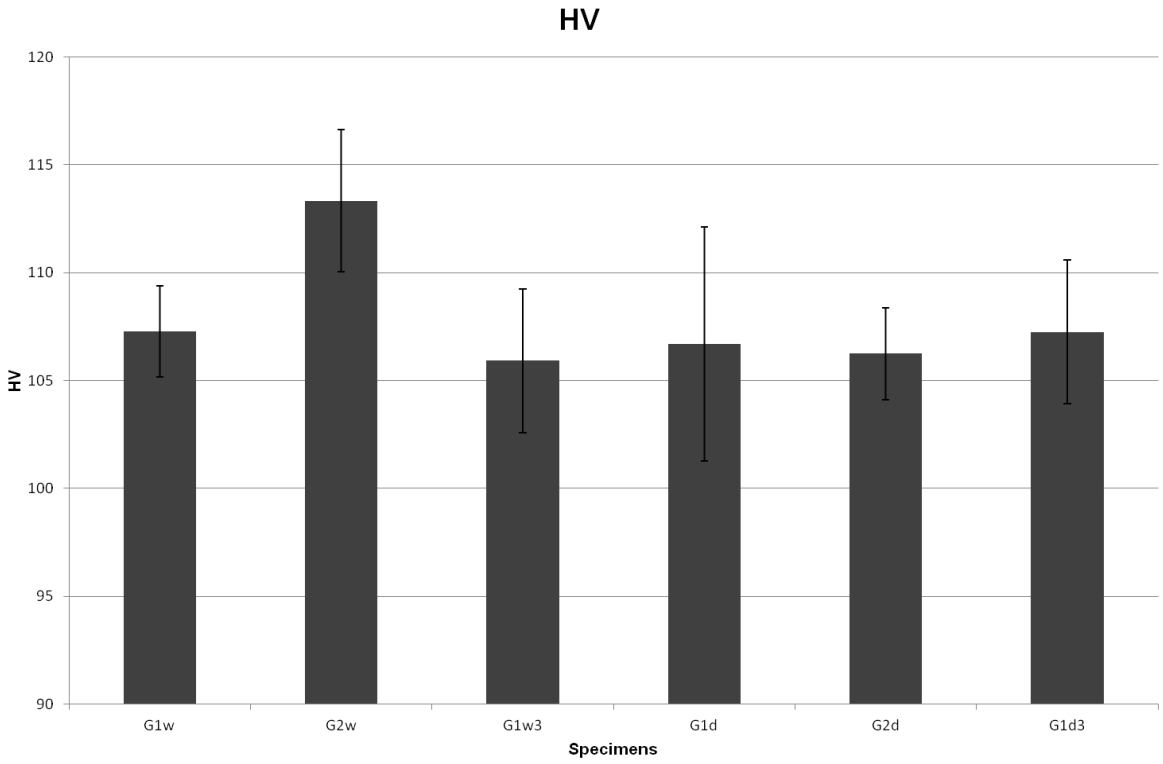

Fig. 44: HV values per specimen.

No statistically significant difference was found when comparing the wet-stored specimens versus the dry-stored specimens, nor when comparing the 1 hour stored specimens versus the 72 hours stored specimens ($p > 0.05$).

6.4. Investigation of the magnitude and influence of water absorption

In this chapter, the results of the investigation of the progression of water absorption through weight measurements, as well as its relationship with post-polymerization and heating will be presented.

6.4.1. Investigation of water absorption of composites through time

The mean difference percentages in weight of the specimens between their original mean weight just after polymerization and their mean weight after each storage condition are given in Table 16. Note that in this measurement, for the same specimens, one storage condition followed the other in continuity. Therefore, Table 17 is a sequel of Table 16 for storages longer than 22 days.

During the first hour after polymerization, the weight of the material was stable, even though the specimens were stored in water. However, they lost weight when heated for 30 min up to 37°C.

The material continued losing weight at a slow rate during a period of approximately 4 weeks, during which it was stored dry in ambient conditions. This phenomenon was reversed after 1 hour storage in water, at the end of these 4 weeks; however the gain in weight caused by this condition was not enough to compensate for the loss of weight that had already taken place until then.

At the end of this 4 week dry- storage period, the total weight loss of the material was 0.067%. Afterwards, the specimens were stored in water for 24 days. This long storage in water resulted in a remarkable gain in weight (0.412%).

The final heating procedure stimulated again a gradual slight loss of weight, as was also observed during the first heating cycle.

	1hour wet	15min on 37°C	27min on 37°C	7 days dry	21 days dry	22 days dry
Mean weight difference [%]	-0.002%	-0.028%	-0.034%	-0.042%	-0.054%	-0.062%
Standard deviation	0.055	0.055	0.055	0.055	0.055	0.055

Table 16: Mean weight difference of the specimens measured after each storage condition, for storages up to 22 days.

22 days +	1 hour wet	1 day dry	24 days wet	15min on 37°	27min on 37°C
Mean weight difference [%]	-0.041%	-0.067%	0.345%	0.296%	0.282%
Standard deviation	0.055	0.055	0.055	0.055	0.055

Table 17: Mean weight difference of the same specimens for storages longer than the initial 22 days as a sequel of Table 16.

6.4.2. Investigation of the relationship between water absorption, post-polymerization and heating

The storage conditions in this second weight measurement were arranged in such a way that potentially different influences of water sorption and post-polymerization procedures on the specimens could be detected. This would be possible by comparing the differences in weight between the various groups.

As explained in Chapter 5.7.2, the first group (1ww) was stored wet for 1 h, then heated to 37°C for 30 min, then stored wet for 72 h and then heated again to 37°C for 30 min. The second group (1wd) was stored wet for 1 h, heated to 37°C for 30 min, then stored dry for 72 h and then heated again to 37°C for 30 min. The third group (3d) was stored dry for 72 hours and then heated to 37°C for 30 min and the fourth group (3w) was stored wet for 72 hours and then heated to 37°C for 30 min.

For all groups, each storage condition followed the other without interruption. The weight percentage differences occurring after each storage condition were calculated in comparison to the initial weight of the specimen [Table 17]. The results are presented in Fig. 45, Fig. 46 and Fig. 47.

	1 hour wet	15 min on 37°C	30 min on 37°C	72 hours wet	72 hours dry	15 min on 37°C	30 min on 37°C
1ww	0.007%	-0.020%	-0.019%	0.224%	-	0.178%	0.168%
1wd	0.018%	-0.019%	-0.019%	-	0.04%	0.023%	0.022%
3d	-	-	-	-	0.07%	0.058%	0.054%
3w	-	-	-	0.243%	-	0.197%	0.192%

Table 17: Weight percentage difference of the specimens between their original weight and their weight after each storage condition.

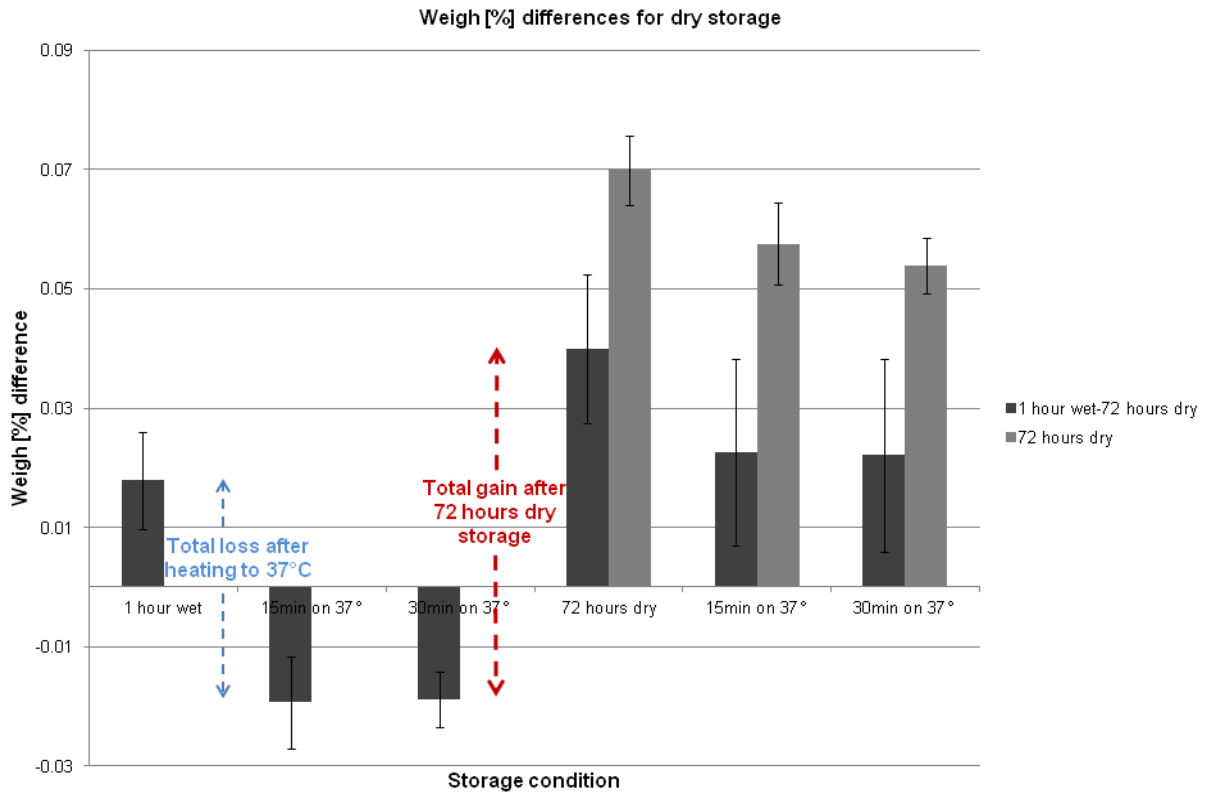

Fig. 45: Weigh percentage differences for the groups of specimens stored dry. The blue arrows show the total loss of weight after 15 min at 37°C. The red arrows indicate the total weight gain that took place in the 1h wet-72h dry group after 72 hours' dry storage.

In Fig. 45 the first column shows that after 1 hour of storage in water, the specimens gained weight. Since what is shown is the difference in weight after each storage condition in comparison to the initial weight of the specimens, it is shown that after the first heating cycle the specimens lost approximately double the weight they had initially gained from the wet storage (blue arrows in Fig. 45).

Both groups of specimens stored dry gained weight after 72 hours' dry storage. For the reason described above, the initially heated specimens also gained the weight percentage they had lost, plus the absolute gain they showed, as the red arrows in Fig. 45 indicate. Additionally, all specimens lost weight during the final heating; however this loss did not bring the weight back to its initial value.

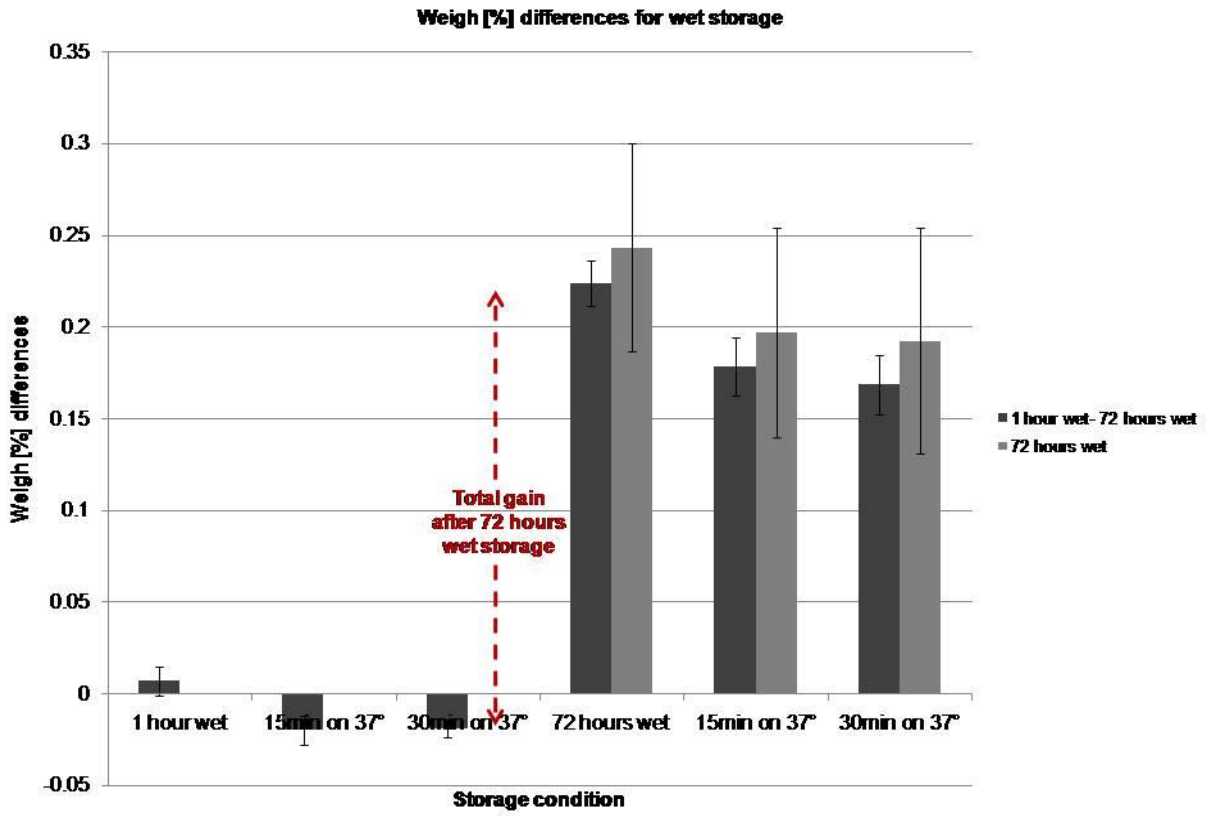

Fig. 46: Weigh percentage differences for the specimens stored wet. The red arrows indicate the total weight gain after 72 hours' wet storage for the specimens that were subjected to the initial heating.

The same behavior of the dry-stored specimens as that seen in Fig. 45 can be seen in Fig. 46 for the wet- stored specimens. After 1 h wet storage, the specimens gained weight that they lost afterwards during the initial heating. This first heating cycle did not affect the gain in weight thereafter, since the total weight gain after 72 h wet storage is the same for both groups, regardless of whether the specimens were initially heated or not.

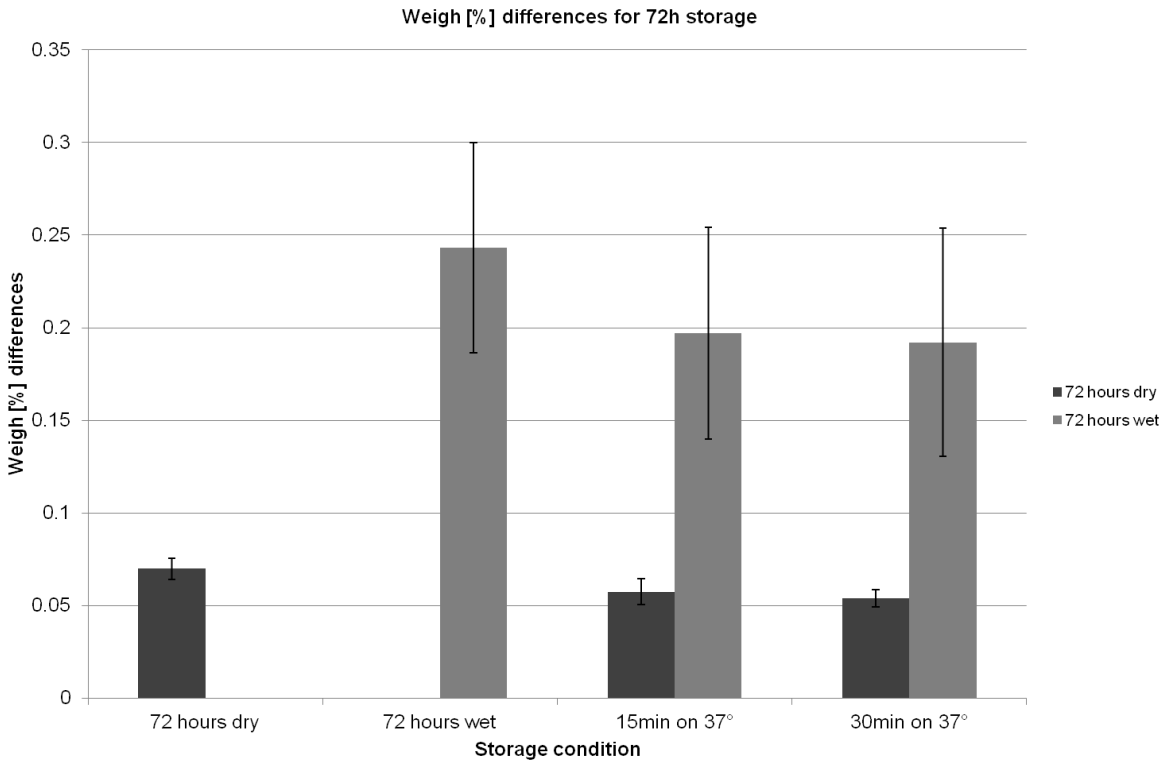

Fig. 47: Weigh percentage differences for the groups of specimens stored for 72 hours.

For the specimens that were not subjected to an initial heating cycle, Fig. 47 shows that they all gained weight after 72 h storage. The storage medium only influenced the magnitude of the gain: the wet- stored specimens gained 0.17% more weight than the dry- stored ones.

Furthermore, all specimens from both groups gradually lost weight when they were heated up to 37°C, after the 72 h storage, for the duration of the rising of the temperature.

7 Discussion

7.1 ESPI potential and restrictions

In order to be able to conduct comparable experiments to investigate the potential differences in the dimensional changes occurring as a result of various storage conditions, a measurement protocol had to be established. The aperture and the focus of the lens were optimized so that they would be in accordance with the distance of the specimen from the camera. The laser intensity had to be arranged in such a way that thermal fluctuations of the lasers would be avoided. These fluctuations can provoke mode hoping, a phenomenon during which the wavelength of the lasers change in such a way that it influences the results [124, 125]. Whenever mode hoping takes place, the measurement cannot be properly phase-unwrapped and quantified. As mentioned in Chapter 5.2.1.5, this problem also occurs when there are distortions from external vibrations.

The inability to phase unwrap results in defective steps that can be recognized as such by a distinctive appearance of the phase map: in the image recorded by ESPI, a big, sudden change is found on the surface displacement slope. The actual image of a defective step acquired by ESPI indicates whether the equivalent deformation slope should be taken into account as a reliable result or not. In Figs. 48 (a) and (b), the deformation images acquired from two reliable steps are given. The slopes are quantifiable and precise, showing the direction of the deformation as well as its magnitude.

In Fig. 48 (c) by contrast, an image acquired from a defective step is shown. A deformation of this kind could not take place on the surface of a single material such as a composite. Furthermore, for these experiments the production of specimens was proved to be reliable as a method since the Vickers hardness values acquired from the specimens (Chapter 6.3) were comparable to each other and also consistent with the values found for this material in the literature [126]. Therefore, the appearance of a slope of a step as the one shown in Fig. 48 (c) does not represent a finding of scientific interest but rather points to an interruption of the ESPI procedure, which could be mode

hopping or one of the factors described in Chapter 5.2.1.5. This drawback is connected with the advantage of measuring deformations of this small magnitude with ESPI.

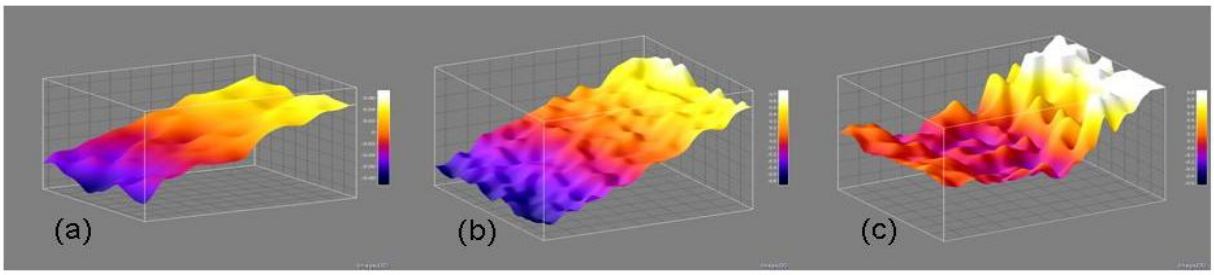

Fig. 48: Deformation slopes acquired from three different measurement steps. (a) and (b) are images of reliable slopes providing actual strain values for the equivalent steps. (c) is an image of an artefact since no single material could present a slope of this kind. Therefore, the strain value acquired from (c) cannot be taken into account as valid.

During these measurements, whenever ‘defective’ steps like this were found, the strain values acquired from them were replaced by the mean value of the strain of their previous 5 steps and their following 5 steps. In Fig. 49, for example, the initial slopes of specimens measured within the framework of investigations of the storage medium (Chapter 6.2.1) are given. The slope marked red on this Figure represents the shrinkage of one specimen according to the values as they were acquired by the ESPI and not corrected yet. This slope differs in terms of smoothness in comparison to the rest shown here and so the occurrence of mode hopping during this measurement is implied. Indeed, after controlling the steps indicated by the red arrows, they proved affected and irrelevant to the measurement of strain and were removed following the aforementioned procedure. Eventually, the same slope after the correction is shown marked red in Fig. 50.

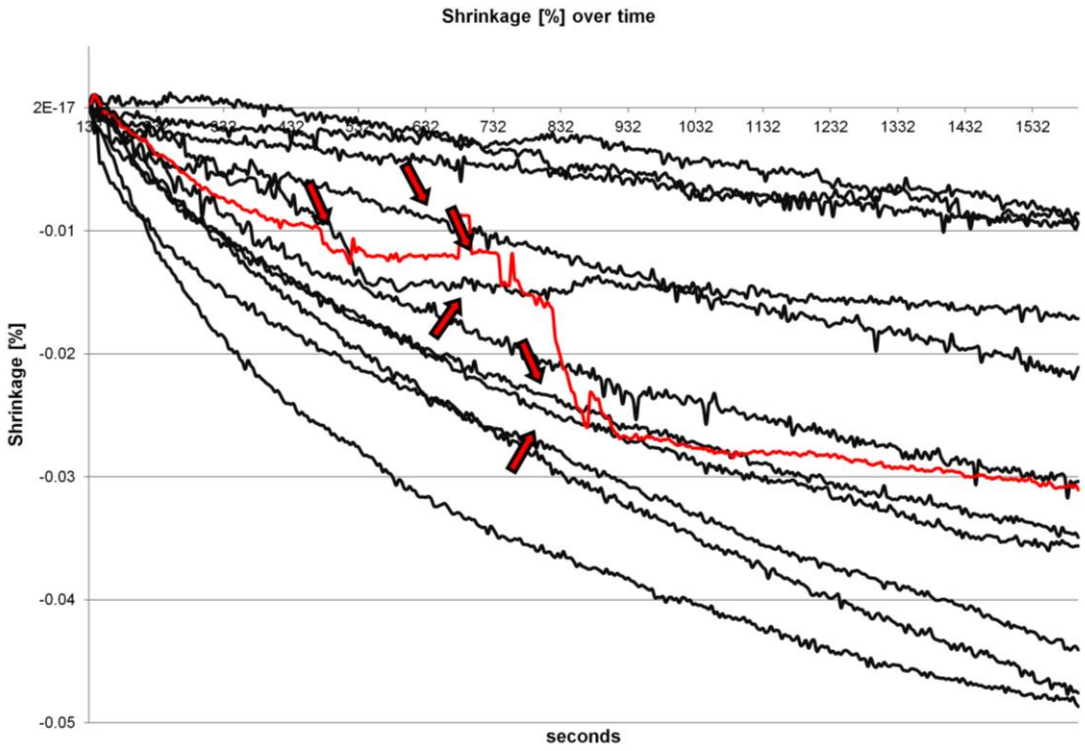

Fig. 49: Original shrinkage slope of a specimen (red slope), implying the occurrence of mode hopping during the measurement. The red arrows indicate the affected steps that had to be removed.

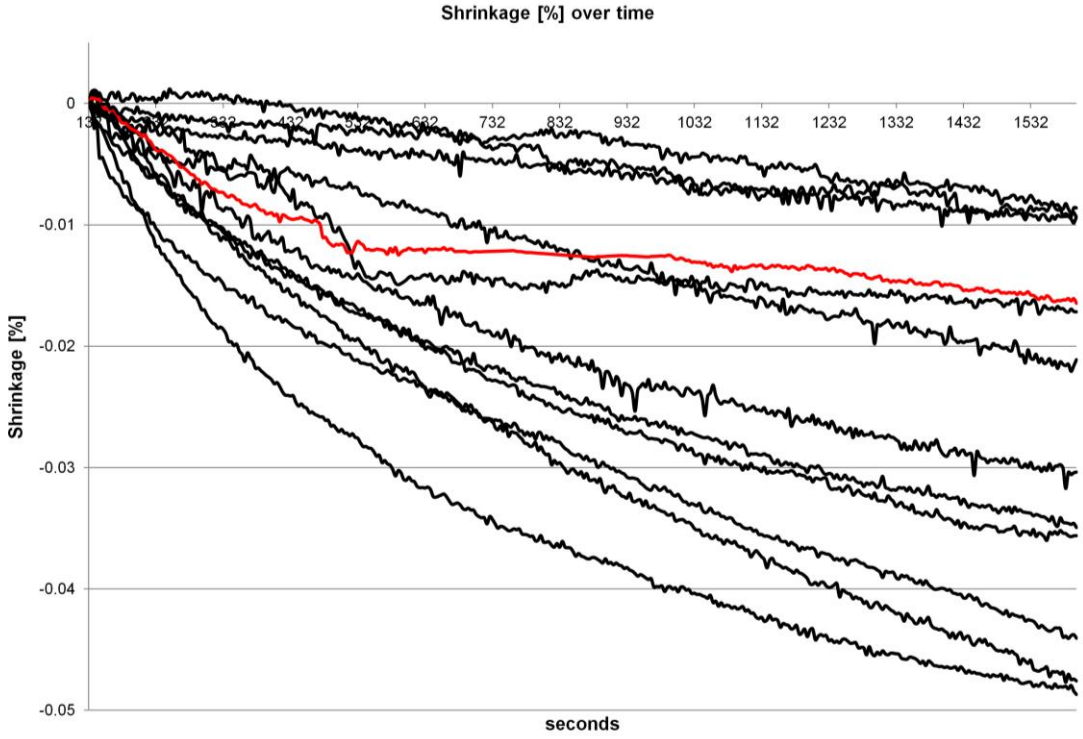

Fig. 50: The same slope after correction was applied (red slope).

7.2 Dimensional behavior of Grandio

As mentioned before, all measurements revealed the same general dimensional behavior of the material, regardless of the special storage conditions of each group tested: the material expanded reaching a peak simultaneously as the temperature reached the designated 37°C, only to shrink afterwards until the end of the measurement.

The expansion taking place during the rise of the temperature is in agreement with the expected behavior of any material during heating: as the temperature rises, the material expands following the CTE.

An initial expansion followed by shrinkage was also observed and described by Ashbee et al. who demonstrated that composites first expands when immersed in hot water, slowly shrinking after this first expansion phase ends [90].

The heating-induced expansion phase is outside the scope of interest of this study. However it is important to take into account the fact that, because of omitting this phase, the final total deformation of the material could not be calculated - some groups exhibited larger shrinkage than their initial expansion, which means that at the end of the measurement they had actually shrunk; other groups didn't. Whether the final result would be shrinkage or expansion was dependent on the storage duration and is also mentioned in the literature [87].

Shrinkage was always exhibited after the temperature was stabilized, more dramatic at first and gradually slowing down until the end of the measurement. Two phenomena influence this shrinkage, post-polymerization and water absorption. Within the frame of investigating these influences, the general layout of the measurements carried out in this study is shown in Fig. 51.

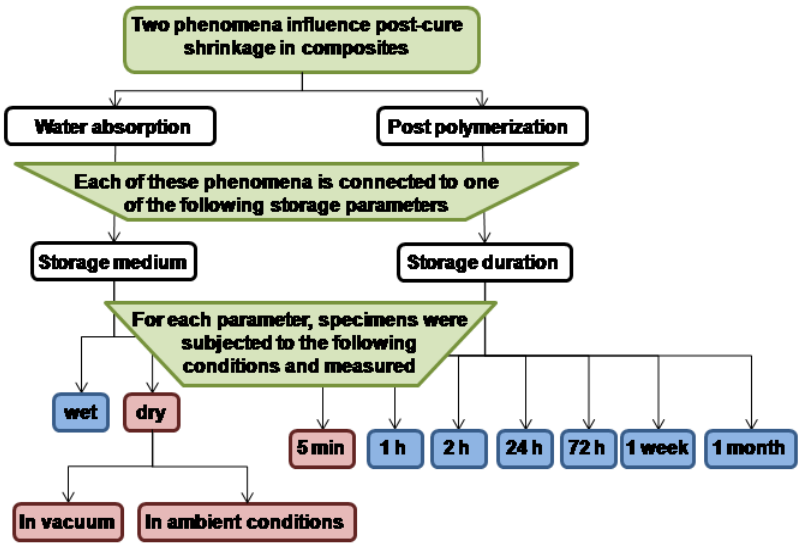

Fig. 51: Experimental procedure followed for the investigation of the different influences of water absorption and post-polymerization on the shrinkage of the composite as it was heated to 37°C.

Already the first small experiment of the evaluation of the ESPI method suggested that the water storage duration influences the deformation of the material. The results of the measurements for the establishment of the ESPI protocol (Chapter 6.1.2) revealed a difference between wet and dry stored specimens. Nevertheless this was a difference of magnitude rather than one of actual response: both storage conditions led to shrinkage however the wet stored specimens shrank more than the dry stored ones.

The more detailed investigation (Chapter 6.2.2) led to the demonstration that the storage medium does not play a role in a statistically significant way, at least for storages up to 72 hours, compared to the storage duration, which does influence the shrinkage. This means that water absorption doesn't play an important role during the first few days following the placement of the restoration in a humid environment.

However, this demonstration can lead to an ambivalence regarding the dry storage. The question concerns the factor responsible for the shrinkage exhibited by the dry stored specimens. It is possible that the specimens already contained water either even before polymerization or through absorption of humidity from the environment during their storage.

Indeed, the fact that the specimens stored in vacuum shrank more than the ones stored in ambient conditions (Chapter 6.2.2) pointed to the plausibility of these two possibilities

[Fig. 52]. Storage in vacuum resulted in the extraction of humidity, both from the mass of the material and from the surrounding environment, so this difference in the shrinkage between the two groups of dry storage showed that the specimens stored dry in ambient conditions were actually less dry than expected.

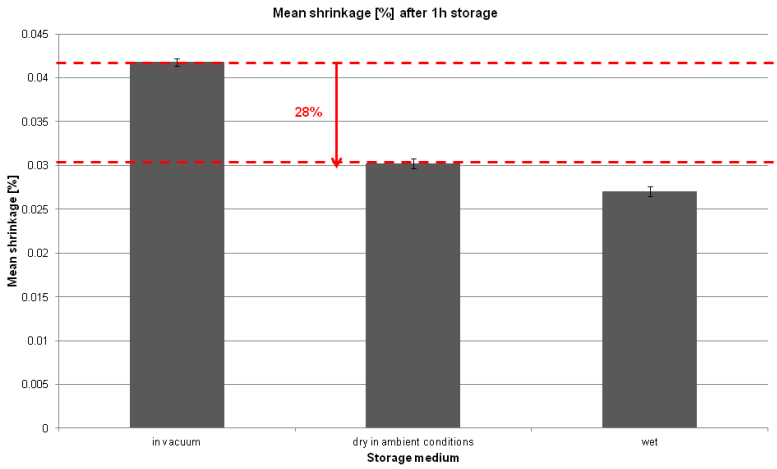

Fig. 52: Differences in the mean shrinkage between specimens stored for 1 h in vacuum, in ambient conditions and in water. The specimens stored in vacuum shrank 28% more than the specimens stored in ambient conditions.

Mortier et al. also demonstrated that non-desiccated specimens exhibited lower sorption but higher solubility compared to desiccated specimens [127]. This finding is in agreement with the results described here. Since water sorption is higher when water is already present in the material and non-desiccated specimens exhibited a lower sorption, the conclusion can be drawn that water was already present in the non-desiccated specimens. This observation is also mentioned elsewhere in the literature [58, 65].

The greater shrinkage observed for the specimens stored in vacuum also suggests that the water in the material may be playing a stabilizing role, even if its content is low. The lower shrinkage observed for the more ‘humid’ specimens that were stored dry in ambient conditions shows that these specimens reacted in a less dramatic way towards the rise of the temperature. These more ‘humid’ specimens therefore appear to be closer to dimensional stability. The reason for this must be the presence of water, since this is the only difference between the two groups under comparison.

The aforementioned facts also contribute to the idea that post-polymerization and not water absorption may be playing the most prominent role in the dimensional behavior of the material during at least 72 h after its actual polymerization. Post-polymerization is expressed in a more radical way during this time period and 72 hours of wet storage is a short period for water absorption to take place in a significant magnitude.

A more complete overview of the influences of post-polymerization and water absorption was given through investigations of specimens stored for longer periods (Chapter 6.2.3). In Fig. 41 it can be seen that the general magnitude of shrinkage induced by heating decreases as the storage durations increased for storages of up to 72 hours. For storage durations longer than 72 hours, the shrinkage values started increasing again.

In detail, the specimens heated and measured 5 min after polymerization exhibited the largest shrinkage values of all. The importance of this observation lies on the fact that this is the time condition closest to the clinical reality: the material is put inside the cavity, polymerizes and starts heating up to mouth temperature. This appears to be the most sensitive period concerning the dimensional behavior of the material.

As time goes by, the shrinkage values decrease but are still relatively high particularly for the specimens measured within the first day after polymerization. During this first day the material exhibits the largest dimensional instability, reaching a more balanced state only 24 or even 72 hours after its polymerization. As discussed before, post-polymerization appears to be the phenomenon predominating in the dimensional response of the material for storages up to 72 hours.

The smallest shrinkage values were exhibited by the specimens stored wet for 72 hours, signifying that at that time, the material was in its least reactive state in terms of its dimensions. The influence of post-polymerization appears at that time to be coming to an end. For storages longer than 72 hours, the material’s dimensional balance diminished again. This observation points out to the fact that the 72 hours after polymerization is a turning point concerning the dimensions of the material [Fig. 53, Fig. 54]. After 1 month of storage in water, the shrinkage values were not different than the values acquired from the 24 hours of water storage. Within 1 month of wet storage, water absorption is expected, according to the literature, to have already taken place. Moreover, post-polymerization is expected to have finished. Consequently, since the

only difference between the groups of specimens was their storage duration, the only phenomenon that could be responsible for this increase in shrinkage of specimens stored for longer periods than 72 hours is water absorption [Fig. 55].

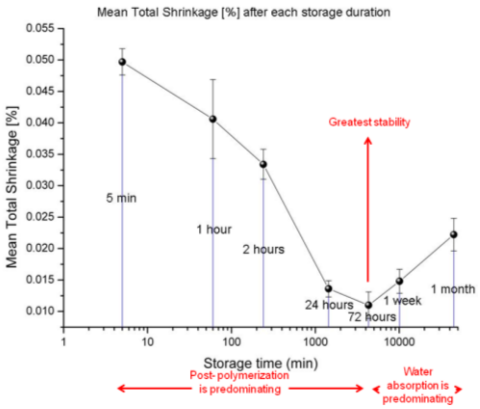

Fig. 53: Until 72 hours of water storage, post-polymerization controls the dimensional behavior of the material, whereas for longer storages, the dominant phenomenon is water absorption.

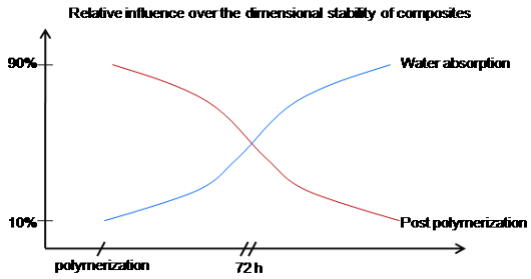

Fig. 54: Model for explanation of time dependency of the influence of post-polymerization and water absorption in composites.

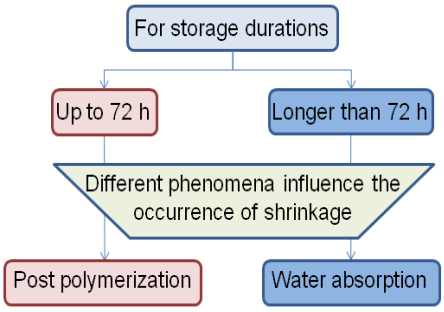

Fig.55: Time frame of the influence of each parameter over shrinkage.

A further point of interest is the fact that no specimen ever reached a completely stable state over the duration of the measurement in any of the measurements. Future studies should involve longer measurements and specimens subjected to longer storage durations.

The definition of what the term post-polymerization implies can provide the information needed in order to understand all the aforementioned processes.

7.3 Post-polymerization, free volume theory and diffusion

The term post-polymerization is used to describe particular phenomena connected to the reduction of the remaining double bonds after the actual curing of the composite, however its meaning, as will be explained, can easily be misunderstood. The chemical processes taking place after curing are actually explained by the free-volume theory for polymers.

7.3.1 Post-polymerization

As mentioned in the literature, in the range of temperatures as the ones used for the measurements described in this study, post-polymerization processes connected with the mobility of residual radicals cannot take place, since the reactive molecules are trapped inside the polymer structure [128]. As a verification of this, it was demonstrated that the degree of conversion was not increasing within the first 24 hours after polymerization, however during that period the material did shrink [90, 129].

Only a higher temperature would impose a change in the polymer structure, ensuring the mobility needed in order for this kind of reactions between the residual radicals to take place [130]. Loza-Herrero et al. have shown that the amount of the remaining double bonds was reduced when the material was heated in the first 6 hours after polymerization. Nevertheless this rise of the temperature only accelerated this process, since after the 6 hours no difference was found in the amount of double bonds between the heated and non-heated specimens [131]. Therefore, it appears as if this reduction of the double bonds takes place under all circumstances.

Consequently, if the residual radicals are not reacting with each other at 37°C, something else must be responsible for this reduction of the double bonds. The leaching of components from the material was found to play a significant role here [90].

Moreover, the half-life of the radicals inside the material was found to reduce logarithmically as temperature rose, even to 37°C. This half-life time was also calculated to be between 2 and 5 days at 37°C [132].

The main explanation for these competing phenomena that take place after polymerization is found in the free-volume theory of diffusion in polymers.

7.3.2 Free-volume theory and diffusion

According to Vrentas et al., the free volume of a polymer- solvent system is defined as the difference between its volume at 0°K and its volume at any other temperature [133]:

$$V_f = V - V_0 \qquad \text{[Eq. 4]}$$

where V_F= the free volume,

V= the volume at any temperature

V_0= the volume at 0°K

The change in volume (V) of the material, which results according to Eq. 4 in an increase of its free volume ($V_{F)}$, is connected to the material's thermal expansion due to the rise of the temperature. Truffier-Boutry et al. had also demonstrated that the free volume changes due to thermal expansion [129].

The free volume consists of two parts. The first one is called interstitial free volume and is a result of the homogenous expansion of the material. The second part is connected with the random appearance of holes in the material and is therefore called hole free volume. The hole free volume is the part of the free volume into which molecular transports, connected to diffusion, can occur [133-136]. A water molecule, for instance, can occupy a hole.

It has been demonstrated that in the first day after the polymerization of composite, a free volume relaxation takes place, during which the storage medium plays no role in the degradation of residual radicals [129, 134]. The free volume relaxation is

responsible for the shrinkage observed in this study during the first 24h after polymerization, as also mentioned by Truffier-Boutry [129]. This time span is too short for water absorption to take place, however it is then, as mentioned, that the elution of species of the material takes place.

After the first day, the storage medium starts to play a role, with the wet specimens loosing radicals at a lower rate than the ones stored dry [128]. This degradation was also found to be influenced by temperature: the lower the temperature, the lower the degradation rate [128] and, as already mentioned, the lower the diffusion. The degradation of the radicals seems consequently to be connected with diffusion.

Therefore, in this study, the stability exhibited by the material 72h after curing implies a threshold at that time [Fig. 56(a)]. The free volume relaxation has finished, and the elution of species from the material and water sorption has not yet acquired a significant magnitude. Therefore, it is then that the specimens exhibit the greatest dimensional stability.

For the specimens of this study stored longer than 72h, water absorption could be responsible for the larger shrinkage values observed. At 37°C, the water molecules in the material cannot evaporate since this can only occur when the temperature reaches the glass transition temperature T_g [105]. Nevertheless water does accelerate the molecular mobility inside the material [71]. The actual reason, however, for the higher shrinkage of these specimens remains obscure and future studies are required in this direction.

For these long storages, the influence of the diffusion of oxygen in the material is also mentioned. Oxygen was demonstrated to play an important role in the degradation of the radicals, directly connected with a higher molecular mobility in the material induced by the rise of the temperature or by water absorption [128].

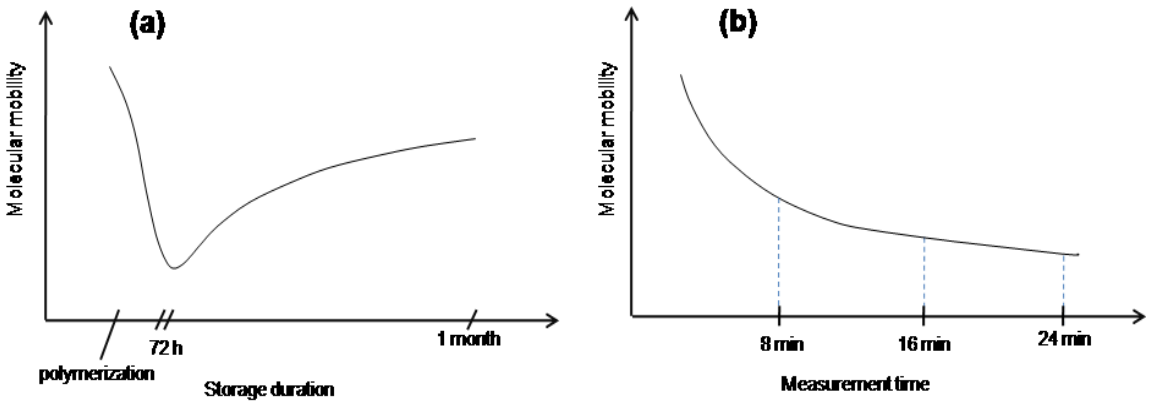

Fig. 56: Models of explanation of the development of molecular mobility in the material in relation to (a): the storage duration and (b): the duration of the measurement.

These molecular phenomena taking place in the material indicate that by recording its dimensional behavior under each condition with ESPI, what is actually recorded - apart from the shrinkage - is the molecular mobility of the material as a response to the change of its temperature. This observation was also made by Wells- Gray et al. [137].

The general trend of the slopes of all specimens additionally underlines this observation. At the start of the measurements, when all slopes had the highest values, the material was balancing in the new temperature in terms of kinetics, gradually slowing down until the end of the measurement [Fig. 56(b)].

7.4. Loss or gain of weight and molecular mobility

When an additional type of investigation of the water absorption was conducted by measuring the weight of the material (Chapters 6.4.1 and 6.4.2), there was always a loss of weight observed when the material was heated, regardless of the storage medium or duration [Fig. 57]. This observation is also mentioned in the literature [75]. Regarding the loss of weight occurring early after the polymerization of the material, post-polymerization could be responsible. The loss of weight however occurring when the specimens were heated to 37°C 2 months after their polymerization cannot be explained by post-polymerization, since by that time it is considered to be complete [Fig. 57 (b)].

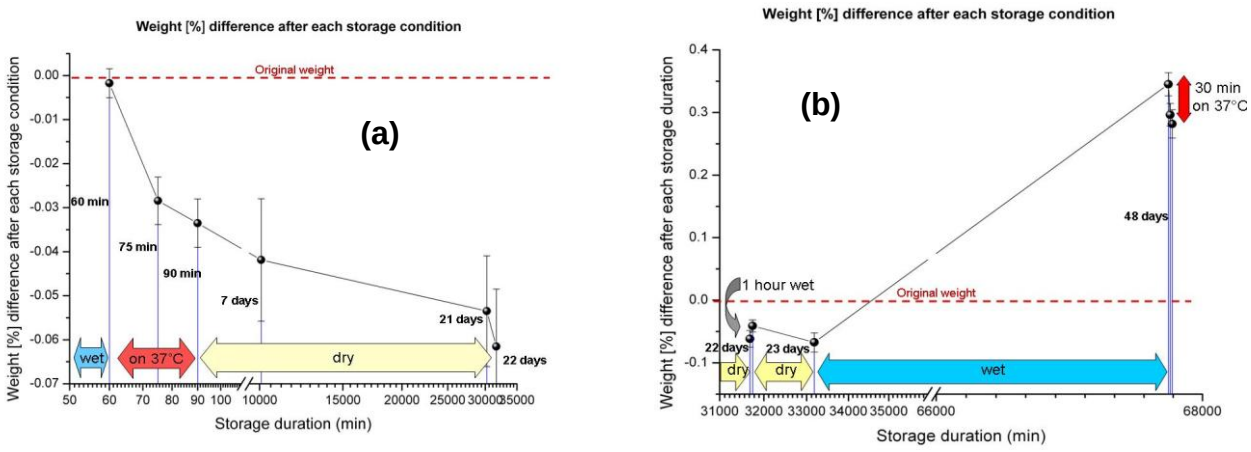

Fig. 57: Mean difference in weight of the same specimens over time after each storage condition, in comparison to their original weight as measured after polymerization (Chapter 6.4.1). Fig. 57 (b) is the sequel of Fig. 57 (a) for storages longer than 22 days.

Moreover, heating to 37°C never influenced the magnitude of water absorption thereafter: the gain of weight after 72 hours of water storage was the same, regardless of whether the material was previously heated for 30 min or not as shown in Fig. 57.

Very little information exists in the literature concerning the weight gain of the material after storage in water. In contrast to the 0.35% gain in weight after 30 days of water storage found in this study (Chapter 6.4.1), Pastila et al. reported a gain of less than 1% for the equivalent storage duration [78]. However many differences exist between the two experimental procedures followed. In this study, the specimens were immersed in water only after 23 days had passed from polymerization and not immediately after it, as is the case in the study of Pastila et al. In these 23 days, chemical reactions, such as

degradation of residual radicals, are expected to have taken place. These reactions influence water absorption and consequently also the gain in weight mentioned above.

Nevertheless, in this study the material always appeared to be losing weight when heated and always gaining weight when stored in water and these two procedures were taking place independent of each other. Furthermore, the loss of weight observed after 22 days of dry storage in ambient conditions point to the existence of a process taking place. This process could be connected to the diffusion of humidity or oxygen in the material, as mentioned above, and its reaction with residual radicals.

Consequently, heating appeared to be influencing the weight of the material only as long as it was applied, which shows that what the rise in temperature was accelerating the molecular mobility. This finding additionally validates the observation that recording by ESPI reveals the molecular mobility of the material.

7.5. Clinical relevance

The measurement setup for the specimens measured 5min after polymerization was arranged to resemble the actual procedures followed *in vivo*: the material is placed in the cavity, polymerizes and then its temperature rises to mouth temperature. These specimens were also the ones that exhibited the most dramatic change in their dimensions during heating to 37°C.

The rest of the groups simulate hypothetical conditions, measured in order to test the impact of the various factors affecting the dimensional behavior. Their recordings demonstrated that the material responds abruptly to the rise in temperature throughout the first day after its polymerization, reaching its most stable state on the third day after polymerization. The temperature rise was neither extreme, nor a phenomenon that can be avoided since it is the actual mouth temperature.

Therefore, particularly in the first hours after a composite filling is placed, its reaction to heating appears to be remarkable, even if the final temperature is the mouth temperature. Within this framework, future investigations should include testing in different temperatures in order to investigate if the patient should be advised to avoid thermal fluctuations in the mouth during the first hours after a filling is placed.

The impact of the observed shrinkages on the filling–tooth interface becomes obvious when compared to the sizes of molecules that could enter the potential gap formed. If the mean total shrinkage percentage of the 5 min stored group was $4.97E^{-02}$% after 30min at 37°C, for a composite filling of 3mm length, the potential gap formed on the interface because of this shrinkage equals 1.5μm. For a 5mm long composite filling, the potential gap would be 2.5 μm.

The radius of a water molecule in liquid state is 193pm, and the energy it requires to enter a micro cavity is 1.1eV, which equals to $1.76239411E^{-19}$J [138, 139].Since, for water only, 1 calorie is the heat needed to raise the temperature of 1 gram of water by 1°C, and 1 calorie equals 4.184J, the energy required for the water molecule to enter a micro cavity could be acquired if its temperature rose by $9.28E^{-23}$°C. Consequently, in the hypothetical situation when no adhesive was used for the filling, or if an inadequate

adhesion was achieved, as often occurs, water could easily enter the aforementioned gap in the interface [Fig. 58].

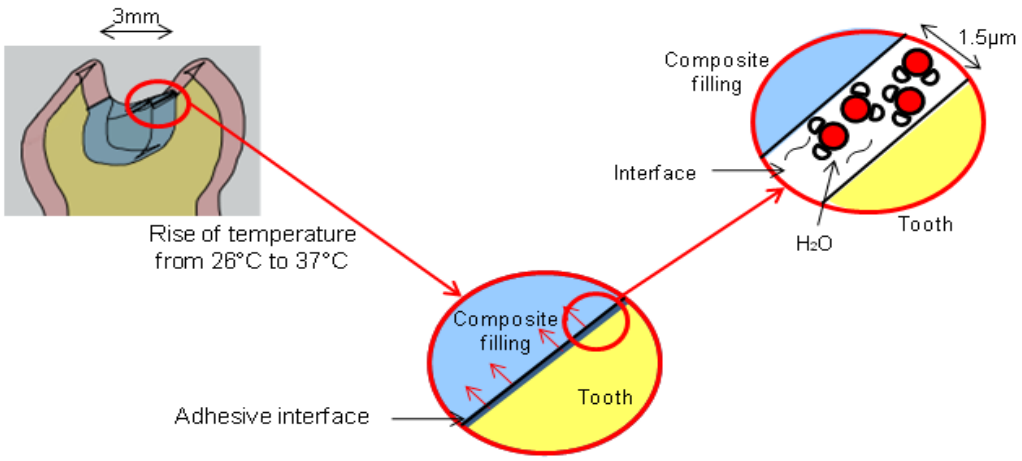

Fig.58: The shrinkage of the composite due to the rise of the temperature is important for the integrity of the adhesive interface. Water molecules can flood the potential gap formed on the interface, as shown for a 3mm long composite filling.

The actual stress developed as the observed shrinkage takes place can be calculated by using the stress-strain equation:

$$\sigma = E \cdot \varepsilon \qquad \text{[Eq. 5]}$$

where σ= stress,

E= Young's Modulus

E= strain

The Young's Modulus of Grandio is calculated to be 14.81GPa [75]. According to this, the stress calculated for the specimens at the end of 5 min at 37°C was 7.36MPa. This was also the largest stress value calculated for the groups of the specimens. After 3 days' water storage, the stress was 1.62MPa and was the lowest for all groups. After 1 month's storage in water, the stress that developed after the heating to 37°C was in the middle, 3.32MPa.

These stresses develop gradually as long as the shrinkage takes place; their values are also remarkable as they are directly applied on the adhesive on the tooth - restoration interface, posing a problem concerning the integrity of this complex.

7.6. Conclusions

From this study, the following conclusions could be drawn:

1. Water was shown not to influence the dimensional stability of the material during the first 72 hours after polymerization, since it is too early for water absorption to take place. However, its influence is expressed after these first 72 hours, as shown by the results of this study and by information published in relevant literature. Post-polymerization was shown to play a role in a statistically significant way, influencing the dimensional behavior of the material during the first 72h after polymerization. Therefore, the null hypothesis of this study must be accepted. The post-cure dimensional behavior of the material is influenced by post-polymerization and water absorption.

2. The potential of performing full–field, non–destructive measurements of deformations with ESPI, as they take place on the nm scale in all three dimensions was validated and the proposed setup can be used as a measurement protocol for conducting deformation measurements with ESPI. The smallest strain value of $-9E^{-05}$ acquired from the measurement aiming to evaluate the ESPI technique (Chapter 6.1.1) validates the high sensitivity of the method and the different responses between specimens that underwent various storage conditions allow comparisons to be made. Thus, the second hypothesis of this study should be accepted.

3. The response of the material towards heating to mouth temperature is substantial, particularly during the first day after polymerization. If an inadequate adhesion to the tooth substances is achieved, water molecules can easily enter the gap formed as a result of the observed shrinkage.

8. Summary

The high qualities of dental composite resins have established them as first choice materials for direct filling restorations. However their longevity is highly dependent on the integrity of the adhesive interface between the restoration and the tooth. This interface is in turn influenced by the dimensional behavior of the material and its response to the various conditions in the mouth.

The composite fillings have to operate in a wet environment under constant thermal fluctuations. Phenomena like water absorption and elution of chemical species from the material, post-polymerization and changes in temperature strongly influence the dimensional behavior of the material, posing a challenge to the adhesive interface.

In order to be able to investigate the impact of these phenomena on the dimensions of the material, and since the magnitude of these deformations is very small, a very sensitive method should be applied. Electronic speckle pattern- correlation interferomentry (ESPI) is a non-contact, non-destructive optical method for measuring small deformations of surfaces taking place in a range of 20 nm to 2 μm, being therefore suitable for performing this kind of measurements.

The aim of this study was to measure the actual deformations of the composite when heated up to 37°C and to investigate the different impact of the factors influencing the dimensional behavior of the material. Accordingly, through these measurements the potential of ESPI for conducting small scale recordings of the deformations taking place in composite materials should be determined and a measurement protocol should be established in order to standardize this procedure.

Within this framework, two materials were chosen, Admira (VOCO, Cuxhaven) for the preliminary measurements and Grandio (VOCO, Cuxhaven) for the main deformation measurements. Each specimen was stored dry (ambient conditions) or wet (water) for particular durations before measurement. The deformations taking place as the specimen was heated from 26°C to 37°C were recorded, with each recording lasting 27 min, corresponding to 400 measurements over the surface. Comparisons were made between the deformations recorded for the various groups.

The impact of water absorption and post-polymerization over the dimensional behavior of the material was investigated with ESPI, as well as the time frame in which these phenomena exert their influence. Additional measurements in this direction included microindentation tests and measurements of the weight. The possibility of water pre-existing in the dry specimens was also examined.

Through the measurements with the ESPI it was demonstrated that as temperature rose from 26°C up to 37°C, following an initial expansion all specimens shrank for the duration of the measurement (-0.05%≤deformation≤-0.011%).

The largest and most dramatic dimensional response of the material was exerted at the first 24 hours after polymerization, regardless of the storage medium. 72 hours after polymerization the material showed the greatest stability. For storages longer than 72 hours and up to 1 month, the shrinkage values started rising again.

Evidently, the first 24 hours are overall the most important period for the dimensional behavior of the material. The shrinkage exhibited as a result of the rise in temperature is the most statistically significant, even when this rise is only up to mouth temperature. During this time, post-polymerization exerts the greatest influence. By contrast, 72 hours after polymerization, the impact of water absorption is greater than that of post-polymerization.

Through all these measurements it was demonstrated that ESPI is capable of measuring nanometer deformations and minute strains related to the molecular dynamics of the composites, relevant to the clinical conditions where these materials are used. Through the measurements with the ESPI, a measurement protocol was established standardizing the method for future investigations.

9. Zusammenfassung

Die hohe Qualität der zahnärztlichen Komposite hat sich als erste Wahl für direkte Restaurationen etabliert. Doch ihre Langlebigkeit ist stark abhängig von der Integrität des adhäsiven Verbunds zwischen Restauration und Zahn. Diese Grenzfläche ist wiederum durch das dimensionale Verhalten des Materials und seine Reaktion auf die verschiedenen Bedingungen im Mund beeinflusst.

Die Kompositfüllungen müssen einer feuchten Umgebung und konstanten thermischen Fluktuationen widerstehen. Phänomene wie Wasseraufnahme und Löslichkeit von chemischen Substanzen aus dem Material, Post-Polymerisation und Änderungen der Temperatur beeinflussen das dimensionale Verhalten des Materials und stellen eine Herausforderung an die Adhäsive Grenzfläche.

Um in der Lage zu sein die Auswirkungen dieser Phänomene auf die Dimensionen des Materials zu untersuchen, insbesondere da die Größe dieser Verformungen sehr klein ist, sollte entsprechend eine sehr empfindliche Methode angewendet werden. Elektronische Speckle-Korrelation Interferometrie (ESPI) ist eine berührungslose, zerstörungsfreie, optische Methode zur Messung von kleinen Verformungen der Oberfläche, in einem Bereich von 20nm bis 2µm und ist deshalb geeignet für die Durchführung dieser Art von Messungen.

Das Ziel dieser Studie war es, die tatsächlichen Verformungen des Kunststoffes zu messen, wenn er bis zu 37 ° C erhitzt ist und die unterschiedlichen Auswirkungen der Faktoren zu untersuchen, die das dimensionale Verhalten des Materials beeinflussen. Durch diese Messungen wird die Möglichkeit kleinste Deformationen im Kunststoff mit ESPI aufzunehmen untersucht. Zur Standardisierung wurde ein Messprotokoll eingerichtet.

Im Rahmen dessen wurden zwei Materialien gewählt: Admira (VOCO, Cuxhaven) für den vorläufigen Messungen und Grandio (VOCO, Cuxhaven) für die Hauptdeformationsmessungen. Für bestimmte Zeiträume vor der Messung wurde jede Probe trocken (Umgebungsbedingungen) bzw. feucht (Wasser) gelagert. Verformungen während des Verfahrens, zwischen dem Heizen von 26°C bis 37°C, wurden gemessen und aufgenommen. Jede Aufnahme dauerte 27 min, bzw. entspricht 400 Messungen

auf der Oberfläche. Vergleiche zwischen den Verformungen der verschiedenen Gruppen wurden durchgeführt.

Die Auswirkungen der Wasseraufnahme und Polymerisation über dem dreidimensionalen Verhalten des Materials wurde mit ESPI untersucht, sowie der Zeitraum, in dem diese Phänomene ihren Einfluss ausüben. Zusätzliche Messungen in diese Richtung enthalten die Mikroindentation- Tests und Messungen des Gewichts. Die Möglichkeit von Wassereinlagerung in den trockenen Proben wurde ebenfalls untersucht.

Durch die Messungen mit dem ESPI wurde gezeigt, dass während des Temperaturanstiegs von 26°C auf 37°C nach einer ersten Expansion alle Proben schrumpften. Für die Dauer der Messung entsprach dies -0,05%≤Verformung≤-0,011%. Die größte und dramatischste dimensionale Reaktion des Materials findet innerhalb der ersten 24 Stunden nach der Polymerisation statt, unabhängig von dem Lagerungsmedium. 72 Stunden nach der Polymerisation zeigt das Material die größte Stabilität. Für Lagerungszeiträume zwischen 72 Stunden und 1 Monat, zeigte sich wieder ein Anstieg der Schrumpfung.

Offensichtlich sind die ersten 24 Stunden insgesamt die wichtigsten für die Dimensionen des Materials. Die Schrumpfung als Folge des Anstiegs der Temperatur ist statistisch signifikant, auch wenn dieser Temperaturanstieg nur auf Niveau der Mundtemperatur ist. Während dieser Zeit übt die Post-Polymerisation den stärksten Einfluss aus. Im Gegensatz dazu sind 72 Stunden nach der Polymerisation die Auswirkungen der Wasseraufnahme größer als die der Polymerisation. Außerdem wurde durch diese Experimente gezeigt, dass die Messung mit ESPI Nanometerverformungen und Spannungen der Kunststoffe, unter klinisch relevanten Bedingungen, möglich ist. Durch die Messungen mit ESPI wurde ein Messprotokoll zur Standardisierung für zukünftige Untersuchungen hergestellt.

10. References

1. O'Brien, W., ed. *Dental Materials and their selection*. Third ed. 2002, Quintessence Publishing Co, Ing: Carol Stream. 113- 131.

2. Attin HK, E.H., J Klimek ed. *Einführung in die Zahnerhaltung*. 2 ed. 1999, Urban & Fischer Verlag: Mühchen- Jena. 160- 167.

3. Anusavice, K., ed. *Phillip's Science of Dental Materials*. Eleventh ed. 2003, Elsevier: St. Louis. 495- 540.

4. Attin HK, E.H., J Klimek, ed. *Einführung in die Zahnerhalung*. 2 ed. 1999, Urban & Fischer Verlag: München- Jena. 170- 190.

5. Anusavice, K., ed. *Phillip's Science of Dentl Materials*. Eleventh ed. 2003, Elsevier: St. Louis. 399- 441.

6. Craig, R.G., ed. *Restorative Dental Materials*. 10th ed. 1997, Mosby- Year Book Inc.: Ann Arbor Michigan. 245- 9.

7. Shalaby SW, U.S., ed. *Polymers for dental and orthopedic applications*. 2007, CRC Press, Taylor & Francis Group: Boka Raton. 14-18.

8. Ferracane, J.L., *Hygroscopic and hydrolytic effects in dental polymer networks.* Dent Mater, 2006. **22**(3): p. 211-22.

9. Kalachandra, S., D.T. Turner, *Water sorption of polymethacrylate networks: bis-GMA/TEGDM copolymers.* J Biomed Mater Res, 1987. **21**(3): p. 329-38.

10. Goncalves, F., C.S. Pfeifer, J.L. Ferracane, R.R. Braga, *Contraction stress determinants in dimethacrylate composites.* J Dent Res, 2008. **87**(4): p. 367-71.

11. Ferracane, J.L., *Current trends in dental composites.* Crit Rev Oral Biol Med, 1995. **6**(4): p. 302-18.

12. Anusavice, K., ed. *Phillip's Science of Dental Materials*. Eleventh ed. 2003, Elsevier: St. Louis. 143- 169.

13. Craig, R.G., ed. *Restorative Dental Materials*. 11th ed. 2002, Mosby, Inc.: St. Louis, Missouri. 231- 257.

14. Ferracane, J.L., *Elution of leachable components from composites.* J Oral Rehabil, 1994. **21**(4): p. 441-52.

15. Oysaed, H., I.E. Ruyter, *Composites for use in posterior teeth: mechanical properties tested under dry and wet conditions.* J Biomed Mater Res, 1986. **20**(2): p. 261-71.

16. von Fraunhofer, J.A., P. Curtis, Jr., *Physical and mechanical properties of anterior and posterior composite restorative materials.* Dent Mater, 1989. **5**(6): p. 365-8.

17. Kim, K.H., J.L. Ong, O. Okuno, *The effect of filler loading and morphology on the mechanical properties of contemporary composites.* J Prosthet Dent, 2002. **87**(6): p. 642-9.

18. Manhart, J., K.H. Kunzelmann, H.Y. Chen, R. Hickel, *Mechanical properties of new composite restorative materials.* J Biomed Mater Res, 2000. **53**(4): p. 353-61.

19. Ferracane, J.L., H.X. Berge, J.R. Condon, *In vitro aging of dental composites in water--effect of degree of conversion, filler volume, and filler/matrix coupling.* J Biomed Mater Res, 1998. **42**(3): p. 465-72.

20. Curtis, A.R., W.M. Palin, G.J. Fleming, A.C. Shortall, P.M. Marquis, *The mechanical properties of nanofilled resin-based composites: characterizing discrete filler particles and agglomerates using a micromanipulation technique.* Dent Mater, 2009. **25**(2): p. 180-7.

21. Soderholm, K.J., M. Zigan, M. Ragan, W. Fischlschweiger, M. Bergman, *Hydrolytic degradation of dental composites.* J Dent Res, 1984. **63**(10): p. 1248-54.

22. Soderholm, K.J., *Degradation of glass filler in experimental composites.* J Dent Res, 1981. **60**(11): p. 1867-75.

23. Sarkar, N.K., *Internal corrosion in dental composite wear.* J Biomed Mater Res, 2000. **53**(4): p. 371-80.

24. Santos, C., R.L. Clarke, M. Braden, F. Guitian, K.W. Davy, *Water absorption characteristics of dental composites incorporating hydroxyapatite filler.* Biomaterials, 2002. **23**(8): p. 1897-904.

25. O'Brien, W., ed. *Dental materials and their selection*. Third ed. 2002, Quintessence Publishing Co, Inc: Carol Stream. 74- 89.

26. Labella, R., P. Lambrechts, B. Van Meerbeek, G. Vanherle, *Polymerization shrinkage and elasticity of flowable composites and filled adhesives.* Dent Mater, 1999. **15**(2): p. 128-37.

27. Stansbury, J.W., *Cyclopolymerizable monomers for use in dental resin composites.* J Dent Res, 1990. **69**(3): p. 844-8.

28. Stansbury, J.W., *Synthesis and evaluation of novel multifunctional oligomers for dentistry.* J Dent Res, 1992. **71**(3): p. 434-7.

29. Ruttermann, S., S. Kruger, W.H. Raab, R. Janda, *Polymerization shrinkage and hygroscopic expansion of contemporary posterior resin-based filling materials--a comparative study.* J Dent, 2007. **35**(10): p. 806-13.

30. Munksgaard, E.C., E.K. Hansen, H. Kato, *Wall-to-wall polymerization contraction of composite resins versus filler content.* Scand J Dent Res, 1987. **95**(6): p. 526-31.

31. Takahashi, H., W.J. Finger, K. Wegner, et al., *Factors influencing marginal cavity adaptation of nanofiller containing resin composite restorations.* Dent Mater. **26**(12): p. 1166-75.

32. Versluis, A., D. Tantbirojn, M.R. Pintado, R. DeLong, W.H. Douglas, *Residual shrinkage stress distributions in molars after composite restoration.* Dent Mater, 2004. **20**(6): p. 554-64.

33. Calheiros, F.C., F.T. Sadek, L.C. Boaro, R.R. Braga, *Polymerization stress related to radiant exposure and its effect on microleakage of composite restorations.* J Dent, 2007. **35**(12): p. 946-52.

34. Barink, M., P.C. Van der Mark, W.M. Fennis, et al., *A three-dimensional finite element model of the polymerization process in dental restorations.* Biomaterials, 2003. **24**(8): p. 1427-35.

35. Asmussen, E., *Factors affecting the quantity of remaining double bonds in restorative resin polymers.* Scand J Dent Res, 1982. **90**(6): p. 490-6.

36. Inoue, K., I. Hayashi, *Residual monomer (Bis-GMA) of composite resins.* J Oral Rehabil, 1982. **9**(6): p. 493-7.

37. Moon, H.J., Y.K. Lee, B.S. Lim, C.W. Kim, *Effects of various light curing methods on the leachability of uncured substances and hardness of a composite resin.* J Oral Rehabil, 2004. **31**(3): p. 258-64.

38. Pearson, G.J., C.M. Longman, *Water sorption and solubility of resin-based materials following inadequate polymerization by a visible-light curing system.* J Oral Rehabil, 1989. **16**(1): p. 57-61.

39. Deliperi, S., D.N. Bardwell, *An alternative method to reduce polymerization shrinkage in direct posterior composite restorations.* J Am Dent Assoc, 2002. **133**(10): p. 1387-98.

40. Cunha, L.G., R.C. Alonso, E.J. de Souza-Junior, et al., *Influence of the curing method on the post-polymerization shrinkage stress of a composite resin.* J Appl Oral Sci, 2008. **16**(4): p. 266-70.

41. Soares, L.E., A.A. Martin, A.L. Pinheiro, M.T. Pacheco, *Vicker's hardness and Raman spectroscopy evaluation of a dental composite cured by an argon laser and a halogen lamp.* J Biomed Opt, 2004. **9**(3): p. 601-8.

42. Poskus, L.T., A.M. Latempa, M.A. Chagas, et al., *Influence of post-cure treatments on hardness and marginal adaptation of composite resin inlay restorations: an in vitro study.* J Appl Oral Sci, 2009. **17**(6): p. 617-22.

43. Oysaed, H., I.E. Ruyter, *Water sorption and filler characteristics of composites for use in posterior teeth.* J Dent Res, 1986. **65**(11): p. 1315-8.

44. Roulet, J.F., C. Walti, *Influence of oral fluid on composite resin and glass-ionomer cement.* J Prosthet Dent, 1984. **52**(2): p. 182-9.

45. Braden, M., R.L. Clarke, *Water absorption characteristics of dental microfine composite filling materials. I. Proprietary materials.* Biomaterials, 1984. **5**(6): p. 369-72.

46. Huang, C., F.R. Tay, G.S. Cheung, et al., *Hygroscopic expansion of a compomer and a composite on artificial gap reduction.* J Dent, 2002. **30**(1): p. 11-9.

47. Koike, T., T. Hasegawa, A. Manabe, K. Itoh, S. Wakumoto, *Effect of water sorption and thermal stress on cavity adaptation of dental composites.* Dent Mater, 1990. **6**(3): p. 178-80.

48. Soderholm, K.J., *Water sorption in a bis(GMA)/TEGDMA resin.* J Biomed Mater Res, 1984. **18**(3): p. 271-9.

49. Bastioli, C., G. Romano, C. Migliaresi, *Water sorption and mechanical properties of dental composites.* Biomaterials, 1990. **11**(3): p. 219-23.

50. Carfagna, C., G. Guerra, L. Nicolais, S. Tartaro, *Effects of postcuring and water sorption on the mechanical properties of composite dental restorative materials.* Biomaterials, 1983. **4**(3): p. 228-9.

51. Ferracane, J.L., V.A. Marker, *Solvent degradation and reduced fracture toughness in aged composites.* J Dent Res, 1992. **71**(1): p. 13-9.

52. Takeshige, F., Y. Kawakami, M. Hayashi, S. Ebisu, *Fatigue behavior of resin composites in aqueous environments.* Dent Mater, 2007. **23**(7): p. 893-9.

53. Braden, M., E.E. Causton, R.L. Clarke, *Diffusion of water in composite filling materials.* J Dent Res, 1976. **55**(5): p. 730-2.

54. Janda, R., J.F. Roulet, M. Latta, S. Ruttermann, *Water sorption and solubility of contemporary resin-based filling materials.* J Biomed Mater Res B Appl Biomater, 2007. **82**(2): p. 545-51.

55. Mair, L.H., *The silver sorption layer in dental composites: three year results.* Dent Mater, 1999. **15**(6): p. 408-12.

56. Kalachandra, S., *Influence of fillers on the water sorption of composites.* Dent Mater, 1989. **5**(4): p. 283-8.

57. Sideridou, I., D.S. Achilias, C. Spyroudi, M. Karabela, *Water sorption characteristics of light-cured dental resins and composites based on Bis-EMA/PCDMA.* Biomaterials, 2004. **25**(2): p. 367-76.

58. Braden, M., *The absorption of water by acrylic resins and other materials.* J Prosthet Dent, 1963. **14**(2): p. 307-16.

59. Labella, R., M. Braden, K.W. Davy, *Novel acrylic resins for dental applications.* Biomaterials, 1992. **13**(13): p. 937-43.

60. Ferracane, J.L., J.R. Condon, *Rate of elution of leachable components from composite.* Dent Mater, 1990. **6**(4): p. 282-7.

61. Ortengren, U., H. Wellendorf, S. Karlsson, I.E. Ruyter, *Water sorption and solubility of dental composites and identification of monomers released in an aqueous environment.* J Oral Rehabil, 2001. **28**(12): p. 1106-15.

62. Ortengren, U., F. Andersson, U. Elgh, B. Terselius, S. Karlsson, *Influence of pH and storage time on the sorption and solubility behaviour of three composite resin materials.* J Dent, 2001. **29**(1): p. 35-41.

63. Braden, M., *Water absorption characteristics of dental microfine composite filling materials. II. Experimental materials.* Biomaterials, 1984. **5**(6): p. 373-5.

64. Sideridou, I., V. Tserki, G. Papanastasiou, *Study of water sorption, solubility and modulus of elasticity of light-cured dimethacrylate-based dental resins.* Biomaterials, 2003. **24**(4): p. 655-65.

65. Venz, S., B. Dickens, *NIR-spectroscopic investigation of water sorption characteristics of dental resins and composites.* J Biomed Mater Res, 1991. **25**(10): p. 1231-48.

66. Sideridou, I.D., D.S. Achilias, M.M. Karabela, *Sorption kinetics of ethanol/water solution by dimethacrylate-based dental resins and resin composites.* J Biomed Mater Res B Appl Biomater, 2007. **81**(1): p. 207-18.

67. Frisch, H.L., *Sorption and Transport in Glassy Polymers- A Review.* Polymer Engineering and Science, 1980. **20**(1): p. 2-13.

68. Kalachandra, S., T.W. Wilson, *Water sorption and mechanical properties of light-cured proprietary composite tooth restorative materials.* Biomaterials, 1992. **13**(2): p. 105-9.

69. Asaoka, K., S. Hirano, *Diffusion coefficient of water through dental composite resin.* Biomaterials, 2003. **24**(6): p. 975-9.

70. Musanje, L., M. Shu, B.W. Darvell, *Water sorption and mechanical behaviour of cosmetic direct restorative materials in artificial saliva.* Dent Mater, 2001. **17**(5): p. 394-401.

71. Lagouvardos, P.E., P. Pissis, A. Kyritsis, D. Daoukaki, *Water sorption and water-induced molecular mobility in dental composite resins.* J Mater Sci Mater Med, 2003. **14**(9): p. 753-9.

72. Indrani, D.J., W.D. Cook, F. Televantos, M.J. Tyas, J.K. Harcourt, *Fracture toughness of water-aged resin composite restorative materials.* Dent Mater, 1995. **11**(3): p. 201-7.

73. Fan, P.L., A. Edahl, R.L. Leung, J.W. Stanford, *Alternative interpretations of water sorption values of composite resins.* J Dent Res, 1985. **64**(1): p. 78-80.

74. Karabela, M.M., I.D. Sideridou, *Effect of the structure of silane coupling agent on sorption characteristics of solvents by dental resin-nanocomposites.* Dent Mater, 2008. **24**(12): p. 1631-9.

75. Sideridou, I.D., M.M. Karabela, E. Vouvoudi, *Physical properties of current dental nanohybrid and nanofill light-cured resin composites.* Dent Mater. **27**(6): p. 598-607.

76. Aliping-McKenzie, M., R.W. Linden, J.W. Nicholson, *The effect of saliva on surface hardness and water sorption of glass-ionomers and "compomers".* J Mater Sci Mater Med, 2003. **14**(10): p. 869-73.

77. McCabe, J.F., S. Rusby, *Water absorption, dimensional change and radial pressure in resin matrix dental restorative materials.* Biomaterials, 2004. **25**(18): p. 4001-7.

78. Pastila, P., L.V. Lassila, M. Jokinen, et al., *Effect of short-term water storage on the elastic properties of some dental restorative materials--A resonant ultrasound spectroscopy study.* Dent Mater, 2007. **23**(7): p. 878-84.

79. Medeiros, I.S., M.N. Gomes, A.D. Loguercio, L.E. Filho, *Diametral tensile strength and Vickers hardness of a composite after storage in different solutions.* J Oral Sci, 2007. **49**(1): p. 61-6.

80. Braden, M., G.J. Pearson, *Analysis of aqueous extract from filled resins.* J Dent, 1981. **9**(2): p. 141-3.

81. Rathburn MA, R.C., CT Hanks, FE Filisko, *Cytotoxicity of a Bis-GMA dental composite before and after leaching in organic solvents.* J Biomed Mater Res, 1991. **25**(4): p. 443-457.

82. Spahl, W., H. Budzikiewicz, W. Geurtsen, *[Study on the residual monomer contents of different light curing hybrid composite resins].* Dtsch Zahnarztl Z, 1991. **46**(7): p. 471-5.

83. Wu, W., E.E. Toth, J.F. Moffa, J.A. Ellison, *Subsurface damage layer of in vivo worn dental composite restorations.* J Dent Res, 1984. **63**(5): p. 675-80.

84. Pham D., F.J.L., *Early elution of uncured components from light-activated dental composites.* J Dent Res, 1989(68): p. 207, Abst. No 205.

85. Zhang, Y., J. Xu, *Effect of immersion in various media on the sorption, solubility, elution of unreacted monomers, and flexural properties of two model dental composite compositions.* J Mater Sci Mater Med, 2008. **19**(6): p. 2477-83.

86. Toledano, M., R. Osorio, E. Osorio, et al., *Sorption and solubility of resin-based restorative dental materials.* J Dent, 2003. **31**(1): p. 43-50.

87. Hirasawa, T., S. Hirano, S. Hirabayashi, I. Harashima, M. Aizawa, *Initial dimensional change of composites in dry and wet conditions.* J Dent Res, 1983. **62**(1): p. 28-31.

88. Sideridou, I.D., M.M. Karabela, E. Vouvoudi, *Volumetric dimensional changes of dental light-cured dimethacrylate resins after sorption of water or ethanol.* Dent Mater, 2008. **24**(8): p. 1131-6.

89. Martin, N., N.M. Jedynakiewicz, A.C. Fisher, *Hygroscopic expansion and solubility of composite restoratives.* Dent Mater, 2003. **19**(2): p. 77-86.

90. Ashbee K.H.G., W.R.C., *Water damage in glass fiber/ resin composites.* Procedings of the Royal Society of London, 1969. **312, No 1511**: p. 553- 564.

91. Riggs, P.D., P. Kinchesh, M. Braden, M.P. Patel, *Nuclear magnetic imaging of an osmotic water uptake and delivery process.* Biomaterials, 2001. **22**(5): p. 419-27.

92. Wang BG, T.Y., SI Nakao, *Solvent diffusion in amorphous glassy polymers.* J Pol Sci: Part B: Polymer Physics, 2000. **38**(6): p. 846-856.

93. Feilzer, A.J., A.J. de Gee, C.L. Davidson, *Relaxation of polymerization contraction shear stress by hygroscopic expansion.* J Dent Res, 1990. **69**(1): p. 36-9.

94. Versluis, A., D. Tantbirojn, M.S. Lee, L.S. Tu, R. DeLong, *Can hygroscopic expansion compensate polymerization shrinkage? Part I. Deformation of restored teeth.* Dent Mater. **27**(2): p. 126-33.

95. Ernst, C.P., K. Canbek, T. Euler, B. Willershausen, *In vivo validation of the historical in vitro thermocycling temperature range for dental materials testing.* Clin Oral Investig, 2004. **8**(3): p. 130-8.

96. Sideridou, I., D.S. Achilias, E. Kyrikou, *Thermal expansion characteristics of light-cured dental resins and resin composites.* Biomaterials, 2004. **25**(15): p. 3087-97.

97. Bullard, R.H., K.F. Leinfelder, C.M. Russell, *Effect of coefficient of thermal expansion on microleakage.* J Am Dent Assoc, 1988. **116**(7): p. 871-4.

98. Craig, R.G., ed. *Restorative Dental Materials*. 10th ed. 1997, Mosby- Year Book Inc.: Ann Arbor Michigan. 253- 4.

99. Powers, J.M., R.W. Hostetler, J.B. Dennison, *Thermal expansion of composite resins and sealants.* J Dent Res, 1979. **58**(2): p. 584-7.

100. Soderholm, K.J., *Influence of silane treatment and filler fraction on thermal expansion of composite resins.* J Dent Res, 1984. **63**(11): p. 1321-6.

101. Souder W, G.P., *Physical properties of dental materials*, W.U.S.D.o. Commerce, Editor. 1942, National Bureau of Standards.

102. Hashinger, D.T., C.W. Fairhurst, *Thermal expansion and filler content of composite resins.* J Prosthet Dent, 1984. **52**(4): p. 506-10.

103. Toparli, M., N. Gokay, T. Aksoy, *An investigation of temperature and stress distribution on a restored maxillary second premolar tooth using a three-dimensional finite element method.* J Oral Rehabil, 2000. **27**(12): p. 1077-81.

104. Sidhu, S.K., T.E. Carrick, J.F. McCabe, *Temperature mediated coefficient of dimensional change of dental tooth-colored restorative materials.* Dent Mater, 2004. **20**(5): p. 435-40.

105. Earnest, C., ed. *Assignment of glass transition temperatures using thermomechanical analysis*. Assignment of the glass transition, ed. R. Seyler. 1994, ASTM STP 1249: Philadelphia: Am Soc Test Mat. 75-87.

106. Chutinan, S., J.A. Platt, M.A. Cochran, B.K. Moore, *Volumetric dimensional change of six direct core materials.* Dent Mater, 2004. **20**(4): p. 345-51.

107. Marchesi, G., L. Breschi, F. Antoniolli, et al., *Contraction stress of low-shrinkage composite materials assessed with different testing systems.* Dent Mater. **26**(10): p. 947-53.

108. Min, S.H., J. Ferracane, I.B. Lee, *Effect of shrinkage strain, modulus, and instrument compliance on polymerization shrinkage stress of light-cured composites during the initial curing stage.* Dent Mater. **26**(10): p. 1024-33.

109. Della Bona, A., V. Rosa, D. Cecchetti, *Influence of shade and irradiation time on the hardness of composite resins.* Braz Dent J, 2007. **18**(3): p. 231-4.

110. Jones R, C.W., ed. *Holographic and speckle interferometry: A discussion of the theory, practice and application of the techniques*. 1989, Press Syndicate of the University of Cambridge: Cambridge. 81-90.

111. DantecDynamics. *http://www.dantecdynamics.com/Default.aspx?ID=854*.

112. Zaslansky, P., A.A. Friesem, S. Weiner, *Structure and mechanical properties of the soft zone separating bulk dentin and enamel in crowns of human teeth: insight into tooth function.* J Struct Biol, 2006. **153**(2): p. 188-99.

113. Zaslansky, P., J.D. Currey, A.A. Friesem, S. Weiner, *Phase shifting speckle interferometry for determination of strain and Young's modulus of mineralized biological*

materials: a study of tooth dentin compression in water. J Biomed Opt, 2005. **10**(2): p. 024020.

114. ImageJ, *http://rsbweb.nih.gov/ij/*.

115. Craig, R.G., ed. *Restorative Dental Materials*. Eighth ed. 1989, The C.V. Mosby Company: St. Louis. 68-69.

116. Yap, A.U., A.C. Tan, C. Quan, *Non-destructive characterization of resin-based filling materials using Electronic Speckle Pattern Interferometry.* Dent Mater, 2004. **20**(4): p. 377-82.

117. Shahar, R., P. Zaslansky, M. Barak, et al., *Anisotropic Poisson's ratio and compression modulus of cortical bone determined by speckle interferometry.* J Biomech, 2007. **40**(2): p. 252-64.

118. Barak, M.M., A. Sharir, R. Shahar, *Optical metrology methods for mechanical testing of whole bones.* Vet J, 2009. **180**(1): p. 7-14.

119. Kishen, A., V.M. Murukeshan, V. Krishnakumar, A. Asundi, *Analysis on the nature of thermally induced deformation in human dentine by electronic speckle pattern interferometry (ESPI).* J Dent, 2001. **29**(8): p. 531-7.

120. Bouillaguet, S., J. Gamba, J. Forchelet, I. Krejci, J.C. Wataha, *Dynamics of composite polymerization mediates the development of cuspal strain.* Dent Mater, 2006. **22**(10): p. 896-902.

121. Nasralla Ramez A, M.A.B., Hisham A Nasr-El-Din, *Investigation of Wettability Alteration by Low Salinity Water*. 2011, Society of Prtroleum Engineers.

122. Chung, S.M., A.U. Yap, K.T. Tsai, F.L. Yap, *Elastic modulus of resin-based dental restorative materials: a microindentation approach.* J Biomed Mater Res B Appl Biomater, 2005. **72**(2): p. 246-53.

123. Lizymol P.P., K.V. K., *A comparison of efficiency of two photoinitiators for polymerization of light-cure dental composite resins.* Journal of Applied Polymer Science, 2007. **107**(5): p. 3337–3342.

124. Petermann, K., ed. *Laser Diode Modulation and Noise*. 1991, Kluwer Academic Publishers Group: Dordrecht, The Netherlands. 170-172.

125. Zappe, H., ed. *Laser Diode Microsystems*. 2004, Springer Verlag: Berlin Heidelberg. 196-200.

126. Fleming, G.J., M. Awan, P.R. Cooper, A.J. Sloan, *The potential of a resin-composite to be cured to a 4mm depth.* Dent Mater, 2008. **24**(4): p. 522-9.

127. Mortier, E., D.A. Gerdolle, A. Dahoun, M.M. Panighi, *Influence of initial water content on the subsequent water sorption and solubility behavior in restorative polymers.* Am J Dent, 2005. **18**(3): p. 177-81.

128. Leprince, J., G. Lamblin, D. Truffier-Boutry, et al., *Kinetic study of free radicals trapped in dental resins stored in different environments.* Acta Biomater, 2009. **5**(7): p. 2518-24.

129. Truffier-Boutry, D., S. Demoustier-Champagne, J. Devaux, et al., *A physico-chemical explanation of the post-polymerization shrinkage in dental resins.* Dent Mater, 2006. **22**(5): p. 405-12.

130. Bagis, Y.H., F.A. Rueggeberg, *The effect of post-cure heating on residual, unreacted monomer in a commercial resin composite.* Dent Mater, 2000. **16**(4): p. 244-7.

131. Loza-Herrero, M.A., F.A. Rueggeberg, W.F. Caughman, et al., *Effect of heating delay on conversion and strength of a post-cured resin composite.* J Dent Res, 1998. **77**(2): p. 426-31.

132. Burtscher, P., *Stability of radicals in cured composite materials.* Dent Mater, 1993. **9**(4): p. 218-21.

133. Vrentas JS, J.D., *Diffusion in polymer-solvent systems; I. Re-examination of the Free-Volume theory.* J Pol Sci: Polymer Physics, 1977a. **15**(3): p. 403-416.

134. Vrentas JS , J. Duda, *A free-volume interpretation of the influence of the glass transition on diffusion in amorphous polymers.* J Appl Pol Science, 1978. **22**(8): p. 2325-2339.

135. Reis RA, J.O., R Nobrega, *Diffusion coefficients in polymer-solvent systems for highly concentrated polymer solutions.* Braz J Chem Eng., 2001. **18**(4): p. 367-384.

136. Vrentas JS, J.D., *Diffusion in polymer-solvent systems; II. A predictive theory for the dependence of diffusion coefficients on temperature, concentration and molecular weight.* J Pol Sci: Polymer Physics, 1977b. **15**(3): p. 417-439.

137. Wells-Gray, E.M., S.J. Kirkpatrick, R.L. Sakaguchi, *A dynamic light scattering approach for monitoring dental composite curing kinetics.* Dent Mater. **26**(7): p. 634-42.

138. Bockris, J.O.M., ed. *Modern Electrochemistry 1: Ionics*. Second ed. 1998, Plenum Press: New York. 48-49.

139. Smirnov IV, V.V., Kornilova AA, *Introduction to the Biophysics of Activated water*. 2005, Boca Raton: Universal Publishers. 35-42.

140. Mezger, T., ed. *The Rheology Handbook*. 2nd ed. 2006, Vincentz Network GmbH & Co.: Hannover. 242-244.

Abbreviations

BisGMA: bisphenol A- glycidyl methacrylate

TEGDMA: triethylene glycol dimethacrylate

BISDMA:bisphenol A- dimethacrylate

EGDMA: ethylene glycol dimethacrylate

UDMA: urethane dimethacrylate

DMAPE: 4-n, n- dimethylamino- phenyl- ethanol

DMAEM: dimethylaminoethyl methacrylate

EDMAB: ethyl-4 – dimethylaminobenzoate

CEMA: n,n- cyanoethylmethylaniline

CTE: coefficient of thermal expansion

ESPI: electronic speckle pattern interferometry

Appendix A

Acquisition of displacement data for each step by ESPI

Following Zaslanksy et al. [113], the total light intensity recorded by the reflection of the surface is calculated by the following formula:

$$I_{total} = I_a + I_b + \sqrt{I_a \cdot I_b}\cos(\varphi_a - \varphi_b) \qquad \text{[Eq. 6]}$$

Where I_a, I_b are the intensities of each interference beams,

φ_a,φ_b are the phases corresponding to the aforementioned intensities

These two phases vary, however the difference between them ($\Delta\varphi_{ab}= \varphi_a - \varphi_b$) is constant for one surface. This difference can be calculated by acquiring four consecutive images of the same surface by changing the phase by π/2 each time.

Therefore, during each ESPI measurement step, four images of the specimen surface are acquired per direction, by the rotation of the reflective mirror of the interferometer by π/2, for one period. The following figures show the procedure followed in order to calculate $\Delta\varphi_{ab}$ [Fig. 59- 62].

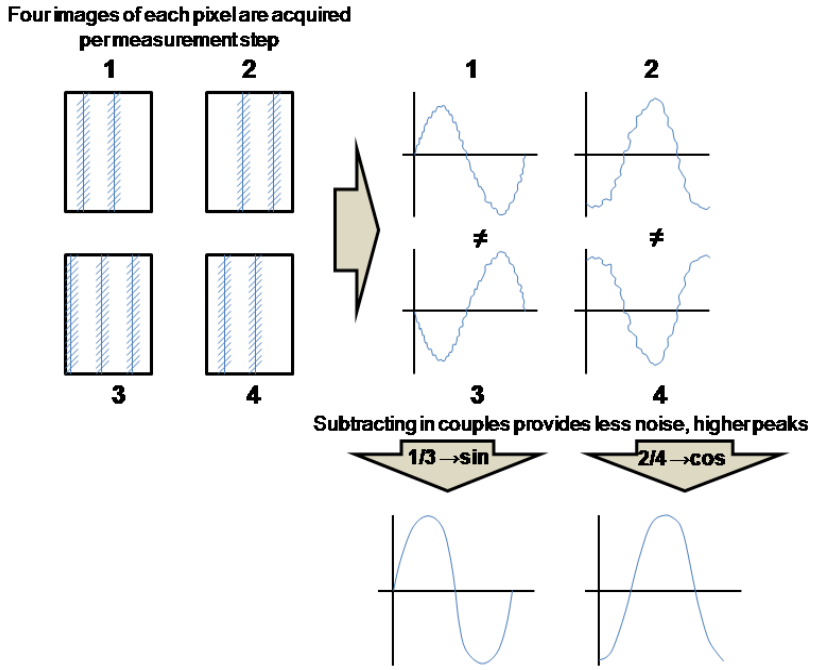

Fig 59: Four images per pixel are taken at each step, by rotating the reflective mirror of the interferometer by π/2 for one period. Subtracting in couples the intensities recorded from the equivalent images 1 to 3 and 2 to 4, the result is a sin for the first couple and a cos for the second, with less noise and higher peaks.

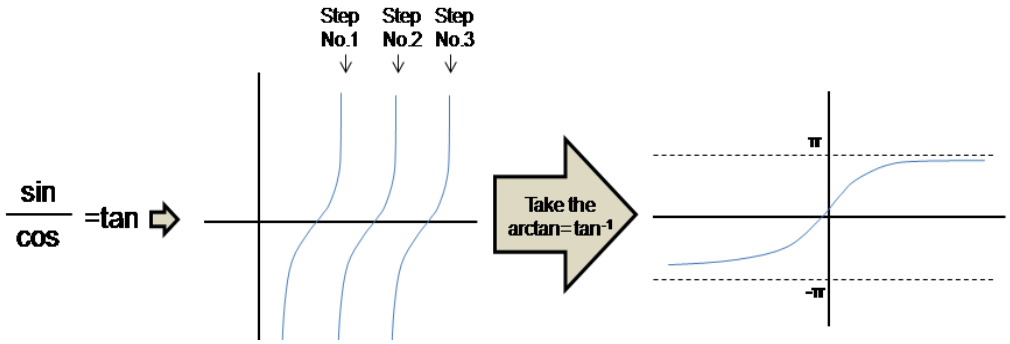

Fig.60: From Fig. 59, sin divided by cos equals tan. This way, out of the four images taken initially, one value is calculated per step. The arctan= $\tan^{-1}$ is used to limit the values of the tan inside the frame of π and –π.

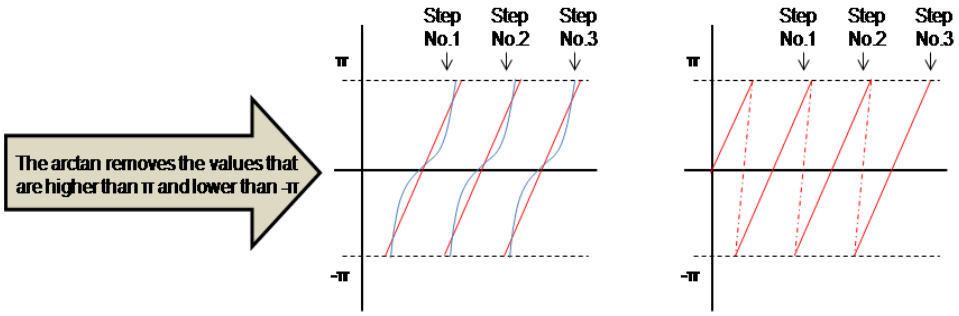

Fig. 61: The arctan removes the values of the tan that are higher than π and lower than –π. From the final graph shown here, the direction of the deformation recorded can be defined, but not yet the actual value of strain.

From this, $\Delta\varphi_{ab}$ can be calculated by using the following formula:

$$\Delta_{\varphi ab} = \arctan\left[\frac{I_1 - I_3}{I_2 - I_4}\right] \qquad \text{[Eq. 7]}$$

Every difference on the Intensity recorded before and after a load is applied is expressed as a difference of the $\Delta\varphi_{ab}$ prior to and after loading. This difference is expressed for every 2π. The phase corresponding to the actual displacement can therefore be calculated following phase shifting, as described in Fig 62.

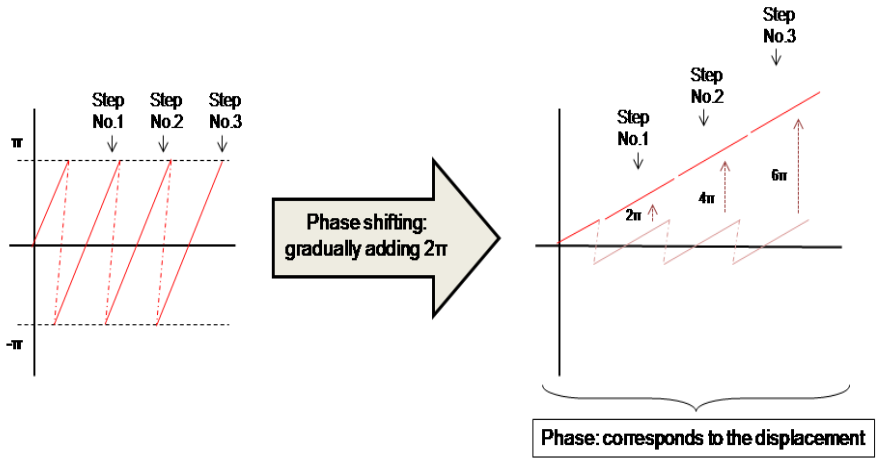

Fig. 62: The actual phase of each step that corresponds to the displacement can now be calculated by consecutively adding 2π for every step. This procedure is called phase shifting.

With this procedure, in order to calculate the actual displacement the following formula is used for the in-plane displacement:

$$d = \frac{N \cdot \lambda \cdot (\Delta\varphi_{post} - \Delta\varphi_{pre})}{4\pi \sin\theta} \qquad \text{[Eq. 8]}$$

and for the out-of-plane displacement:

$$d = \frac{N \cdot \lambda \cdot (\Delta\varphi_{post} - \Delta\varphi_{pre})}{4\pi} \qquad \text{[Eq. 9]}$$

Where: N: the number of fringes

λ: the wavelength of the lasers

θ: the illumination angle

The strain of the material can now be calculated from the acquired displacement map in relation to a reference point on the surface, as explained in Chapter 5.2.1.2.

Appendix B

1. Basic principles of the Peltier element

The Peltier element generally consists of two different materials, through which a current flow is achieved [140]. This current flow causes a difference in temperature between the two materials: one side is heated while the other cools. In this way, the heating of the specimen can be achieved, if it is placed in close contact to the heated side of the Peltier element.

By raising the current that passes through the Peltier, the rise in temperature of a specimen can be achieved in a controlled way if the temperature gradient between the two sides of the Peltier is kept constant. In order for this gradient to be constant, the low temperature of the cooling side of the Peltier must be kept stable. This can be achieved in various ways, as for example by attaching a water bath.

2. Use of the Peltier element in this study

On the Peltier element used for this study, the constant low temperature of the reverse side was achieved by mounting a fan beneath it. However, in order for this system to operate smoothly, a slow heating procedure during the measurement should be used, so that there would be enough time for the fan to keep the low temperature on this side stable.

At the high speed of temperature rising on this study (2 min), the fan is unable to keep the temperature gradient constant. Therefore, the Peltier operates at intervals: the temperature rises for as long as the gradient is kept constant, and then stops until the fan restabilizes it. This excluded the possibility of taking into account the part of the measurement corresponding to this phase. After the first two minutes, as the temperature reaches 37°C and is stabilised, the temperature gradient on the Peltier is also stable and therefore the measurement can take place.

Appendix C

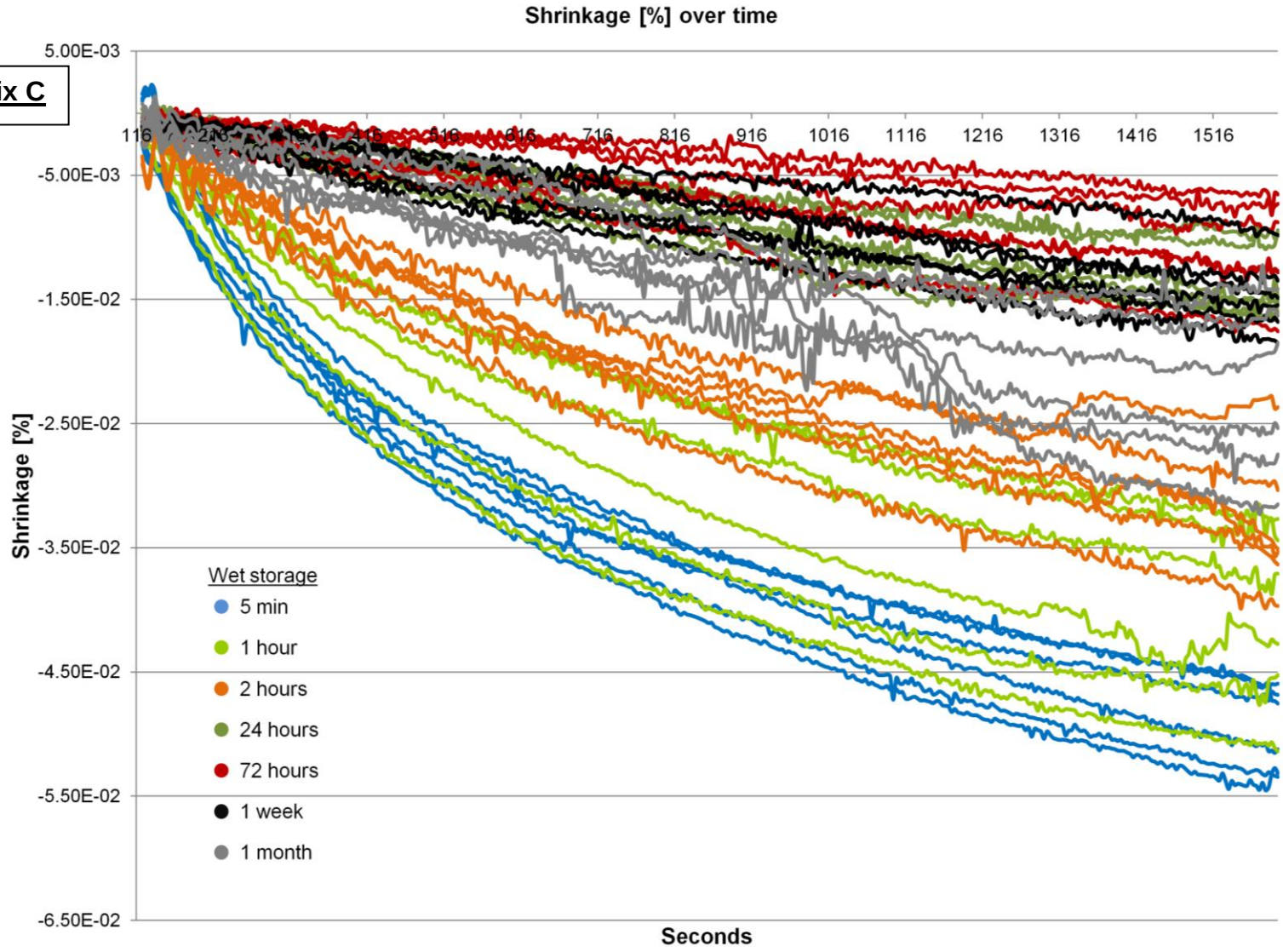

Shrinkage percentage over time for all the specimens of the measurement.

Lebenslauf

Mein Lebenslauf wird aus datenschutzrechtlichen Gründen in der elektronischen Version meiner Arbeit nicht veröffentlicht.

Publikationsliste

1. Kollia P, Kachrimanis N, Pelekanos S: Prothetische Versorgung im Oberkiefer von teilbezahnten Patienten in Kennedy Klass I, Referat am 11. Kongress der griechischen Studenten der Zahnmedizin, 2006, Athen.

2. Kachrimanis N, Belouka S, Paximada H: Treatment of aesthetic problems with stratified layering technique: a clinical report. (Contemporary Dentist Journal of Greece 27(2) 56-67,2007)

3. Kachrimanis N, Zaslansky P, Müller WD: Nanometer deformations of wet and dry composites determined by Speckle Interferometry, Poster, Annual Meeting of the ADM 07-09.10.2010, Trieste, Italien.

4. Kachrimanis N, Zaslansky P, Müller WD: A post-cure nano-scale shrinkage study of dry and wet stored composite. Poster, 45th Meeting of the CED-IADR with the Scandinavian Devision 31.08-03.09.2011, Budapest, Ungarn.

Berlin, den 20. September 2012

Eidesstattliche Versicherung

„Ich, Nikolaos Kachrimanis, versichere an Eides statt durch meine eigenhändige Unterschrift, dass ich die vorgelegte Dissertation mit dem Thema: *The submicron dimensional behavior of post-cure dental composites: an Electronic Speckle Pattern-correlation Interferometry study* selbstständig und ohne nicht offengelegte Hilfe Dritter verfasst und keine anderen als die angegebenen Quellen und Hilfsmittel genutzt habe.

Alle Stellen, die wörtlich oder dem Sinne nach auf Publikationen oder Vorträgen anderer Autoren beruhen, sind als solche in korrekter Zitierung (siehe „Uniform Requirements for Manuscripts (URM)“ des ICMJE -*www.**icmje**.org*) kenntlich gemacht. Die Abschnitte zu Methodik (insbesondere praktische Arbeiten, Laborbestimmungen, statistische Aufarbeitung) und Resultaten (insbesondere Abbildungen, Graphiken und Tabellen) entsprechen den URM (s.o) und werden von mir verantwortet.

Meine Anteile an etwaigen Publikationen zu dieser Dissertation entsprechen denen, die in der untenstehenden gemeinsamen Erklärung mit dem/der Betreuer/in, angegeben sind. Sämtliche Publikationen, die aus dieser Dissertation hervorgegangen sind und bei denen ich Autor bin, entsprechen den URM (s.o) und werden von mir verantwortet.

Die Bedeutung dieser eidesstattlichen Versicherung und die strafrechtlichen Folgen einer unwahren eidesstattlichen Versicherung (§156,161 des Strafgesetzbuches) sind mir bekannt und bewusst.“

Berlin, den 22. Mai 2013